NATIONAL ADVISORY COMMITTEE FOR AERONAUTICS

TECHNICAL NOTE

No. 1446

THEORY OF THE INLET AND EXHAUST PROCESSES OF INTERNAL-COMBUSTION ENGINES

By Tsung-chi Tsu

Massachusetts Institute of Technology

Washington

January 1949

NATIONAL ADVISORY COMMITTEE FOR AERONAUTICS

TECHNICAL NOTE NO. 1446

THEORY OF THE INLET AND EXHAUST PROCESSES OF INTERNAL-COMBUSTION ENGINES

By Tsung-chi Tsu

SUMMARY

A theory, based on the First Law of Thermodynamics and hydrodynamic laws governing the flow of gases, is developed for the calculation of the mass of fluid pumped per stroke and of indicator diagrams for the pumping process of internal-combustion engines, compressors, or vacuum pumps. The data needed are few and easily obtainable. Thus, the volumetric efficiency and the indicator diagrams for the inlet and exhaust processes of an internal-combustion engine can be obtained even before the engine is actually built.

The differential equations of the theory, although incapable of ordinary mathematical integration, can be solved by means of a differential analyzer, or, more laboriously, by a method of step-by-step calculation.

A large number of inlet and exhaust processes of three different gasoline engines are calculated and, although the theoretical volumetric efficiencies, owing to some approximations made in the theory, are, on the average, 5 percent higher than the measured values, the trends predicted by the theory are correct.

The agreement between the calculated and measured indicator diagrams seems to be within the precision of the measuring indicator, with indications that in certain cases the calculated pressures are more accurate. In some cases where the agreement is poor, the discrepancy can be traced to (1) a zero shift of the atmospheric lines in the measured indicator diagrams, (2) gross errors in estimating the initial pressures of the theoretical indicator diagrams, (3) a combination of causes (1) and (2), or (4) vibrations set up in the inlet and exhaust pipes of the test engine.

It is found from theoretical calculations that by varying the inlet pressure p_i and the exhaust pressure p_e, other things being kept constant, the volumetric efficiency varies with the ratio p_i/p_e regardless of the individual levels of either p_i or p_e.

The theory also indicates that for the inlet process, the effect of decreasing the piston speed is the same as increasing the relative size of the inlet valve to the piston or increasing the velocity of sound in the intake charge; and for the exhaust process, the effect of decreasing the piston speed is the same as increasing the relative size of the exhaust valve to the piston or increasing the velocity of sound in the ideal residual gas (defined in the text).

With the aid of the theory, it is possible to calculate some hypothetical inlet and exhaust processes which are impossible to obtain on actual engines, such as the cases where the valves open and close instantaneously.

INTRODUCTION

Of the four strokes that make up an Otto- or Diesel-engine cycle, the compression stroke can be analyzed with a good degree of accuracy; that is, calculated pressure-volume-temperature relations agree reasonably well with experimental results. Since the publication of thermodynamic charts for the working fluid in internal-combustion engines by Hottel and coworkers in 1936 (reference 1), the thermodynamic changes caused by combustion and expansion can also be predicted with a fair degree of accuracy. However, despite the efforts of many investigators (of whom the more important and representative ones are cited in references 2 to 8), there has been no satisfactory method of analyzing the inlet and exhaust processes.

Most of the past researches on this subject consist of experimental work that applies only to a particular set of conditions; and the few analytical treatments are either unsatisfactory or very limited in scope. Thus, the relation of cylinder pressure to crank angle of the inlet and exhaust processes and the volumetric efficiency of the cylinder cannot be known until after the engine is actually built and tested.

To the design engineer as well as to the research engineer, this certainly is a great handicap and inconvenience; for air capacity is perhaps the most important single factor limiting the maximum power output of an engine. A method of predicting air capacity would be especially convenient when a new design or certain changes in design or operating conditions are contemplated.

With these views in mind, research was undertaken by the author under the supervision of Prof. Edward S. Taylor, and the findings were embodied in a thesis (reference 9) and submitted to the Massachusetts Institute of Technology in June 1944. The method developed therein applies to any single-cylinder engine with very short inlet and exhaust pipes. The data needed for the analytical solutions are few and very simple to obtain, and the agreement between the calculated and experimental results is quite satisfactory. The material in this report is based on the theory developed in that thesis, plus an extensive check of the theory with experimental results. This covers three different engines and the following ranges of variables:

$\dfrac{\text{Average effective inlet-valve opening area}}{\text{Piston area}}$	0.058 – 0.026
$\dfrac{\text{Average effective exhaust-valve opening area}}{\text{Piston area}}$	0.056 – 0.026
Inlet opening, degrees B.T.C.	45 – 3
Inlet closing, degrees A.B.C.	33 – 127
Exhaust opening, degrees B.B.C.	132 – 60
Exhaust closing, degrees A.T.C.	3 – 45
Inlet-valve opening duration; crank angle, degrees	216 to 352
Exhaust-valve opening duration; crank angle, degrees	243 to 352
$\dfrac{\text{Inlet pressure}}{\text{Exhaust pressure}}$	0.5 – 4.0
$\dfrac{\text{Mean piston speed}}{\text{Velocity of sound in intake mixture}}$	0.0055 – 0.0420

It may be well to point out that, although the theory was intended for the pumping process of the internal-combustion engine, it is equally applicable to reciprocating compressors or vacuum pumps in which the working medium is a gaseous substance.

This work was conducted at the Massachusetts Institute of Technology under the sponsorship and with the financial assistance of the National Advisory Committee for Aeronautics.

EQUATION OF THE INLET PROCESS – VOLUMETRIC EFFICIENCY

During the inlet process, the energy content in the cylinder continuously changes for the following three reasons: (1) fresh energy is brought in by the fuel-air mixture through the inlet valve; (2) work is performed on the piston by the cylinder contents; and (3) heat is transferred between the cylinder contents and their surroundings. In symbols,

$$dE = dH - p\ dV + dQ \tag{1}$$

where

dE change of internal energy in the cylinder

dH enthalpy brought into the cylinder by the fresh charge

p cylinder pressure

dV change of cylinder volume

dQ heat transferred into the cylinder contents

All the changes take place during the same time interval dt. (For a list of symbols used in this report see appendix A.)

If the cylinder contents are assumed to be homogeneous and a perfect gas, then

$$E = MC_vT \tag{2}$$

and

$$dE = C_v d(MT) \tag{3}$$

where

M mass of cylinder contents

T absolute temperature of cylinder contents

C_v mean specific heat (at constant volume) of the cylinder contents, assumed to be constant

Also

$$dH = C_pT_i\ dM \tag{4}$$

where

C_p mean specific heat at constant pressure of the fresh charge, assumed constant

T_i absolute temperature of the fresh mixture at station i (fig. 1(a)). Station i is a station upstream of the inlet valve where pressure and temperature are sensibly constant and where the velocity of flow of the intake charge is considerably lower than that through the valve; T_i is what is usually referred to as the inlet temperature.

dM mass of charge admitted into the cylinder in time dt

Combining equations (1), (3), and (4) yields

$$C_v \, d(MT) = C_p T_i \, dM - p \, dV + dQ \tag{5}$$

which is the general differential equation of the inlet process. It should be noted that in equation (5) dQ really consists of two parts: the heat picked up by the fresh charge dM on its way from station i to the valve and the heat transferred into the contents enclosed in the cylinder during time dt. It has been shown, however, that unless there is an unusually large temperature difference between the walls of the inlet system and the incoming charge, the effect of heat transfer on either volumetric efficiency or cylinder pressure is small (references 9 and 10). Besides, a reasonably accurate estimate of the magnitude of dQ is not usually possible. So for practical purposes, the term dQ is omitted and equation (5) is simplified to

$$C_v \, d(MT) = C_p T_i \, dM - p \, dV \tag{6}$$

From the perfect-gas law

$$pV = (M/m) \, RT \tag{7}$$

where m is the molecular mass of the gas (mass per mole of gas; M/m, number of moles), and R, the universal gas constant. It is observed that:

$$d(pV) = (R/m) \, d(MT) \tag{8}$$

From equations (6) and (8) is obtained

$$(mC_v/R) \, d(pV) = C_p T_i \, dM - p \, dV \tag{9}$$

Dividing equation (9) by mC_v/R, transposing terms, and noting that

$$C_p/C_v = k \tag{10}$$

and

$$R/(mC_v) = k - 1 \tag{11}$$

finally results in

$$d(pV) + (k_i - 1) p \, dV = (R/m_i) k_i T_i \, dM \tag{12}$$

the subscript i being used to denote the intake charge.

On equating the terms of the left-hand side of equation (12) to zero, the familiar equation of the isentropic process is obtained. The difference between the inlet process and the isentropic process is the term of the right-hand side, which represents the energy brought into the cylinder by the fresh charge.

In order to put equation (12) into a mathematically soluble form, dM must be evaluated in terms of more convenient variables, such as the pressures on both sides of the inlet valve and the effective valve opening area. The flow of the intake charge through the inlet valve, it must be noted, is unsteady, and the hydrodynamic rule governing such flow is Euler's equation (reference 11):

$$\frac{\partial w}{\partial t} + w \cdot \text{grad } w = \text{grad } U - \frac{1}{\rho} \text{grad } p \tag{13}$$

where

w velocity field

U gravitational force function

p pressure field

t time

ρ density of the fluid

In the case under consideration where the fluid is a gas, the gravitational force (weight of the gas) may be neglected in the presence of other forces. By concentrating on one particular streamline C and denoting by u and x the velocity and the distance, respectively, along that streamline, the result at that particular instant is

$$\frac{\partial u}{\partial t} + u \frac{du}{dx} = -\frac{1}{\rho} \frac{dp}{dx} \tag{14}$$

Integration along the streamline gives

$$\int_c \frac{\partial u}{\partial t} dx + \frac{u^2}{2} + \int_c \frac{dp}{\rho} = \text{Constant} \tag{15}$$

For the isentropic relation p/ρ^k = Constant, it becomes

$$\int_c \frac{\partial u}{\partial t} dx + \frac{u^2}{2} + \frac{k}{k-1} \frac{p}{\rho} = \text{Constant} \tag{16}$$

which differs from Bernoulli's equation by the first term. Bernoulli's equation, of course, is valid only for steady flow; but in dealing with general hydrodynamic problems in which a gas (not a liquid) is involved, the inertia force due to the unsteadiness of flow is usually small compared with other forces. In the particular case of the flow through an engine valve, this statement will be supported by an example given in appendix B. Therefore, the first term in equation (16) will be dropped, leaving simply

$$\frac{u^2}{2} + \frac{k}{k-1}\frac{p}{\rho} = \text{Constant} \tag{17}$$

from which the velocity through the valve in terms of the upstream and downstream pressures (that is, inlet pressure p_i and cylinder pressure p) is easily computed and the mass rate of flow through the valve is found to be

$$\frac{dM}{dt} = A_i p_i \sqrt{\frac{2m_i}{RT_i}\frac{k}{k-1}\left[\left(\frac{p}{p_i}\right)^{\frac{2}{k}} - \left(\frac{p}{p_i}\right)^{\frac{k+1}{k}}\right]} \tag{18}$$

where A_i is the effective inlet-valve opening area (actual valve opening area multiplied by flow coefficient), and T_i, the absolute inlet temperature. If a dimensionless quantity is further defined

$$F_i = \sqrt{\frac{k}{k-1}\left[\left(\frac{p}{p_i}\right)^{\frac{2}{k}} - \left(\frac{p}{p_i}\right)^{\frac{k+1}{k}}\right]} \tag{19}$$ [1]

then

$$dM/dt = A_i p_i F_i \sqrt{2m_i/RT_i} \tag{20}$$

[1] F_i refers to the flow factor for inward flow, as distinguished from F_e, the flow factor for outward flow. (See equation (39).)

By going back to equation (12), it is seen that the term on the right-hand side

$$\left(R/m_i\right) k_iT_i \ dM = \left(R/m_i\right) k_iT_i(dM/dt) \ dt$$

$$= \left(R/m_i\right) k_iT_i\left(A_ip_iF_i \sqrt{2m_i/RT_i}\right)dt$$

$$= k_iA_ip_iF_i \sqrt{2RT_i/m_i} \ dt$$

$$= A_ip_iF_i \sqrt{2k_i} \sqrt{k_iRT_i/m_i} \ dt$$

$$= \sqrt{2k_i} \ A_ip_iF_iC_i \ dt \tag{21}$$

where $C_i \equiv \sqrt{k_iRT_i/m_i}$ is the velocity of sound in the intake mixture.

With an engine running at N revolutions per unit time, the time t and the crank angle θ are connected by the relation

$$dt = d\theta/360N \tag{22}$$

Combining equations (12), (21), and (22) yields

$$d(pV) + \left(k_i - 1\right)p \ dV = \sqrt{2k_i} \ A_ip_iF_iC_i \ d\theta/360N \tag{23}$$

Dividing equation (23) through by p_iV_d, where p_i is the inlet pressure and V_d, the piston displacement, gives

$$d\left(\frac{p}{p_i} \frac{V}{V_d}\right) + \left(k_i - 1\right)\frac{p}{p_i} \, d\left(\frac{V}{V_d}\right) = \frac{\sqrt{2k_i}A_iF_iC_i \ d\theta}{360NV_d} \tag{24}$$

Noting that the piston displacement V_d is the product of the piston area A_p and the stroke S and also that $2SN$ represents the mean piston speed s results in

$$d\left(\frac{p}{p_i}\frac{V}{V_d}\right) + \left(k_i - 1\right)\frac{p}{p_i}\,d\left(\frac{V}{V_d}\right) - \frac{\sqrt{2k_i}}{180}\,\frac{C_i}{s}\,\frac{A_i}{A_p}\,F_i\,d\theta = 0 \qquad (25)$$

which is the final form of the equation of the inlet process.

All terms in equation (25) are expressed in dimensionless ratios except θ, which is in degrees. The constants p_i, C_i, k_i, and s are easily obtainable. Thus, when the relations V/V_d and A_i/A_p against θ are known, the equation becomes immediately soluble. The relation between the flow factor F_i and the ratio p/p_i may be obtained from figure 2(b). As equation (19) shows, the flow factor F_i is a function both of k the ratio of specific heats and of the ratio p/p_i. Fortunately, by defining F_i as it is, it becomes practically independent of k for the range $1.25 < k < 1.40$, which, incidentally, covers fuel-air mixtures of all fuels and all mixture ratios used in practical operation of internal-combustion engines.

As can be seen from equation (20), with constant upstream conditions, the flow factor is proportional to the mass rate of flow per unit effective valve opening area (mass per unit time per unit area). Thus, the flow factor increases as the pressure ratio p/p_i decreases, but a critical pressure ratio is soon reached beyond which there is no further increase of flow and the flow factor becomes constant. This is clearly shown in figure 2(b). The critical pressure ratio is a function of k and is given by

$$\text{Critical pressure ratio} = \left(\frac{2}{k+1}\right)^{\frac{k}{k-1}}$$

Unfortunately, equation (25) cannot be solved by ordinary mathematical integration, as the relation between A_i/A_p and θ must, in general, be presented in graphical form and F_i is not an easily integrable function; but it can be readily solved by means of a differential analyzer, or, more laboriously, by a method of step-by-step calculation.

From equations (20) and (22), it follows that

$$dM = A_i p_i F_i \sqrt{\frac{2m_i}{RT_i}}\,\frac{d\theta}{360N}$$

Therefore the total mass of fresh charge admitted into the cylinder during the inlet process is

$$M_t = \int_{M_o}^{M_c} dM = \sqrt{\frac{2m_i}{RT_i}}\,\frac{p_i}{360N}\int_{\theta_o}^{\theta_c} A_i F_i \, d\theta \tag{26}$$ [2]

where θ_o is the crank angle at which the inlet valve opens and θ_c the crank angle at which the valve is completely closed; M_t, of course, is the total mass of air plus fuel, and the mass of air alone is

$$M_a = M_t/(1 + f) \tag{27}$$

where f is the fuel-air ratio by weight. If the mass of air M_a taken into the cylinder during the entire intake process is known, the volumetric efficiency of the cylinder can easily be calculated (reference 12).

EQUATION OF THE EXHAUST PROCESS

By analogy to the equation of the inlet process, the equation of the exhaust process can be written as follows:

$$d\left(\frac{p}{p_e}\frac{V}{V_d}\right) + \left(k_e - 1\right)\frac{p}{p_e}\,d\left(\frac{V}{V_d}\right) - \frac{\sqrt{2k_e}}{180}\,\frac{C_e}{s}\,\frac{A_e}{A_p}\,F_e\,d\theta = 0 \tag{28}$$

where the symbols have the same meaning as defined before except that here p_e is the exhaust pressure, k_e the ratio of specific heats of the exhaust gas, C_e the velocity of sound in the residual gas, A_e the effective exhaust-valve opening area, and F_e the flow factor for outward flow which will be defined later.

---

[2] As equation (26) is dimensional, consistent units must be used. One convenient system would be to use m_i in slugs per mole, R in ft-lb per mole per $^{\circ}R$, T_i in $^{\circ}R$, p_i in lb/sq in., A_i in sq in., N in rps, and θ in degrees. M_t will then be in slugs.

However, for the sake of completeness and in order to clarify the definition of C_e and to show the difference between the flow factors F_e and F_i, the derivation is repeated.

Referring to figure 1(b), at time t, the cylinder volume is V, its pressure, p, and its absolute temperature, T. If the cylinder contents are considered as a perfect gas, its mass is $M = (m/R)(pV/T)$ and its internal energy is $E = MC_vT$ where C_v is the mean specific heat at constant volume of the cylinder contents.

$$E = MC_vT = (m/R)(pV/T)C_vT = (mC_v/R)(pV) \tag{29}$$

After an infinitesimal length of time dt, the time is $t + dt$, the cylinder volume $V + dV$, the pressure $p + dp$, and the absolute temperature $T + dT$. The mass of the cylinder contents becomes $M + dM$ and its internal energy

$$E + dE = (M + dM)C_v(T + dT) \tag{30}$$

The term C_v is assumed to be constant during this change. Again using the perfect-gas law, equation (30) may be written

$$\begin{aligned} E + dE &= (M + dM)C_v(T + dT) \\ &= \frac{m(p + dp)(V + dV)}{R(T + dT)} C_v(T + dT) \\ &= (mC_v/R)(p + dp)(V + dV) \end{aligned} \tag{31}$$

Subtracting equation (29) from equation (31) and neglecting infinitesimal of the second order leaves

$$dE = (mC_v/R)(p\ dV + V\ dp) = (mC_v/R)\ d(pV) \tag{32}$$

This change of internal energy in the cylinder during time dt is caused by two things: (1) work is done by the piston on the cylinder contents and (2) energy is discharged through the exhaust valve by the outgoing gas. Any heat exchange between the cylinder contents and their surroundings will be neglected as in the case of the inlet process.

The energy carried out by a unit mass of gas flowing through the exhaust valve is equal to its internal energy plus the flow work. In other words it is equal to the enthalpy, which in turn, for a perfect gas, is equal to C_pT, where C_p is the specific heat at constant pressure. Therefore, from the First Law of Thermodynamics,

$$dE = \left(mC_v/R\right) d(pV) = -C_pT\ dM - p\ dV \tag{33}$$

dM being the mass of gas flowing out through the exhaust valve during time dt. Dividing equation (33) through by mC_v/R and remembering that $C_p/C_v = k_e$, $C_p - C_v = R/m$, and $R/(mC_v) = k_e - 1$ yields

$$d(pV) + \left(k_e - 1\right) p\ dV = -\left(R/m_e\right) k_e T\ dM \tag{34}$$

Now $dM = (dM/dt)\ dt$, $dt = d\theta/360N$, and

$$\frac{dM}{dt} = A_e p \sqrt{\frac{2m_e}{RT} \frac{k}{k-1} \left[\left(\frac{p_e}{p}\right)^{\frac{2}{k}} - \left(\frac{p_e}{p}\right)^{\frac{k+1}{k}}\right]} \tag{35}$$

(This equation usually appears in textbooks on fluid mechanics or thermodynamics. See, for example, reference 13, p. 317, equation 160.)

Therefore

$$\begin{aligned}
\left(R/m_e\right) k_e T\ dM &= \left(R/m_e\right) k_e T (dM/dt)\ dt \\
&= \frac{R}{m_e} k_e T A_e p \sqrt{\frac{2m_e}{RT} \frac{k}{k-1} \left[\left(\frac{p_e}{p}\right)^{\frac{2}{k}} - \left(\frac{p_e}{p}\right)^{\frac{k+1}{k}}\right]}\ \frac{d\theta}{360N} \\
&= k_e A_e p_e \sqrt{\frac{2RT}{m_e} \frac{k}{k-1} \left(\frac{p}{p_e}\right)^2 \left[\left(\frac{p_e}{p}\right)^{\frac{2}{k}} - \left(\frac{p_e}{p}\right)^{\frac{k+1}{k}}\right]}\ \frac{d\theta}{360N}
\end{aligned} \tag{36}$$

The temperature of the cylinder contents T in expression (36) is inconvenient to handle, since it varies during the exhaust process as the cylinder pressure falls. For this reason a temperature T_r, defined by the following equation, will be introduced:

$$\frac{T}{T_r} = \left(\frac{p}{p_e}\right)^{\frac{k-1}{k}} \tag{37}$$

That is, T_r would be the temperature of the cylinder contents if they had expanded isentropically from the pressure p and temperature T to the exhaust pressure p_e; T_r will hence be called the ideal residual-gas temperature. Since the expansion of the gases inside the cylinder during the exhaust process is very nearly isentropic, T_r in practice could be regarded as fixed for a given exhaust process. It should be noted that T_r is different from the exhaust temperature in its usual sense, because exhaust temperature is ordinarily measured in the exhaust pipe or the exhaust receiver. The exhaust temperature is the average temperature of many portions of exhaust gases that come out from the exhaust valve at various times; whereas the ideal residual-gas temperature is the temperature of the residual gas after it has expanded isentropically to a certain well-defined pressure. The flow of gases through the valve is an irreversible process, and since flow work is done upon the exhaust gas by the gas remaining in the cylinder, the exhaust temperature in its usual sense is, in general, higher than T_r unless there is considerable cooling of the exhaust system.

In actual application, T_r can be calculated from the air capacity and the cylinder pressure at some point during the expansion stroke before the opening of the exhaust valve. This pressure can be obtained from the heavy-spring indicator diagram if such is available. Otherwise, T_r can still be calculated, but less accurately, by an analysis of the fuel-air cycle (reference 12).

Putting equation (37) into equation (36) and simplifying gives

$$(R/m_e)k_eT\ dM = \frac{\sqrt{2k_e}\ \sqrt{k_eRT_r/m_e}\ A_ep_e}{360N}\sqrt{\frac{k}{k-1}\left[\left(\frac{p}{p_e}\right)^{\frac{3k-3}{k}} - \left(\frac{p}{p_e}\right)^{\frac{2k-2}{k}}\right]}\ d\theta \tag{38}$$

Denoting $\sqrt{k_e R T_r / m_e}$ by C_e, which is the velocity of sound in the ideal residual gas, and defining

$$F_e = -\sqrt{\frac{k}{k-1}\left[\left(\frac{p}{p_e}\right)^{\frac{3k-3}{k}} - \left(\frac{p}{p_e}\right)^{\frac{2k-2}{k}}\right]} \tag{39}$$

finally gives

$$-(R/m_e)k_e T\ dM = \frac{\sqrt{2k_e}\ A_e p_e C_e F_e\ d\theta}{360N} \tag{40}$$

By combining equations (34) and (40), dividing the resultant equation through by $p_e V_d$, and using the relations $V_d = A_p S$ and $2SN = s$, as was done in the analysis of the inlet process, equation (28) is again obtained.

$$d\left(\frac{p}{p_e}\frac{V}{V_d}\right) + (k_e - 1)\frac{p}{p_e}\ d\left(\frac{V}{V_d}\right) - \frac{\sqrt{2k_e}}{180}\frac{C_e}{s}\frac{A_e}{A_p}F_e\ d\theta = 0 \tag{28}$$

Equation (28), the equation of the exhaust process, is similar in appearance to equation (25), the equation of the inlet process. It can, of course, also be solved by means of a differential analyzer or by a method of step-by-step calculation.

The most important difference between the equation of the inlet process and the equation of the exhaust process lies in the flow factor F about which the following may be noted:

(1) Theoretically, equation (35) is valid only for steady flow. The flow through the exhaust valve, like the flow through the inlet valve, is unsteady. So, to be theoretically rigorous, it is necessary to derive from Euler's equation another expression for the mass rate of flow instead of equation (35), which is based on Bernoulli's equation. Since the effect of unsteadiness of the flow of gases through engine valves is negligible, the equation for steady flow has been used here for the sake of simplicity.

(2) Although the form of the flow factor for outward flow (equation (39)) is quite similar to that of the flow factor for inward flow (equation (19)) their physical meanings are different. The flow factor for inward flow F_i is proportional to the mass rate of flow per unit area or the mass velocity; whereas according to equation (40) and the relation $d\theta/360N = dt$

$$\dot{F}_e = -\sqrt{\frac{k_e}{2}}\,\frac{R}{m_e}\,\frac{1}{p_e C_e}\,T\left(\frac{1}{A_e}\,\frac{dM}{dt}\right) \tag{41}$$

where the quantities R, k_e, m_e, p_e, and C_e are constants for a given exhaust process and therefore F_e is proportional to the product of the absolute temperature of the cylinder contents T and the mass velocity through the exhaust valve $(1/A_e)(dM/dt)$. In other words, F_e is a measure of the rate of decrease of energy content in the cylinder per unit of effective valve opening area.

(3) The flow factor for outward flow is plotted against p/p_m for different values of k ranging from 1.20 to 1.40 in figure 2. This flow factor is applicable whenever the flow is outward either in the inlet process or in the exhaust process, that is, whenever gases flow out from the cylinder into the inlet port or the exhaust port. In the former case the flow factor is a function of p/p_i, whereas in the latter case it is a function of p/p_e. Therefore the symbol p_m is used to represent either p_i or p_e.

(4) For actual calculation of the inlet or exhaust process the flow factors are plotted in such a way (fig. 2) that the calculator automatically distinguishes between the flow factor for inward flow and the flow factor for outward flow. When p/p_m is less than unity, the flow factor is plotted for inward flow, and when p/p_m is greater than unity the flow factor for outward flow is plotted.

(5) For inward flow at a given inlet pressure p_i, the maximum mass velocity (mass of fluid per unit time per unit valve opening area) is limited by the critical pressure ratio beyond which it ceases to increase and the flow factor F becomes constant. (See fig. 2(b).) The case of outward flow is different. During the exhaust process, at a given exhaust pressure p_e, the mass velocity could increase indefinitely if the upstream pressure (that is, the cylinder pressure p) were increased indefinitely, as will be explained further in appendix C.

(6) As can be seen from equation (39) and figure 2, the flow factor for outward flow is always negative and for inward flow it is always positive. Thus in actual numerical calculations where backflow[3] or valve overlap is involved, no confusion is possible as to the sign of F.

GENERAL EQUATION OF THE INLET AND EXHAUST PROCESSES

Equation (25), the equation of the inlet process, is applicable when only the inlet valve is open and equation (28), the equation of the exhaust process, is applicable when only the exhaust valve is open. For modern high-speed internal-combustion engines, there is always valve overlap to a greater or lesser extent. During the period when both the inlet and the exhaust valves are open, it follows from the same reasoning as used in the previous derivations that

$$d(pV) + (k - 1)p dV = (R/m_i)k_i T_i \, dM_i - (R/m_e)k_e T \, dM_e \tag{42}$$

where dM_i is the mass of fluid flowing through the inlet valve and dM_e is the mass of fluid flowing through the exhaust valve, during the time interval dt. Both dM_i and dM_e may be either positive or negative, depending on whether the flow is a normal one or a backflow. It is true that when dM_i is negative $(k_i/m_i)T_i$ should be replaced by $(k/m)T$, where the subscript i refers to the intake charge and the quantities without subscripts refer to the cylinder contents; when dM_e is negative T should be replaced by T_e, the exhaust temperature. If this were done, however, the actual calculation would be unduly complicated and lengthy. Besides, during the overlap period, T and T_e are as a rule not very different. Thus, by using equation (41), inaccuracy should be expected only when p_i is much lower than p_e (severely throttled operation), the valve overlap period is long, and the engine speed is very low, as the combination of these three conditions contributes to serious backflow through the inlet valve.

Another question arises as to whether k_i or k_e should be used in conjunction with the $p\,dV$ term, where k is the ratio of specific heats of the cylinder contents and strictly speaking a variable depending on the composition and the temperature of the cylinder contents. A study in regard

---

[3]The term "backflow" is used here to describe the type of flow the direction of which is opposite to the normal one. Thus, during the inlet process, if gases flow out of the cylinder into the inlet port, it is a backflow; whereas during the exhaust process, if gases flow back from the exhaust port into the cylinder, it is a backflow.

to the effect of variations in k was made, and it was decided that such refinement is unnecessary for practical purposes. Thus, for the inlet process, even with valve overlap, k_i will be used; and for the exhaust process, k_e will be used.

Now if equation (42) is treated mathematically in the same way as the equations of the inlet and exhaust processes, there is obtained

$$d\left(\frac{p}{p_i}\frac{V}{V_d}\right) + (k_i - 1)\frac{p}{p_i}d\left(\frac{V}{V_d}\right) - \frac{\sqrt{2k_i}}{180}\frac{C_i}{s}\frac{A_i}{A_p}F_i\,d\theta$$

$$- \frac{\sqrt{2k_e}}{180}\frac{p_e}{p_i}\frac{C_e}{s}\frac{A_e}{A_p}F_e\,d\theta = 0 \qquad (43)$$

which is applicable to the inlet process during the overlap period.

Equations (25), (28), and (43) have the same general form and may be represented by the following general equation:

$$d\left(\frac{p}{p_m}\frac{V}{V_d}\right) + A\frac{p}{p_m}d\left(\frac{V}{V_d}\right) - B\frac{A_i}{A_p}F_i\,d\theta - C\frac{A_e}{A_p}F_e\,d\theta = 0 \qquad (44)$$

where

p cylinder pressure

p_m either inlet pressure p_i or exhaust pressure p_e

V cylinder volume

V_d piston displacement volume

θ crank angle, degrees

A_i effective inlet-valve opening area

A_e effective exhaust-valve opening area

F_i flow factor for inlet valve, a function[4] of p/p_i

F_e flow factor for exhaust valve, a function[4] of p/p_e

A,B,C constants which are defined in the following table

	Inlet process	Exhaust process	Inlet process, including over-lap period
p_m =	p_i	p_e	p_i
A =	$k_i - 1$	$k_e - 1$	$k_i - 1$
B =	$\frac{\sqrt{2k_i}}{180} \frac{c_i}{s}$	0	$\frac{\sqrt{2k_i}}{180} \frac{c_i}{s}$
C =	0	$\frac{\sqrt{2k_e}}{180} \frac{c_e}{s}$	$\frac{\sqrt{2k_e}}{180} \frac{p_e}{p_i} \frac{c_e}{s}$

Equation (44) is the general equation of the inlet and exhaust processes. It is convenient to use when many inlet processes, with or without valve overlap, and exhaust processes are to be solved. It is especially convenient when the solutions are to be obtained on a differential analyzer, since only one setup of the connections on the analyzer is necessary for all cases, with changes only in the constants and in the numerical ranges of the different quantities.

---

[4]The function is represented by the curves in figure 2. Note that the meanings of F_i and F_e here are slightly different from those in footnote 1. The old definitions were made for the sake of clarity in the derivation of the equations. In actual application, since the flow through both the inlet and the exhaust valves may be either inward or outward, it is much more convenient to identify the flow factors with the valves rather than with the directions of flow. Thus for the inlet valve, F_i is a function of p/p_i; whereas for the exhaust valve, F_e is a function of p/p_e. Thus both F_i and F_e are plus when the flow is inward and minus when the flow is outward.

NUMERICAL CALCULATIONS – INDICATOR DIAGRAMS AND VOLUMETRIC EFFICIENCIES

In order to solve equation (44), it is necessary to know the conditions at the starting point, the pressure p_m, the constants A, B, and C, and the relations of V/V_d, A_i/A_p, and A_e/A_p against θ. These factors will be discussed as follows.

Initial conditions.– Integration of equation (44) may be started at any point during the inlet or exhaust process, but it is convenient to start the inlet process at the point of inlet-valve opening and the exhaust process at the point of exhaust-valve opening. Let the crank angle at such a point be designated by θ_o. Then the cylinder volume V_o corresponding to θ_o can be easily determined from the geometry of the engine. The initial cylinder pressure p_o for the exhaust process can be estimated by an analysis of the fuel-air cycle starting with an assumed volumetric efficiency. Judgment is to be used in this respect because the actual pressure is likely to be lower than the fuel-air cycle pressure.

The initial cylinder pressure for the inlet process can be obtained from the solution of the corresponding exhaust process, but when an inlet process is to be solved alone without solving the corresponding exhaust process, p_o may be taken as equal to the exhaust pressure p_e for low-to-medium engine speed with adequate exhaust-valve size and adequate exhaust-valve opening duration. For medium-to-high engine speed with small exhaust-valve size or with short exhaust-valve opening duration, p_o may be as high as 3 pounds per square inch above p_e. In some exceptional cases where high engine speed, short exhaust-valve opening duration, large A_i/A_e ratio, and large p_i/p_e ratio are combined, the blow-down of exhaust gases (during which the cylinder pressure drops very rapidly) may never be complete and p_o of the inlet process may be much higher than p_e. In such cases p_o is best obtained by solving the exhaust process preceding the inlet process.

It will be shown later that any reasonable error in estimating p_o, either of the inlet or of the exhaust process, has no appreciable effect on pressures at the end of the process or on volumetric efficiency. Thus it is not necessary to repeat any solutions unless the estimate of p_o is very far off.

Pressure p_m.– This pressure is equal to the inlet pressure p_i for the inlet process and to the exhaust pressure p_e for the exhaust process (see preceding table).

Constant A.– This constant is equal to $k_i - 1$ for the inlet process and $k_e - 1$ for the exhaust process. A curve of k_i against percentage of theoretical fuel (gasoline) is shown in figure 3; k_e, unfortunately, cannot be determined so easily and accurately as k_i. In most cases, however, a value of 1.25 for k_e is adequate. In a study where k_e is changed from 1.25 to 1.30 and the same solution repeated, it was found that the difference caused by this change is very small (reference 9).

Constant B.– This constant is equal to $\left(\sqrt{2k_i}/180\right)\left(C_i/s\right)$ for the inlet process. It vanishes for the exhaust process.

The quantity k_i can be read from figure 3; s is the mean piston speed of the engine at which the solution is desired; C_i is the velocity of sound in the intake mixture and is equal to $\sqrt{k_iRT_i/m_i}$ where R is the universal gas constant, m_i the molecular mass of the intake mixture, and T_i the absolute inlet temperature. The terms C_i and s, of course, should be in the same units.

Constant C.– This constant is equal to $\left(\sqrt{2k_e}/180\right)\left(C_e/s\right)$ for the exhaust process or $\left(\sqrt{2k_e}/180\right)\left(p_e/p_i\right)\left(C_e/s\right)$ for the overlap period of the inlet process. It vanishes during the main part of the inlet process when only the inlet valve is open.

As before, k_e may be taken equal to 1.25. The inlet pressure p_i, exhaust pressure p_e, and piston speed s are known quantities for a given solution. The velocity of sound in the ideal residual gas C_e is equal to $\sqrt{k_eRT_r/m_e}$, where R is the universal gas constant, m_e the molecular mass of the exhaust gas, and T_r the ideal residual-gas temperature.

The quantity T_r is obtained as follows: If the actual indicator diagram is available, the cylinder pressure at some point during the expansion stroke before the exhaust valve opens may be measured from the diagram. With a knowledge of the air consumption per stroke of the cylinder and the cylinder volume at the point where the pressure is measured, the corresponding temperature may be obtained from a suitable thermodynamic chart for combustion products (references 1 and 12). Then expansion along a constant-entropy line to the exhaust pressure p_e gives T_r. If there is no actual indicator diagram to begin with, as is very often the case, T_r could be estimated by analyzing the fuel-air cycle (references 1 and 12) in which the volumetric efficiency has to be assumed. An engineer experienced in internal-combustion-engine cycles, however, can estimate T_r pretty accurately without going through the entire fuel-air cycle.

As C_e is proportional to the square root of T_r a small percentage error in T_r will be approximately halved in the constant C.

<u>V/V_d against θ</u>.- For ordinary engines in which the crank-connecting-rod mechanism is used, the ratio of cylinder volume to displacement volume at any crank angle can always be closely approximated by the following relation

$$V/V_d = a - (1/2) \cos \theta - b \cos 2\theta \tag{45}$$

where

$$a = \frac{1}{r-1} + \frac{1}{2}\left[1 + \frac{1}{4}\left(\frac{R}{L}\right) + \frac{3}{64}\left(\frac{R}{L}\right)^3 + \frac{5}{256}\left(\frac{R}{L}\right)^5 + \ldots\right]$$

$$b = \frac{1}{8}\left(\frac{R}{L}\right) + \frac{1}{32}\left(\frac{R}{L}\right)^3 + \frac{15}{1024}\left(\frac{R}{L}\right)^5 + \ldots$$

r compression ratio

R crank radius

L length of connecting rod

θ crank angle

The constants a and b converge very quickly, as the ratio R/L is usually small.

A_i/A_p against θ.— Here A_i is the effective inlet-valve opening area and is equal to the actual valve opening area multiplied by the flow coefficient. The flow coefficients at various valve lifts are obtained by means of a model test under steady-flow conditions with a small pressure drop (say 10 in. of alcohol) across the valve. The flow coefficients are calculated from the test data according to the procedures in reference 14 and the flow-test apparatus used for determining the flow coefficients in this report is described in references 15 and 16.

The use of steady-flow coefficients is allowable because the effect due to the unsteadiness of flow through the valves is neglected anyway.

A_e/A_p against θ.— This ratio is obtained in the same way as in the preceding case.

In reference 9 several inlet and exhaust processes of two different engines[5] are solved and the calculated and experimental results agree well. In the present report, a large number of solutions covering three different engines and a wide range of the different variables, as outlined in the INTRODUCTION, will be recorded.

---

[5]These engines were a CFR engine and an experimental engine consisting of a Cyclone G-200 cylinder mounted on a universal test crankcase. Both engines were tested at the Sloan Laboratories, M.I.T.

Data for Solutions

CFR engine

Bore, in.	3.25
Stroke, in.	4.50
Compression ratio	4.92
$\frac{\text{Crank radius}}{\text{Length of connecting rod}}$	0.225

$$\frac{V}{V_d} = 0.7835 - 0.5000 \cos \theta - 0.0285 \cos 2\theta$$

Inlet valve: Two combinations – large valve with large lift, and small valve with small lift

Large-valve diameter, in.	1.050
Large lift, in.	0.262
Small-valve diameter, in.	0.830
Small lift, in.	0.208

Exhaust valve

Diameter, in.	1.344
Maximum lift, in.	0.277

Valve timing: 7 different timings. (See fig. 4.)

Inlet and exhaust pressures: Four combinations.

p_i (in. Hg abs.)	p_e (in. Hg abs.)	p_i/p_e
20	40	0.5
30	30	1
40	20	2
40	10	4

Inlet temperature, T_i, $^{\circ}R$	580
Fuel-air ratio	0.078

CFR engine tests were made at the Sloan Laboratories, Massachusetts Institute of Technology, and reported in reference 16, except for the series where $p_i/p_e = 0.5$. This reference also gives a detailed description of the test setup.

The data for the CFR engine solutions in this report were prepared before the tests were started and the theoretical and experimental results were obtained independently of each other.

Inlet-exhaust engine

Engine: Pratt & Whitney Wasp, Jr., cylinder (R-985) mounted on a special crankcase

Bore, in.	$5\frac{3}{16}$
Stroke, in.	$5\frac{1}{2}$
Compression ratio	5.5
$\frac{\text{Crank radius}}{\text{Length of connecting rod}}$	0.2562

$$\frac{V}{V_d} = 0.7546 - 0.5000 \cos \theta - 0.0325 \cos 2\theta$$

Inlet- and exhaust-valve sizes, lifts and timing: (See table I.)

Inlet pressure, p_i, in. Hg abs.	33
Exhaust pressure, p_e, in. Hg abs.	33
Inlet temperature, T_i, $^{\circ}R$	580
Fuel-air ratio	0.075

This engine was used at the Sloan Laboratories, Massachusetts Institute of Technology, in a study of the effect of changing the ratio of exhaust-valve flow capacity[6] to inlet-valve flow capacity on volumetric efficiency and power output. Hence it will be referred to in this report as the inlet-exhaust engine. A description of the test setup and the test results are given in reference 17.

[6]Flow capacity is defined as the product of the square of the valve diameter and the average flow coefficient over the entire valve-opening period.

Bore-stroke engine

Engine: Liquid-cooled Lycoming cylinder mounted on a heavy crankcase

Bore, in.	5.25
Stroke, in.	4.25, 5.25, and 6.25
Compression ratio	6.0
$\dfrac{\text{Crank radius}}{\text{Length of connecting rod}}$	0.25

$$\frac{V}{V_d} = 0.7316 - 0.5000 \cos \theta - 0.0318 \cos 2\theta$$

Inlet- and exhaust-valve data: (See figs. 5 and 6.)

Inlet pressure, p_i, in. Hg abs.	27.4, 40, and 50
Exhaust pressure, p_e, in. Hg abs.	31.4
Inlet temperature, T_i, $^{\circ}R$	580
Fuel-air ratio	0.075

This engine was used at the Sloan Laboratories, Massachusetts Institute of Technology, in a study of the effect of changing the bore-stroke ratio on air capacity, power output, and detonation. Hence, it will be referred to in this report as the bore-stroke engine. A description of the test setup and the test results are given in reference 18.

A list of the initial conditions, constants, and curve numbers for A_i/A_p against θ and A_e/A_p against θ for all solutions is given in table II.

Calculations

Most of the solutions, for which the data are listed in table II, were obtained by means of the electrical differential analyzer at the Massachusetts Institute of Technology, although about one-third of them were solved by a method of step-by-step calculation. Eight solutions were made by both methods, and the results are substantially identical.

Results

The results are presented in table III and figure 7, which compare the calculated and measured volumetric efficiencies; and table IV, which compares the calculated and measured indicator diagrams.

Other volumetric-efficiency curves are plotted in figures 8 to 12 and indicator diagrams are plotted in figures 13 to 47.

DISCUSSION OF RESULTS

During the inlet process, the cylinder contents change from pure residual gas at the beginning of the process to a mixture of residual gas and increasing quantities of fresh charge. The cylinder temperature decreases as more and more fresh charge is admitted. Therefore the value k (ratio of specific heats) of the cylinder contents changes accordingly. Solutions 1 to 6 were made to study the effect of changing k. For residual gas at 2500° R, k is about 1.270, whereas for a gasoline-air mixture with a fuel-air ratio of 0.078 k is 1.346 according to figure 3. In solutions 1 to 6 four different values of k ranging from 1.270 to 1.346 and two engine speeds (2000 and 3600 rpm) were used. The corresponding test data on a CFR engine were taken from reference 15. A comparison of the calculated and measured volumetric efficiencies and indicator diagrams showed that the two low values of k did not give satisfactory agreement, as expected; whereas the two high values of k gave about equally good agreement, with the value 1.346 being slightly superior. Therefore it was decided that for all the subsequent solutions, k_i would be taken as 1.346 for a gasoline-air ratio of 0.078; and for other fuel-air ratios, k_i would be read directly from figure 3.

Since the possibility always exists that the estimated initial pressure p_o may be in error, a study was made to determine the effect of varying p_o on the solution as a whole. Five exhaust solutions (solutions 39 to 43) and four inlet solutions (solutions 44 to 47) were made with p_o as the only variable. The results are plotted in figures 9, 13, and 14. It can be seen that wide variations in p_o affect the cylinder pressures only during the initial period of the solution, and cylinder pressures during most of the process (either inlet or exhaust) are not affected at all. Figure 9 shows that high p_o results in lower calculated volumetric efficiency, but the effect is very small. It is therefore concluded that any ordinary inaccuracy in estimating p_o is unimportant.

From equation (44) and the definition of the constants, B and C, it may be noted that for the inlet process the effect of decreasing the piston speed s is the same as that of increasing the velocity of sound C_i (which is proportional to the square root of the inlet temperature T_i) or as that of increasing the size of the inlet valve relative to the piston. For the exhaust process, the effect of decreasing s is the same as that of increasing C_e (which is proportional to the square root of the ideal residual-gas temperature T_r) or as that of increasing the relative size of the exhaust valve to the piston.

Therefore, these three variables $\left(1/s, \sqrt{T_i}\right.$ or $\sqrt{T_r}$, A_i/A_p or $\left.A_e/A_p\right)$ need not be studied separately, as the effect of varying one is the same as that of varying either of the other two variables. In solutions 48 to 52, inclusive, the constant B was varied. The results are plotted in figure 8. Although the abscissa of figure 8 is labeled engine speed, it can be easily translated into an inlet-temperature scale or a valve-size scale.

In solutions 53 to 57 the exhaust pressure p_e is kept constant at 15 pounds per square inch absolute and the inlet pressure p_i is varied. The calculated volumetric efficiencies are plotted in figure 10. In solutions 58 to 61 p_i is held constant at 15 pounds per square inch absolute and p_e is varied. The calculated volumetric efficiencies are plotted in figure 11. The results in figures 10 and 11 are further combined and plotted against p_i/p_e in figure 12(a) and against p_e/p_i in figure 12(b). The fact that the points fall on a smooth curve indicates that volumetric efficiency is a function of the ratio p_i/p_e, regardless of the individual level of either p_i or p_e. Figure 12 also contains curves representing the equation

$$e_v = 1 + \frac{1 - (p_e/p_i)}{k_i(r - 1)} \tag{46}$$

where r is the compression ratio of the cylinder. This equation, suggested by Prof. Edward S. Taylor of the Massachusetts Institute of Technology (reference 16), is based on the assumptions that valve events occur at dead centers and that the cylinder pressure is equal to p_i during the entire inlet process and equal to p_e during the entire exhaust process. It gives results approximating fairly well those from the more exact theory and is convenient to use when a quick estimate of the ratio of volumetric efficiencies at two different p_i/p_e ratios is desired.

In figure 12 are also shown a few experimental points which were obtained on the CFR engine at 2500 rpm with cam 2, large valve and large lift. The inlet and exhaust pressures were:

p_i (in. Hg abs.)	p_e (in. Hg abs.)	p_i/p_e	p_e/p_i
30	30	1	1
40	20	2	.5
40	10	4	.25

Although these points are not sufficient to give an over-all comparison with the curves in figure 12, it may at least be added that the shape of the theoretical curves is typical of those obtained in actual engine operations where the p_i/p_e ratio is varied.

Some inlet-process solutions were made wherein the effect of valve overlap was arbitrarily omitted, that is, the exhaust valve was arbitrarily assumed to shut abruptly and completely at the point of inlet-valve opening. (See figs. 17, 22, and 24 to 26.) The purpose was to determine the effects caused by valve overlap and to ascertain under what circumstances the calculation might be simplified by neglecting valve overlap without introducing appreciable error. The calculated indicator diagrams (dashed curves) in figures 17, 22, and 24 to 26, however, show that by neglecting valve overlap, the cylinder pressures are seriously in error during the overlap period. The calculated volumetric efficiencies are also inaccurate when the effect of overlap is omitted. It is therefore recommended that valve overlap should be considered in calculations unless the overlap period is very short (such as cams 4, 5, and 6 in fig. 4).

In table III and figure 7, an over-all comparison of the calculated and measured volumetric efficiencies is shown. Another comparison of volumetric efficiencies is shown in figures 8 and 28 to 31. In figure 7, the solid line is a 45° line, whereas the dashed line represents theory 5 percent higher than measurement. The dashed line seems to be more representative of all the points than the solid line, although there are a few points too far below the line and a few too far above the line. The former group consists of solutions 9 and 16, which are both for a p_i/p_e ratio of 0.5, valve overlap of 60°, and piston speed of 1500 feet per minute on the CFR engine. These conditions cause considerable backflow through the inlet valve during the overlap period, and therefore inaccuracy in the theoretical volumetric efficiencies is to be expected. Solutions 27, 28, 30, and 31 are also for $p_i/p_e = 0.5$ and an even greater valve-overlap period of 90°. The calculated volumetric efficiencies are negative for solutions 28 and 30, 0.246 for solution 27, and 0.366 for solution 31. The CFR engine would not operate under these conditions and therefore for these four solutions no points were plotted in figure 7. In the other group of points are solutions 11, 12, and 29. These are all for a high p_i/p_e ratio (4) and a low piston speed (375 ft/min) on the CFR engine. The overlap period is 60° for solutions 11 and 12 and 90° for solution 29. Under these circumstances, during the overlap period some of the fresh charge which comes in through the inlet valve immediately goes out through the exhaust valve, carrying some residual gas with it. This process may be called "short-circuiting." In equation (42), the temperature of the cylinder contents T is defined by equation (37), but during the period of short-circuit flow, this definition of T evidently is no longer true. Inaccuracy in the calculated volumetric efficiency is therefore encountered when high p_i/p_e ratio, long valve-overlap period, and low engine speed are combined to cause serious short-circuit flow. It may be pointed out that high p_i/p_e ratio alone does not necessarily lead to poor agreement between calculated and measured volumetric efficiencies. Thus solutions 10, 22, and 23 are also for a p_i/p_e ratio of 4. In solution 10, although the valve-overlap period is 60°, the relatively high piston speed (1500 ft/min) prevents much short-circuiting. Although the piston speed is only 375 feet per minute, the valve-overlap period for solutions 22 and 23 is very short (6°) and prevents much short-circuiting. Thus, the agreement between calculated and measured volumetric efficiencies for solutions 10, 22, and 23 is much better than for solutions 11, 12, and 29.

On the whole, it appears that the calculated volumetric efficiency averages 5 percent higher than the measured value, although there are a few cases for which the calculated values are lower. This discrepancy is believed to be the combined result of several approximations used in the theory, such as (1) the approximations involved during the short-circuiting and backflow periods, (2) neglecting the acceleration of the gas columns ahead of the valves (first term of equation (16)), (3) the fact that the flow coefficients for the valves were obtained under steady-flow conditions with very small pressure drop across the valves, whereas under actual operating conditions the flow is unsteady and the pressure drop is sometimes much larger than that used in obtaining the flow coefficients, (4) inaccuracies in the estimation of the initial pressure p_o and the ideal residual-gas temperature T_r, (5) the assumption that the ratio of specific heats k of the cylinder contents is constant during the inlet process, and (6) the effect of heat transfer during the inlet process. The effect of heat transfer, although small, may make itself felt in the calculated volumetric efficiencies of some of the solutions in which the piston speed is very low. It is believed that none of these approximations alone could possibly cause an error of 5 percent, but the combination of some or all of them conceivably might.

The degree of agreement between calculated and measured indicator diagrams is given in table IV. For most diagrams the agreement is good, for some it is good except for an apparent shift in the point of zero pressure, and for the others it is not so good. Representative diagrams in each class are reproduced in figures 15 to 27 and 32 to 47.

In general, the agreement between actual and theoretical indicator diagrams of the exhaust processes is excellent and much better than for the inlet processes because (1) the initial pressure p_o for the exhaust processes was always measured from the experimental indicator diagrams and the ideal residual-gas temperature T_r was obtained from the experimental diagrams (by a method outlined under NUMERICAL CALCULATIONS, Constant C), (2) for most exhaust processes there is no back-flow and even when there is, it occurs at the very end of the process and therefore the main part of the solution is not affected, and (3) the ordinate scale of the exhaust diagrams in pressure units (lb/sq in.) per inch is much larger than that of the inlet diagrams; hence any difference between calculated and measured pressures is not so conspicuous as in the inlet diagrams.

Many diagrams would be in close agreement were it not for an approximately constant difference between the calculated and measured pressures. This difference is attributed to a zero shift in the atmospheric line of the experimental indicator diagrams. The experimental diagrams were taken with the Massachusetts Institute of Technology balanced-pressure, point-by-point indicator (reference 8) which users at Sloan Laboratories, Massachusetts Institute of Technology, believe sometimes gives inaccurate atmospheric lines. This belief is further substantiated by the diagrams for solutions 77 and 82.1 (figs. 23 and 25, respectively) in both of which the measured cylinder pressure during the inlet process is always higher than the inlet pressure p_i, which is physically impossible. In the diagram for solution 16 (fig. 16), the starting point p_o of the measured curve is lower than p_e. This is also impossible since on the CFR engine there is no evidence of pressure oscillation in the inlet and exhaust pipes and hence the cylinder pressure at the point of inlet-valve opening could not be lower than the exhaust pressure p_e. It is therefore probable that this type of error (constant difference between calculated and measured pressures) lies in the measured rather than in the calculated diagram. The exhaust diagrams are measured partly from the heavy-spring experimental indicator diagram and partly from the light-spring diagram. Thus, in the diagram for solution 63 (fig. 21), it appears that the light-spring part has a zero shift.

Two measured diagrams obtained on two different dates but presumably under the same operating conditions are shown in figure 15 (solution 11). It can be seen that the difference between the two measured diagrams is as much as that between the theoretical and measured diagrams.

A few diagrams have a discontinuity in the measured curve. (See fig. 16.) This obviously should not happen and its existence must be due to some imperfection in the functioning of the indicator.

In some of the inlet-process diagrams the estimated initial pressure p_o is too low (figs. 17 and 19). The worst cases in this category are solutions 17 and 35, which are both for large inlet valve with large lift, $p_i/p_e = 2$, and high engine speed. It is believed that when the inlet valve opens under these conditions the cylinder pressure is considerably above p_e because of the comparatively large mass of gases inside the cylinder when the exhaust valve opens and because of the comparatively short time during which the exhaust valve remains open. The mass is large because the inlet valve and lift are large and p_i is high; and the time is short because the engine speed is high. It is regrettable that this fact was not foreseen when the data were being prepared for solution. It became apparent only when the results were known. It is recommended that for solutions of this nature, p_o be obtained by a complete analysis of the corresponding exhaust processes.

In another category the poor agreement between the calculated and measured diagrams is believed to be due to the combination of low estimated p_o and a zero shift of the atmospheric line in the measured diagram. This fact is evident from the shape of the curves in figures 18 and 20.

In the case of the bore-stroke engine, the agreement of indicator diagrams is not very good for either the inlet or the exhaust processes (figs. 26 and 27). This is believed to be due to the use of inlet and exhaust pipes each 2 inches in diameter and about 1 foot in length. In the other two engines, the inlet and exhaust pipes were very large and short and carefully rounded at the connections. The assumption that the poor agreement is caused by pipes is substantiated by two things: (1) unpublished data at the Sloan Laboratories, Massachusetts Institute of Technology, show that if the pipes on the bore-stroke engine were enlarged without changing their lengths, the volumetric efficiency of the engine dropped about 2 percent; and (2) the shape of the measured diagram in figure 26 is typical of those where vibration is set up in the inlet pipe (reference 19). In the theory it has been assumed that the conditions upstream of the inlet valve and downstream of the exhaust valve are constant. This is approximated in practice when very short inlet and exhaust pipes are used and when the inlet pressure p_i, temperature T_i, and exhaust pressure p_e are held constant and measured in adequately large surge tanks. In the experimental work on the CFR and inlet-exhaust engines these conditions were fulfilled. In the case of the bore-stroke engine, the inlet and exhaust pipes were longer and smaller than desired.

A correlation of volumetric efficiencies is attempted in appendix D.

CONCLUSIONS

1. The trends of volumetric efficiency predicted by the theory are correct, except when the p_i/p_e ratio is far from 1, the valve-overlap period is long, and the piston speed is low.

2. Owing to several approximations used in the theory, the volumetric efficiencies calculated from the theory are on the average 5 percent too high.

3. Except for the bore-stroke engine, the agreement between calculated and measured indicator diagrams seems to be within the precision of the measuring indicator, with indications that in some cases the calculated pressures are more accurate. In the case of the bore-stroke engine, the failure of the indicator diagrams to agree is probably due to dynamic disturbances set up in the inlet and exhaust pipes.

4. Ordinary inaccuracies in estimating the initial pressure p_o of either an inlet or an exhaust solution affect only the first part of the calculated indicator diagram. Variations in p_o of as much as 4 pounds per square inch for an inlet solution and as much as 20 pounds per square inch for an exhaust solution still give indicator diagrams which converge quite rapidly. The effect of varying p_o on calculated volumetric efficiency is small.

5. Reasonable inaccuracies in estimating the ideal residual-gas temperature T_r are unimportant.

6. In varying the inlet pressure p_i and the exhaust pressure p_e with other things kept constant, the volumetric efficiency depends on the ratio p_i/p_e, irrespective of the individual levels of either p_i or p_e.

7. For the inlet process, the effect of decreasing the piston speed s is the same as that of increasing the relative size of the inlet valve to the piston (that is, A_i/A_p) or as that of increasing the velocity of sound in the intake charge c_i.

8. For the exhaust process, the effect of decreasing the piston speed s is the same as that of increasing the relative size of the exhaust valve to the piston (that is, A_e/A_p) or as that of increasing the velocity of sound in the ideal residual gas c_e.

9. For the inlet process, the use of k (ratio of specific heats) for the intake charge to replace the actual variable k of the cylinder contents gives satisfactory results. Results are unsatisfactory if k is taken equal to or nearly equal to that for the residual gas in the cylinder at the beginning of the inlet process.

10. With the aid of this theory, it is possible to predict the volumetric efficiencies and indicator diagrams for the inlet and exhaust processes even before the actual engine is built, provided the flow

coefficients of the valves can be obtained on a model. It is also possible to calculate some hypothetical inlet or exhaust processes which are impossible to obtain on actual engines, such as the cases where the valves open and close instantaneously.

11. The theory in this report is applicable not only to the pumping process of internal-combustion engines but also to reciprocating compressors or vacuum pumps in which the working medium is a gaseous substance.

Sloan Laboratories for Aircraft and Automotive Engines
Massachusetts Institute of Technology
Cambridge, Mass., October 2, 1945

APPENDIX A

SYMBOLS

A,B,C	constants
A_e	effective exhaust-valve opening area
A_i	effective inlet-valve opening area
A_p	piston area
C_1,C_2	constants
c_e	velocity of sound in ideal residual gas
c_i	velocity of sound in intake mixture
c_p	mean specific heat at constant pressure, assumed constant
c_v	mean specific heat at constant volume, assumed constant
c_x	velocity of sound at station x
E	internal energy of cylinder contents
e_v	volumetric efficiency
F_e	flow factor for outward flow
F_i	flow factor for inward flow
F_s	flow factor for sonic flow
f	fuel-air ratio
H	enthalpy
k	ratio of specific heats (c_p/c_v)
L	length of connecting rod
M	mass of cylinder contents
M_a	mass of air

M_t	total mass of air plus fuel
m	molecular mass of gas
N	number of revolutions per unit time
p	cylinder pressure
p_e	exhaust pressure
p_i	inlet pressure
p_m	either p_e or p_i
p_o	initial cylinder pressure
Q	total heat
R	universal gas constant
r	compression ratio of cylinder
S	stroke
s	mean piston speed
T	absolute temperature of cylinder contents
T_r	absolute temperature of ideal residual gas
t	time
u	velocity along streamline C
u_x	velocity of flow at any station x
V	cylinder volume
V_d	piston displacement
V_o	cylinder volume corresponding to θ_o
w	velocity field
ρ	density of fluid
θ	crank angle

θ_c crank angle at which valve is completely closed

θ_o crank angle at which valve opens

Subscripts:

1 upstream station where velocity of flow is negligible (see fig. 1(a))

av average

cr critical

e exhaust

i inlet; station upstream of inlet valve where pressure and temperature are sensibly constant and where velocity of flow of intake charge is considerably lower than that through valve (see fig. 1(a)).

APPENDIX B

STEADY AND UNSTEADY FLOW OF A GAS

It has been pointed out (under EQUATION OF THE INLET PROCESS) that the difference between steady and unsteady flows is the term $\int_c \frac{\partial u}{\partial t} dx$. This term will now be approximately evaluated in the case of flow through valves.

If the density ρ of the fluid is assumed to be constant, the equation of continuity calls for

$$Au = A_1 u_1$$

where

A area of equipotential surface at distance x from valve

u velocity of flow at distance x from valve

A_1 effective valve opening area

u_1 velocity of flow through valve

Therefore
$$u = (A_1/A)u_1 = f(x)u_1$$

$$\frac{\partial u}{\partial t} = \frac{du_1}{dt} f(x)$$

and
$$\int_c \frac{\partial u}{\partial t} dx = \frac{du_1}{dt} \int_c f(x)\, dx \tag{47}$$

The integral $\int_c f(x)\, dx$ has the dimension of length.

In order to integrate equation (47) the flow pattern (potential function) must be known. In its absence the integration can be carried out only approximately.

The flow toward an engine valve may be treated similarly as that toward a "sink." This is at least very nearly true at large distances from the valve. According to this assumption the equipotential surfaces at large distances are semispherical.

Let a represent the equivalent radius of the inlet-valve opening and assume equipotential surfaces to be semispherical at distances greater than 10a from the valve; then

$$A = 2\pi(ya)^2 \quad \text{for} \quad 10 < y < \infty$$

where ya is the distance from the inlet port $(= x)$; y is a nondimensional quantity.

Another expression for A is required for $0 < y < 10$. It is known that when $y = 0$, $A = \pi a^2$; and when $y = 10$, $A = 200\pi a^2$; and if A is plotted against y, the two curves (one for $0 < y < 10$ and the other for $10 < y < \infty$) must be tangent to each other at $y = 10$. These conditions can be satisfied by the simple quadratic equation

$$A = \pi a^2\left(1 - 0.2y + 2.01y^2\right) \quad \text{for} \quad 0 < y < 10$$

which, from a theoretical point of view, may of course be in error but is satisfactory to use as a first approximation.

$$\int_c f\ (x)\ dx = \int_c (A_1/A)\ dx = \int_c (A_1/A)a\ dy$$

Now

$$A = \pi a^2\left(1 - 0.2y + 2.01y^2\right) \quad \text{for} \quad 0 < y < 10$$

$$A = 2\pi a^2\ y^2 \qquad \text{for } 10 < y < \infty$$

and

$$A_1 = (A)_{y=0} = \pi a^2$$

therefore

$$\int_c \frac{A_1}{A} a\ dy = \int_0^{10} \frac{a\ dy}{1 - 0.2y + 2.01y^2} + \int_{10}^{\infty} \frac{a\ dy}{2y^2}$$

$$\int_0^{10} \frac{a\ dy}{1 - 0.2y + 2.01y^2} = \frac{2a}{\sqrt{8}}\left[\tan^{-1}\frac{4.02y - 0.2}{\sqrt{8}}\right]_0^{10}$$

$$= \frac{2a}{\sqrt{8}}\left[\tan^{-1}\left(40/\sqrt{8}\right) - \tan^{-1}\left(-0.2/\sqrt{8}\right)\right]$$

$$= 0.707(1.50 + 0.07)a$$

$$= 1.11a$$

$$\int_{10}^{\infty} \frac{a\ dy}{2y^2} = \frac{a}{2}\left[-\frac{1}{y}\right]_{10}^{\infty} = \frac{a}{20} = 0.05a$$

and thus

$$\int_c \frac{\partial u}{\partial t}\ dx = \frac{du_1}{dt}(1.11 + 0.05)a$$

$$= 1.16a\left(du_1/dt\right) \tag{48}$$

If the point of tangency is assumed to be at $y = 20$ instead of at $y = 10$ and the foregoing calculation is repeated

$$\int(\partial u/\partial t)\ dx = 1.14a\ \left(du_1/dt\right) \tag{48a}$$

The next step is to examine the size of the term $\int(\partial u/\partial t)\ dx$ as compared with $u_1{}^2/2$ in equation (16). From equation (20) it is seen that

$$A_i p_i F_i\ \sqrt{2m_i/RT_i} = dM/dt = \rho_1 u_1 A_1$$

therefore

$$u_1 = \frac{F_i p_i}{\rho_1}\sqrt{\frac{2m_i}{RT_i}} \tag{49}$$

When it is considered that $\rho_1/\rho_i = (p/p_i)^{\frac{1}{k}}$, the velocity u_1 or the velocity ratio u_1/C_i can be calculated from equation (49), the pressure ratio p/p_i, and the flow factor F_i at different crank angles obtained in the solution. From a curve of u_1/C_i against crank angle it is possible by measuring the slope of the curve to obtain

$$\frac{d}{d\theta}\left(\frac{u_1}{C_i}\right)$$

from which it is easy to get du_1/dt. Substitution of this into equation (48) immediately results in the integral $\int(\partial u/\partial t)dx$; the radius a is calculated from the effective valve opening area A_i by means of the relation $a = \sqrt{A_i/\pi}$. Then the ratio of $\int(\partial u/\partial t)\,dx$ to $u_1^2/2$ is readily obtained.

This has been done for one actual case in reference 9 and it was found that this ratio was 0.114 at $\theta = 30^\circ$, 0.015 at $\theta = 60^\circ$, and 0.008 at $\theta = 180^\circ$ A.T.C. This ratio therefore is very small for most of the inlet process. Its magnitude is comparatively large during only the first 10° or 20° after the valve opens when the velocity of flow through the valve is still low but its acceleration is high. As far as the whole inlet process is concerned, it seems safe to neglect the term $\int(\partial u/\partial t)\,dx$ in equation (16), which is thus simplified to Bernoulli's equation.

Although the foregoing discussion and the computation of the ratio of $\int(\partial u/\partial t)\,dx$ to $u_1^2/2$ are based on the inlet process, it is not difficult to see that the conclusion is also valid for the exhaust process. In other words, the effect of unsteadiness of flow through the exhaust valve can also be neglected.

APPENDIX C

DISCUSSION OF THE FLOW FACTOR FOR OUTWARD FLOW

It has been mentioned in the text that for inward flow through the inlet valve, the mass velocity (mass of fluid per unit time per unit area) is

$$\frac{1}{A_i}\frac{dM}{dt} = p_i\sqrt{\frac{2m_i}{RT_i}\frac{k}{k-1}\left[\left(\frac{p}{p_i}\right)^{\frac{2}{k}} - \left(\frac{p}{p_i}\right)^{\frac{k+1}{k}}\right]} \tag{18}$$

and for outward flow through the exhaust valve, the mass velocity is

$$\frac{1}{A_e}\frac{dM}{dt} = p\sqrt{\frac{2m_e}{RT}\frac{k}{k-1}\left[\left(\frac{p_e}{p}\right)^{\frac{2}{k}} - \left(\frac{p_e}{p}\right)^{\frac{k+1}{k}}\right]} \tag{35}$$

where T is given by

$$\frac{T}{T_r} = \left(\frac{p}{p_e}\right)^{\frac{k-1}{k}} \tag{37}$$

Eliminating T from equations (35) and (37) and simplifying results in

$$\frac{1}{A_e}\frac{dM}{dt} = p_e\sqrt{\frac{2m_e}{RT_r}\frac{k}{k-1}\left[\left(\frac{p}{p_e}\right)^{\frac{k-1}{k}} - 1\right]} \tag{50}$$

On the right-hand side of equation (18), all quantities except p are constant; similarly, on the right-hand side of equation (50), p is the only variable. These equations can therefore be written

$$\frac{1}{A_i}\frac{dM}{dt} = C_1\sqrt{\left[\left(\frac{p}{p_i}\right)^{\frac{2}{k}} - \left(\frac{p}{p_i}\right)^{\frac{k+1}{k}}\right]} \tag{18a}$$

and $$\frac{1}{A_e}\frac{dM}{dt} = C_2\sqrt{\left(\frac{p}{p_e}\right)^{\frac{k-1}{k}} - 1} \qquad (50a)$$

where C_1 and C_2 are constants.

It is well known that equation (18a) has a maximum when

$$\frac{p}{p_i} = \left(\frac{k+1}{2}\right)^{\frac{k}{k-1}}$$

at which pressure ratio (the critical pressure ratio) the velocity of flow is equal to the local velocity of sound. When the pressure ratio p/p_i is further decreased, the velocity of flow and the mass velocity remain constant at their critical values. This explains why the flow factor for inward flow becomes constant when the critical pressure ratio is reached (fig. 2(b)). Equation (50a), however, is different. If the mass velocity $(1/A_e)(dM/dt)$ is plotted against the pressure ratio p/p_e, it always increases as p/p_e increases, though the increase is rather slow when p/p_e is large. (In equation (50a) p_e is considered a constant. So for a given exhaust process the mass velocity is a function of the cylinder pressure p only.) In mathematical terms, the mass velocity as defined by equation (50a) is a monotonic increasing function of p/p_e. It has neither maximums nor minimums.

The velocity of flow through the exhaust valve increases as p/p_e increases. It becomes equal to the local velocity of sound when

$$\frac{p}{p_e} = \left(\frac{k+1}{2}\right)^{\frac{k}{k-1}} \qquad \text{(See equation (53))}$$

beyond which, unlike the flow through the inlet valve, the velocity becomes supersonic and the mass velocity continues to increase according to equation (50). This is substantiated by the calculated results of many exhaust processes and will be further explained a little later.

In a recent research by Hu at the Massachusetts Institute of Technology (references 20 and 21), he measured the mass velocity of flow through exhaust valves from a pressure tank storing compressed air. The range of pressure ratio covered is, approximately, from 2 to 7. When this ratio is high (about 6 or 7), the mass velocity from Hu's measurement is higher than that indicated by equation (50). According to Hu's experiment, then, the velocity of flow at the exhaust valve does not exceed the local velocity of sound, at least not to the extent implied by equation (50).

An investigation was therefore made to see what would happen if the velocity through the exhaust valve was limited to the local sonic velocity. According to Bernoulli's equation for compressible fluids, the velocity of flow u_x at any station x along the path of flow is given by

$$\frac{u_x^2}{2} = \frac{k}{k-1}\left(\frac{p_1}{\rho_1} - \frac{p_x}{\rho_x}\right) \tag{51}$$

where k is the ratio of specific heats of the fluid, p the pressure, and ρ the density. Subscript 1 indicates an upstream station where the velocity of flow is negligible. For an isentropic process, $\rho_1/\rho_x = \left(p_1/p_x\right)^{\frac{1}{k}}$. The local velocity of sound at x is $C_x = \sqrt{k\ p_x/\rho_x}$. Therefore, equation (51) yields the relation

$$\left(\frac{u_x}{C_x}\right)^2 = \frac{2}{k-1}\left[\left(\frac{p_1}{p_x}\right)^{\frac{k-1}{k}} - 1\right] \tag{52}$$

The ratio u_x/C_x is often referred to as the Mach number. From equation (52) it is readily seen that the condition for Mach number equal to 1 is

$$\frac{p_1}{p_x} = \left(\frac{k+1}{2}\right)^{\frac{k}{k-1}} \tag{53}$$

which is the condition at the throat of the exhaust-gas stream where the velocity of flow is equal to the local sonic velocity. For $k = 1.30$, equation (53) gives a pressure ratio of 1.83.

Let $p/p_e = 1.83$ in equation (35); then

$$\frac{1}{A_e}\frac{dM}{dt} = p\sqrt{\frac{2m_e}{RT}\frac{k}{k-1}(0.05136)} \tag{54}$$

The substitution of 1.83 for p/p_e means that by passing through the exhaust valve the pressure of the exhaust gas does not drop to the exhaust pressure p_e but to 1/1.83 of the cylinder pressure p with the expansion from $p/1.83$ to p_e taking place in the exhaust port and the exhaust pipe.

Equation (54) indicates that even when p/p_e is greater than 1.83, the mass velocity increases as the upstream pressure p increases or as the square root of the absolute upstream temperature T decreases. Also, for p/p_e greater than 1.83, the mass velocity given by equation (54) is greater than that given by equation (35).

By using equation (54) and doing the same thing as was done in formulating the equation of the exhaust process, a new flow factor for sonic flow

$$F_s = 0.4718\left(\frac{p}{p_e}\right)^{\frac{3k-1}{2k}} \tag{55}$$

is obtained for $k = 1.30$ and $p/p_e \geq 1.83$.

In reference 9, one exhaust process was solved using both the original flow factor for outward flow F_e and the new flow factor for sonic flow F_s. Although the solution based on F_e agreed very nicely with the experimental indicator diagram, the recalculation based on F_s deviated noticeably from the measured curve. In the present report all the exhaust solutions are based on F_e and the agreement with measured indicator diagrams is almost perfect. If F_s were used, the calculated diagrams would be lower than the measured curves and the agreement would not be nearly so good.

This fact, unless there are other unknown reasons, would seem to indicate that the velocity of flow through the exhaust valve under actual engine operating conditions may be supersonic. Supersonic velocity is possible only when the throat of the exhaust-gas stream is inside the cylinder and ahead of the exhaust valve. The pressure at the throat is, by definition, $p/1.83$; and if F_e is used when p/p_e is greater than 1.83, it is implied that the pressure at the exhaust valve is p_e.

The apparent contradiction between the findings in this report and those in Hu's experiment was first thought to be due to the fact that in calculating the exhaust processes, the effective exhaust-valve opening area was based on flow coefficients obtained by steady-flow tests with very small pressure drop across the valve, whereas under actual engine operating conditions the flow is unsteady and the pressure drop across the exhaust valve is very large. However, experiments by Hu (unsteady flow, large pressure drop) and by Weiss and Yee (reference 22) (steady flow, pressure drop only 10 in. of alcohol) indicate that the difference in flow coefficients from their experiments is small and no consistent trend in the variation of flow coefficients could be attributed to these changes.

It may be pointed out, however, that Hu's experimental conditions did not correspond entirely to actual conditions of engine operation. Thus, in Hu's experiment the valve lift was fixed during each test run, whereas in actual engine operation the valve lift changes rapidly with time. It is conceivable that when the exhaust valve is opening, the changing valve position might cause the vena contracta of the exhaust-gas stream to shift in position accordingly. Thus the throat of the gas stream might fall inside the cylinder and ahead of the valve, and consequently the velocity at the exhaust valve might become supersonic.

APPENDIX D

CORRELATION OF VOLUMETRIC EFFICIENCIES

OBTAINED UNDER DIFFERENT CONDITIONS

If there is no serious backflow or short-circuit flow during the inlet process, the volumetric efficiency can be calculated with reasonable accuracy from

$$e_v = \frac{m_i/m_a}{k_i(1 + f)} Y_c \tag{56}$$

in which

$$Y_c = B \int_{\theta_o}^{\theta_c} \frac{A_i}{A_p} F_i \, d\theta$$

$$= \frac{\sqrt{2k_i}}{180} \frac{C_i}{s} \int_{\theta_o}^{\theta_c} \frac{A_i}{A_p} F_i \, d\theta \tag{57}$$

Combining equations (56) and (57), yields

$$e_v = \frac{\sqrt{2}(m_i/m_a)}{180\sqrt{k_i}(1 + f)} \frac{C_i}{s} \int_{\theta_o}^{\theta_c} \frac{A_i}{A_p} F_i \, d\theta \tag{58}$$

It is apparent from equation (58) that in order to correlate volumetric efficiencies obtained under different test conditions, the proper parameter or criterion to use would be

$$\alpha = \frac{C_i}{s}\left(\frac{A_i}{A_p} F_i\right)_{av}(\theta_c - \theta_o) \tag{59}$$

where

$$\left(\frac{A_i}{A_p} F_i\right)_{av} = \frac{1}{\theta_c - \theta_o} \int_{\theta_o}^{\theta_c} \frac{A_i}{A_p} F_i \, d\theta$$

In actual engine operation, the molecular mass of intake mixture m_i and that of air m_a are nearly equal, and therefore m_i/m_a is nearly equal to 1; $\sqrt{k_i}$ and $1 + f$ do not vary greatly. Besides, $1 + f$ and $\sqrt{k_i}(m_a/m_i)$ change in opposite directions. Thus the quantity

$$\frac{m_i/m_a}{\sqrt{k_i}(1 + f)}$$

is practically constant and therefore does not enter the parameter α.

The parameter α has one disadvantage, however, in that the quantity $\left(\frac{A_i}{A_p} F_i\right)_{av}$ involves the flow factor F_i which cannot be evaluated unless the indicator diagram (either measured or calculated) is available.

In references 15 and 16, from considerations independent of this report, the following criterion for volumetric efficiency has been used

$$\phi = \frac{s}{C_i} \frac{A_p}{(A_i)_{av}}$$

where

$$(A_i)_{av} = \frac{1}{\theta_c - \theta_o} \int_{\theta_o}^{\theta_c} A_i \, d\theta$$

The parameter ϕ correlates volumetric efficiencies satisfactorily when certain operating variables are changed within reasonable ranges.

In reference 23, similarly, the following criterion has been used:

$$\phi' = \left(\frac{s}{C_i}\,\frac{A_p}{(A_i)_{av}}\,\frac{1}{\theta_c - \theta_o}\right) \times \text{Constant}$$

and a large number of volumetric efficiencies obtained under different conditions of test were plotted against ϕ' as abscissa; the correlation was fairly good except when ϕ' was small.

It is to be expected that neither ϕ nor ϕ' will give satisfactory all-round correlation of volumetric efficiencies because they do not include the flow factor F_i which, although inconvenient to evaluate, is nevertheless important since it is proportional to the mass velocity through the inlet valve. The problem is further complicated when conditions giving rise to serious backflow or short-circuit flow are involved.

It seems unlikely that any simple, easily evaluable parameter could be found to correlate volumetric efficiencies when a great many variables are changed over wide ranges. But when normal, moderate changes are made on a few variables, the volumetric efficiencies should be correlated successfully by using either ϕ or ϕ'.

REFERENCES

1. Hershey, R. L., Eberhardt, J. E., and Hottel, H. C.: Thermodynamic Properties of the Working Fluid in Internal-Combustion Engines. SAE Jour., vol. 39, no. 4, Oct. 1936, pp. 409-424.

2. Kemble, E. C.: Calculation of Low-Pressure Indicator Diagrams. NACA Rep. No. 50, 1918.

3. Tanaka, Keikiti: Air Flow through Suction Valve of Conical Seat. Rep. Nos. 50 and 51 (vol. IV, nos. 9, 10), Aero. Res. Inst., Tokyo Imperial Univ., Oct., Nov. 1929, pp. 259-424.

4. Dennison, E. S., Kuchler, T. C., and Smith, D. W.: Experiments on the Flow of Air through Engine Valves. Trans. A.S.M.E., vol. 53, no. 17, Oil and Gas Power 53-6, 1931, pp. 79-97.

5. Dennison, E. S.: Inertia Supercharging of Engine Cylinders. Trans. A.S.M.E., OGP-55-5, vol. 55, no. 14, Nov. 30, 1933, pp. 53-64.

6. Aschenbrenner, Josef: Der Einsluss der Gasträgheit auf den Liefergrad. Forsch. Geb. Ing.-Wes., Bd. 8, Nov.-Dec. 1937, pp. 285-294.

7. Reynolds, B.: Dynamics of Air Flow through Intake Valve. S.M. Thesis, M.I.T., 1938.

8. Reynolds, Blake, Schecter, Harry, and Taylor, E. S.: The Charging Process in a High-Speed, Single-Cylinder, Four-Stroke Engine. NACA TN No. 675, 1939.

9. Tsu, Tsung-chi: A Mathematical Analysis of the Intake and Exhaust Processes of the Internal Combustion Engine. Sc. D. Thesis, M.I.T., June 1944.

10. Forbes, J. E., and Taylor, E. S.: Rise in Temperature of the Charge in Its Passage through the Inlet Valve and Port of an Air-Cooled Aircraft Engine Cylinder. NACA TN No. 839, 1942.

11. Prandtl, L., and Tietjens, O. G. (L. Rosenhead, trans.): Fundamentals of Hydro- and Aeromechanics. McGraw-Hill Book Co., Inc., 1934, p. 110.

12. Taylor, C. Fayette, and Taylor, Edward S.: The Internal Combustion Engine. Int. Textbook Co. (Scranton), 1938.

13. Keenan, Joseph H.: Thermodynamics. John Wiley & Sons, Inc., 1941.

14. Anon: Fluid Meters - Their Theory and Application. Pt. 1. Report of A.S.M.E. Special Research Comm. on Fluid Meters. Fourth ed. A.S.M.E. (New York), 1937.

15. Livengood, James C., and Stanitz, John D.: The Effect of Inlet-Valve Design, Size, and Lift on the Air Capacity and Output of a Four-Stroke Engine. NACA TN No. 915, 1943.

16. Livengood, James C., and Eppes, James V. D.: Effect of Changing Manifold Pressure, Exhaust Pressure, and Valve Timing on the Air Capacity and Output of a Four-Stroke Engine Operated with Inlet Valves of Various Diameters and Lifts. NACA TN No. 1366, 1947.

17. Eppes, James V. D., Livengood, James C., and Taylor, C. Fayette: The Effect of Changing the Ratio of Exhaust-Valve Flow Capacity to Inlet-Valve Flow Capacity on Volumetric Efficiency and Output of a Single-Cylinder Engine. NACA TN No. 1365, 1947.

18. Livengood, J. C., and Eppes, J. V. D.: Effect of Changing the Stroke on Air Capacity, Power Output, and Detonation of a Single-Cylinder Engine. NACA ARR No. 4E24, 1945.

19. Boden, R. H., and Schecter, Harry: Dynamics of the Inlet System of a Four-Stroke Engine. NACA TN No. 935, 1944.

20. Hu, Seng-chiu: A Study of Exhaust-Valve Design from Gas Flow Standpoint. Sc. D. Thesis, M.I.T., May 1942.

21. Hu, Seng-chiu: Study of Exhaust-Valve Design from Gas Flow Standpoint. Jour. Aero. Sci., vol. 11, no. 1, Jan. 1944, pp. 13-20.

22 Weiss, Harold J., and Yee, Yet-lin: Investigation of Exhaust-Valve Design Using Steady Flow. S. B. Thesis, M.I.T., Jan. 1943.

23. Kano, C., and Wadleigh, K. R.: Effect of Inlet-Valve Size, Lift and Timing upon the Air Capacity and Output of a Four-Stroke Cycle Engine. S. M. Thesis, M.I.T., May 1943.

TABLE I

SCHEDULE OF VALVE LIFT, VALVE TIMING, AND FLOW

COEFFICIENTS FOR TESTS ON INLET-EXHAUST ENGINE

[L_{max}, max. valve lift; D, valve diameter;

C_{av}, average flow coefficient over entire

valve opening period.]

Run	Valve lift (in.)		L_{max}/D		C_{av}		D^2C_{av}		Valve timing (1)			
									I.O.	I.C.	E.O.	E.C.
	Inlet	Exhaust	Inlet	Exhaust	Inlet	Exhaust	Inlet	Exhaust	(deg B.T.C.)	(deg A.B.C.)	(deg B.B.C.)	(deg A.T.C.)
1	0.500	0.244	0.225	0.110	0.319	0.163	1.569	0.802	19	66	72	14
2	.405	.290	.183	.131	.281	.193	1.380	.948	19	66	72	14
3	.333	.358	.150	.162	.234	.235	1.151	1.155	19	66	72	14
4	.284	.428	.128	.193	.197	.273	.969	1.343	19	66	72	14
5	.248	.500	.112	.225	.170	.305	.836	1.500	19	66	72	14
6	.248	.500	.112	.225	.170	.305	.836	1.500	(2)	94	72	14
7	.500	.244	.225	.110	.319	.163	1.569	.802	19	66	97	(3)
8	.459	.500	.207	.225	.305	.305	1.500	1.500	19	66	72	14
9	.244	.250	.110	.113	.167	.167	.821	.821	19	66	72	14
10	.500	.244	.225	.110	.319	.163	1.569	.802	19	66	106	14
11	.333	.358	.150	.162	.234	.235	1.151	1.155	19	66	106	14
12	.248	.500	.112	.225	.170	.305	.836	1.500	19	101	72	14
13	.333	.358	.150	.162	.234	.235	1.151	1.155	19	101	72	14

[1]This is the nominal timing when the normal cam clearance of 0.070 in. is used. Since the running cam clearance is adjusted to only 0.045 in., the actual valve opening durations are longer than those listed in the table.

[2]8° A.T.C.

[3]12° B.T.C.

TABLE II

DATA FOR ALL SOLUTIONS[1]

(a) CFR engine

[Compression ratio, 4.92;

$$\frac{V}{V_d} = 0.7835 - 0.5000 \cos \theta - 0.0285 \cos 2\theta;$$

$$\frac{d}{d\theta}\left(\frac{V}{V_d}\right) = \frac{\pi}{180} (0.5000 \sin \theta + 0.0570 \sin 2\theta);$$

$\frac{V_o}{V_d}$ is the value of $\frac{V}{V_d}$ corresponding to θ_o.]

Solution	Designation (1)	θ_o	p_o	p_i	p_e	p_m	A	B	C	A_i/A_p against θ curve (1)	A_e/A_p against θ curve (1)
1	C-s20001e	332	16.22	13.45	15.42	13.45	0.336	0.4077	0.958	C-00SL	C-0000e
1.1	C-x20001e	332	16.22	13.45	15.42	13.45	.300	.3562	.958	C-00SL	C-0000e
2	C-sl20001e	332	16.22	13.45	15.42	13.45	.270	.3276	.958	C-00SL	C-0000e
3	C-sh20001e	332	16.22	13.45	15.42	13.45	.346	.4198	.958	C-00SL	C-0000e
4	C-s36001e	332	16.73	13.45	15.42	13.45	.336	.2265	.542	C-00SL	C-0000e
4.1	C-x36001e	332	16.73	13.45	15.42	13.45	.300	.1979	.542	C-00SL	C-0000e
5	C-sl36001e	332	16.73	13.45	15.42	13.45	.270	.1820	.542	C-00SL	C-0000e
6	C-sh36001e	332	16.73	13.45	15.42	13.45	.346	.2332	.542	C-00SL	C-0000e
7	C-32131e	330	16.0	14.74	14.74	14.74	.346	.2282	.446	C-3200	C-3000e
8	C-32121e	330	15.5	14.74	14.74	14.74	.346	.4108	.804	C-3200	C-3000e
9	C-32021e	330	20.5	9.82	19.64	9.82	.346	.4108	1.71	C-3200	C-3000e
10	C-32421e	330	5.7	19.64	4.91	19.64	.346	.4108	.174	C-3200	C-3000e
11	C-32411e	330	5.3	19.64	4.91	19.64	.346	1.6432	.676	C-3200	C-3000e

[1]See explanation of designation system and remarks about A_i/A_p and A_e/A_p curves following this table.

NACA

TABLE II.– DATA FOR ALL SOLUTIONS[1] – Continued

(a) CFR engine – Continued

Solution	Designation (1)	θ_o	p_o	p_i	p_e	p_m	A	B	C	A_i/A_p against θ curve (1)	A_e/A_p against θ curve (1)
12	C-3141ie	330	5.3	19.64	4.91	19.64	0.346	1.6432	0.695	C-3100	C-3000e
13	C-3113ie	330	16.0	14.74	14.74	14.74	.346	.2282	.456	C-3100	C-3000e
14	C-1113ie	330	16.0	14.74	14.74	14.74	.346	.2282	.451	C-1100	C-1000e
15	C-1213ie	330	16.0	14.74	14.74	14.74	.346	.2282	.442	C-1200	C-1000e
16	C-1202ie	330	20.5	9.82	19.64	9.82	.346	.4108	1.67	C-1200	C-1000e
17	C-2223ie	330	11.1	19.64	9.82	19.64	.346	.2282	.208	C-2200	C-2000e
18	C-2223i	330	11.1	19.64	9.82	19.64	.346	.2282	0	C-2200	--------
19	C-5223i	357	11.1	19.64	9.82	19.64	.346	.2282	0	C-5200	--------
19.1	C-5222 $\frac{1}{2}$ i	357	11.0	19.64	9.82	19.64	.346	.2567	0	C-5200	--------
20	C-4213i	357	16.0	14.74	14.74	14.74	.346	.2282	0	C-4200	--------
20.1	C-4212 $\frac{1}{2}$ i	357	15.9	14.74	14.74	14.74	.346	.2567	0	C-4200	--------
21	C-4113i	357	16.0	14.74	14.74	14.74	.346	.2282	0	C-4100	--------
21.1	C-4112 $\frac{1}{2}$ i	357	15.9	14.74	14.74	14.74	.346	.2567	0	C-4100	--------
22	C-4141i	357	5.3	19.64	4.91	19.64	.346	1.6432	0	C-4100	--------
23	C-6241i	357	5.3	19.64	4.91	19.64	.346	1.6432	0	C-6200	--------
24	C-6222i	357	10.6	19.64	9.82	19.64	.346	.4108	0	C-6200	--------
25	C-6113i	357	16.0	14.74	14.74	14.74	.346	.2282	0	C-6100	--------
25.1	C-6112 $\frac{1}{2}$ i	357	15.9	14.74	14.74	14.74	.346	.2567	0	C-6100	--------
26	C-7113ie	315	16.0	14.74	14.74	14.74	.346	.2282	.465	C-7100	C-7000e
27	C-7103ie	315	20.9	9.82	19.64	9.82	.346	.2282	.982	C-7100	C-7000e
28	C-7101ie	315	20.0	9.82	19.64	9.82	.346	1.6432	6.95	C-7100	C-7000e

[1]See explanation of designation system and remarks about A_i/A_p and A_e/A_p curves following this table.

NACA

TABLE II.– DATA FOR ALL SOLUTIONS[1] – Continued

(a) CFR engine – Continued

Solution	Designation (1)	θ_o	p_o	p_i	p_e	p_m	A	B	C	A_i/A_p against θ curve (1)	A_e/A_p against θ curve (1)
29	C-7141ie	315	5.3	19.64	4.91	19.64	0.346	1.6432	0.716	C-7100	C-7000e
30	C-7201ie	315	20.0	9.82	19.64	9.82	.346	1.6432	6.83	C-7200	C-7000e
31	C-7203ie	315	20.9	9.82	19.64	9.82	.346	.2282	.965	C-7200	C-7000e
32	C-7213ie	315	16.0	14.74	14.74	14.74	.346	.2282	.455	C-7200	C-7000e
33	C-72131	315	16.0	14.74	14.74	14.74	.346	.2282	0	C-7200	-------
34	C-72231	315	11.1	19.64	9.82	19.64	.346	.2282	0	C-7200	-------
35	C-72231e	315	11.1	19.64	9.82	19.64	.346	.2282	.208	C-7200	C-7000e
36	C-011e	122	66.7	13.45	15.42	15.42	.250	0	.805	------	C-0000e
37	C-012e	122	59.2	13.45	15.42	15.42	.250	0	.582	------	C-0000e
38	C-013e	122	48.7	13.45	15.42	15.42	.250	0	.455	------	C-0000e
39	C-021e	122	85.0	15.00	15.00	15.00	.250	0	.656	------	C-0000e
40	C-022e	122	80.0	15.00	15.00	15.00	.250	0	.656	------	C-0000e
41	C-023e	122	75.0	15.00	15.00	15.00	.250	0	.656	------	C-0000e
42	C-024e	122	70.0	15.00	15.00	15.00	.250	0	.656	------	C-0000e
43	C-025e	122	65.0	15.00	15.00	15.00	.250	0	.656	------	C-0000e
44	C-0311	330	15.0	15.00	15.00	15.00	.346	.3286	0	C-2200	-------
45	C-0321	330	16.0	15.00	15.00	15.00	.346	.3286	0	C-2200	-------
46	C-0331	330	17.0	15.00	15.00	15.00	.346	.3286	0	C-2200	-------
47	C-0341	330	19.0	15.00	15.00	15.00	.346	.3286	0	C-2200	-------
48	C-0421	330	16.2	15.00	15.00	15.00	.346	.2570	0	C-2200	-------
49	C-0431	330	16.4	15.00	15.00	15.00	.346	.2108	0	C-2200	-------

[1]See explanation of designation system and remarks about A_i/A_p and A_e/A_p curves following this table.

TABLE II.– DATA FOR ALL SOLUTIONS[1] – Continued

(a) CFR engine – Concluded

Solution	Designation (1)	θ_o	p_o	p_i	p_e	p_m	A	B	C	A_i/A_p against θ curve (1)	A_e/A_p against θ curve (1)
50	C-044i	330	16.9	15.00	15.00	15.00	0.346	0.1788	0	C-2200	--------
51	C-045i	330	15.7	15.00	15.00	15.00	.346	.5480	0	C-2200	--------
52	C-046i	330	15.4	15.00	15.00	15.00	.346	1.643	0	C-2200	--------
53	C-051ie	330	16.0	15.00	15.00	15.00	.346	.3286	.643	C-2200	C-0000e
54	C-052ie	330	16.0	11.00	15.00	11.00	.346	.3286	.905	C-2200	C-0000e
55	C-053ie	330	16.0	7.00	15.00	7.00	.346	.3286	1.463	C-2200	C-0000e
56	C-054ie	330	16.0	20.00	15.00	20.00	.346	.3286	.461	C-2200	C-0000e
57	C-055ie	330	16.0	25.00	15.00	25.00	.346	.3286	.344	C-2200	C-0000e
58	C-062ie	330	11.0	15.00	10.00	15.00	.346	.3286	.410	C-2200	C-0000e
59	C-063ie	330	6.0	15.00	5.00	15.00	.346	.3286	.191	C-2200	C-0000e
60	C-064ie	330	21.0	15.00	20.00	15.00	.346	.3286	.885	C-2200	C-0000e
61	C-065ie	330	26.0	15.00	25.00	15.00	.346	.3286	1.140	C-2200	C-0000e

[1]See explanation of designation system and remarks about A_i/A_p and A_e/A_p curves following this table.

NACA

TABLE II.– DATA FOR ALL SOLUTIONS[1] – Continued

(b) Inlet-exhaust engine

$$\left[\frac{V}{V_d} = 0.7546 - 0.5000 \cos\theta - 0.0325 \cos 2\theta;\right.$$

$$\frac{d}{d\theta}\left(\frac{V}{V_d}\right) = \frac{\pi}{180}(0.5000 \sin\theta + 0.0650 \sin 2\theta);$$

$\frac{V_o}{V_d}$ is the value of $\frac{V}{V_d}$ corresponding to θ_o.

For all the solutions of part (b),

$$\left. p_i = p_e = p_m = 16.20 \text{ lb/sq in. abs.}\right]$$

Solution	Designation (1)	θ_o	p_o	A	B	C	A_i/A_p against θ curve (1)	A_e/A_p against θ curve (1)
62	I-011e	85	108	0.250	0	2.478	-----	I-010e
63	I-013e	85	120	.250	0	.527	-----	I-010e
64	I-051e	85	114	.250	0	2.516	-----	I-050e
65	I-053e	85	108	.250	0	.554	-----	I-050e
66	I-071e	60	159	.250	0	2.504	-----	I-070e
67	I-073e	60	165	.250	0	.539	-----	I-070e
68	I-101e	48	220	.250	0	2.504	-----	I-100e
69	I-103e	48	255	.250	0	.535	-----	I-100e
70	I-111e	48	223	.250	0	2.520	-----	I-110e
71	I-113e	48	256	.250	0	.531	-----	I-110e
72	I-0131e	318	31.38	.348	.2693	.527	I-010	I-010e
73	I-0231e	318	24.54	.348	.2693	.528	I-020	I-020e

[1]See explanation of designation system and remarks about A_i/A_p and A_e/A_p curves following this table.

NACA

TABLE II.– DATA FOR ALL SOLUTIONS[1] – Continued

(b) Inlet-exhaust engine – Concluded

Solution	Designation (1)	θ_o	p_o	A	B	C	A_i/A_p against θ curve (1)	A_e/A_p against θ curve (1)
74	I-032ie	318	18.23	0.348	0.4488	0.874	I-030	I-030e
75	I-032i	318	18.23	.348	.4488	0	I-030	------
76	I-033ie	318	20.33	.348	.2693	.528	I-030	I-030e
77	I-051ie	318	17.14	.348	1.3464	2.516	I-050	I-050e
78	I-052ie	318	17.49	.348	.4488	.895	I-050	I-050e
79	I-052i	318	17.49	.348	.4488	0	I-050	------
80	I-061i	345	17.50	.348	1.3464	0	I-060	------
81	I-063i	345	18.50	.348	.2693	0	I-060	------
82	I-071i	318	19.08	.348	1.3464	0	I-070	------
82.1	I-071ie	318	19.08	.348	1.3464	2.504	I-070	I-070e
83	I-073i	318	32.63	.348	.2693	0	I-070	------
83.1	I-073ie	318	32.63	.348	.2693	.539	I-070	I-070e
84	I-082ie	318	18.10	.348	.4488	.897	I-080	I-080e
85	I-083ie	318	19.55	.348	.2693	.535	I-080	I-080e
86	I-092ie	318	18.92	.348	.4488	.881	I-090	I-090e
87	I-093ie	318	25.72	.348	.2693	.551	I-090	I-090e
88	I-103ie	318	29.04	.348	.2693	.535	I-100	I-100e
89	I-132ie	315	17.95	.348	.4488	.895	I-130	I-130e

[1]See explanation of designation system and remarks about A_i/A_p and A_e/A_p curves following this table.

TABLE II.– DATA FOR ALL SOLUTIONS[1] – Concluded

(c) Bore-stroke engine

$\left[\frac{V}{V_d} = 0.7316 - 0.5000 \cos \theta - 0.0318 \cos 2\theta;\ \frac{d}{d\theta}\left(\frac{V}{V_d}\right) = \frac{\pi}{180}(0.5000 \sin \theta + 0.0635 \sin 2\theta);\right.$

$\frac{V_o}{V_d}$ is the value of $\frac{V}{V_d}$ corresponding to θ_o. For all the solutions in part (c), use A_i/A_p against θ curve B-000 and A_e/A_p against θ curve B-000e. Note that in solution 92 only the A_i/A_p against θ curve is needed and in solutions 96, 97, and 98, only the A_e/A_p against θ curve is needed.]

Solution	Designation (1)	θ_o	p_o	p_i	p_e	p_m	A	B	C
90	B-011ie	343	16.05	13.46	15.42	13.46	0.348	0.3740	0.836
91	B-012ie	343	16.25	13.46	15.42	13.46	.348	.2743	.611
92	B-012i	343	16.25	13.46	15.42	13.46	.348	.2743	0
93	B-014ie	343	17.20	13.46	15.42	13.46	.348	.2165	.493
94	B-023ie	343	16.36	19.64	15.42	19.64	.348	.2571	.378
95	B-033ie	343	16.36	24.54	15.42	24.54	.348	.2571	.297
96	B-011e	119	82	13.46	15.42	15.42	.250	0	.729
97	B-012e	119	81	13.46	15.42	15.42	.250	0	.534
98	B-014e	119	81	13.46	15.42	15.42	.250	0	.430

[1]See explanation of designation system and remarks about A_i/A_p and A_e/A_p curves following this table.

EXPLANATION OF DESIGNATION SYSTEM OF TABLE II

In table II a designation system is used to identify the solutions. There are four different designation types:

From solution number	To solution number	Designation type	Example
[a]7	35	C-wxyz( )	C-3213ie
36	61	C-xxy ( )	C-043i
62	89	I-xxy ( )	I-103ie
90	98	B-xxy ( )	B-012e

[a]Solutions 1 to 6, inclusive, are made in a preliminary investigation to see the effect of changing k_i (ratio of specific heats of the intake charge) on volumetric efficiency and indicator diagram. They are made at two engine speeds (2000 and 3600 rpm) with different values of k_i. To compare the calculated results, test data are taken from reference 15.

Type C-wxyz( ) signifies a systematic investigation using different cams, valve sizes and lifts, and p_i/p_e ratios on the CFR engine.

C denotes CFR engine

w denotes cam number (See fig. 4.)

x denotes inlet-valve size and lift

2 = large valve, large lift

1 = small valve, small lift

y denotes p_i/p_e ratio

0 means $p_i/p_e = 0.5$

1 means $p_i/p_e = 1$

2 means $p_i/p_e = 2$

4 means $p_i/p_e = 4$

z denotes engine speed

$1 = 500$ rpm

$2 = 2000$ rpm

$2\frac{1}{2} = 3200$ rpm

$3 = 3600$ rpm

( ) denotes nature of solution

i = inlet process, without valve overlap

ie = inlet process, with valve overlap

e = exhaust process

Thus C-3213ie represents a solution of the inlet process with valve overlap on the CFR engine with cam 3, large valve, large lift, $p_i/p_e = 1$, at 3600 rpm.

Type C-xxy( ) signifies other investigations on the CFR engine.

C denotes CFR engine

xx denotes series number which always begins with zero (0)

01 = checking of some exhaust processes by theory with experimental results under test condition same as those reported in reference 15

02 = varying initial conditions, exhaust process

03 = varying initial conditions, inlet process

04 = effect of piston speed or inlet temperature on volumetric efficiency

05 = constant p_e, varying p_i

06 = constant p_i, varying p_e

y denotes solution number in a given series

( ) denotes nature of solution

Thus C-043i represents solution 3 of the inlet process, without overlap, in a study of the effect of piston speed or inlet temperature on the volumetric efficiency of a CFR engine.

I-xxy( )

I denotes inlet-exhaust engine

xx denotes series number which corresponds to the run number in table I

y denotes engine speed

1 = 500 rpm

2 = 1500 rpm

3 = 2500 rpm

( ) denotes nature of solution

Thus I-103ie represents a solution of the inlet process, considering valve overlap, on the inlet-exhaust engine at 2500 rpm. Other conditions same as those in run 10, table I.

B-xxy( )

B denotes bore-stroke engine

xx denotes series number

01 for p_i = 27.4 in. Hg abs., p_e = 31.4 in. Hg abs.

02 for p_i = 40 in. Hg abs., p_e = 31.4 in. Hg abs.

03 for p_i = 50 in. Hg abs., p_e = 31.4 in. Hg abs.

y denotes piston speed

1 = 1650 ft/min

2 = 2250 ft/min

3 = 2400 ft/min

4 = 2850 ft/min

( ) denotes nature of solution

Thus B-012e represents a solution of the exhaust process on the bore-stroke engine, with p_i = 27.4 inches of mercury absolute, p_e = 31.4 inches of mercury absolute and at a piston speed of 2250 feet per minute.

In solutions 7 to 98 of this table, it may be noticed that the A_i/A_p and A_e/A_p curves are numbered according to the designation number. Thus for solution 10, which is designated C-3242ie, the A_i/A_p curve is numbered C-3200 and the A_e/A_p curve numbered C-3000e.

For part (a), which is for the CFR engine, three master curves numbered C-0100, C-0200, and C-0000e are shown in figure 48. All the curves for solutions 7 to 61, are generated from these master curves by uniformly expanding or shrinking the crank-angle scale according to the valve opening duration of the particular cam. Thus curve C-3200 is generated from curve C-0200 by expanding the crank-angle scale in the ratio 300:266. Curve C-3200, of course, starts at 330° A.T.C. and ends at 270° A.T.C. (See timing diagram for cam 3, fig. 4.)

For part (b), which is for the inlet-exhaust engine, several A_i/A_p and A_e/A_p curves are shown in figures 49 and 50.

For part (c), which is for the bore-stroke engine, curves B-000 and B-000e are shown in figures 5 and 6.

TABLE III

COMPARISON OF THEORETICAL AND MEASURED VOLUMETRIC EFFICIENCIES

[The last two columns of this table are plotted in fig. 7.]

Solution	Designation[1]	Y_c	e_v (theoretical)	e_v (measured)
3	C-sh2000ie	1.0746	0.782	0.790
6	C-sh3600ie	.7805	.568	.570
7	C-3213ie	1.072	.780	.794
8	C-3212ie	1.100	.801	.763
9	C-3202ie	.639	.465	.605
10	C-3242ie	1.360	.990	.882
11	C-3241ie	1.588	1.156	.955
12	C-3141ie	1.513	1.102	.951
13	C-3113ie	.844	.614	.590
14	C-1113ie	.674	.491	.482
15	C-1213ie	.992	.722	.673
16	C-1202ie	.737	.537	.655
17	C-2223ie	1.250	.910	.832
19.1	C-5222$\frac{1}{2}$i	1.211	.882	.816
20	C-4213i	.993	.723	.661
20.1	C-4212$\frac{1}{2}$i	1.073	.781	.714
21.1	C-4112$\frac{1}{2}$i	.738	.537	.500
22	C-4141i	1.499	1.091	1.003
23	C-6241i	1.207	.879	.831
24	C-6222i	1.194	.870	.805
25.1	C-6112$\frac{1}{2}$i	.883	.642	.650
26	C-7113ie	.747	.544	.526
27	C-7103ie	.339	.246	(2)

[1]Explanation of designation system is given after table II.

[2]Unable to run CFR engine under conditions of solution.

TABLE III

COMPARISON OF THEORETICAL AND MEASURED VOLUMETRIC

EFFICIENCIES — Concluded

Solution	Designation	Y_c	e_v (theoretical)	e_v (measured)
28	C-7101ie	Negative	Negative	(1)
29	C-7141ie	2.270	1.653	1.264
30	C-7201ie	Negative	Negative	(1)
31	C-7203ie	.502	.366	(1)
32	C-7213ie	1.055	.768	.738
35	C-7223ie	1.330	.968	.870
72	I-013ie	.972	.706	.694
73	I-023ie	1.080	.784	.744
74	I-032ie	1.171	.850	.764
76	I-033ie	1.089	.791	.722
77	I-051ie	1.148	.833	.774
78	I-052ie	1.161	.843	.756
80	I-061i	.829	.602	.665
81	I-063i	.880	.639	.601
82.1	I-071ie	1.027	.746	.683
83.1	I-073ie	.702	.510	.553
84	I-082ie	1.166	.846	.758
85	I-083ie	1.157	.840	.796
86	I-092ie	1.140	.828	.723
87	I-093ie	.840	.610	.543
88	I-103ie	.974	.707	.687
89	I-132ie	.978	.710	.654
90	B-011ie	1.213	.881	.873
91	B-012ie	1.196	.868	.872
93	B-014ie	1.140	.828	.845
94	B-023ie	1.276	.926	.947
95	B-033ie	1.304	.947	.983

[1]Unable to run CFR engine under conditions of solution.

NACA

TABLE IV

DEGREE OF AGREEMENT BETWEEN CALCULATED

AND MEASURED INDICATOR DIAGRAMS

[Numbers in this table correspond to solution numbers in table II. Those underlined are reproduced in this report.]

	Inlet processes	Exhaust processes
Good agreement	7, 8, 9, 10, 11, 12, 15, 32; 72, 73, 74, 81, 83.1, 86, 87, 88, 89	36, 37, 38 62, 64, 65, 66, 67 68, 69, 70, 71
Good agreement, except for zero shift	13, 14, [a]16, 22, 23, [a]26; 76, 77, 78, 80, 82.1, 84, 85	63
Poor agreement	[b]17, [c]19.1, [b]20, [b]21.1, [c]24, [c]25.1, [c]29, [b]35 [d]90, [d]91, [d]93	[d]96, [d]97, [d]98

[a]Has discontinuity in measured diagram. (Each occurs at high engine speed; 3600 rpm.) Solution 16: Worst agreement of all.

[b]Estimated initial pressure p_o is too low.

[c]Poor agreement probably due to combination of zero shift and low estimated p_o.

[d]Poor agreement probably due to lengths of inlet and exhaust pipes.

NACA

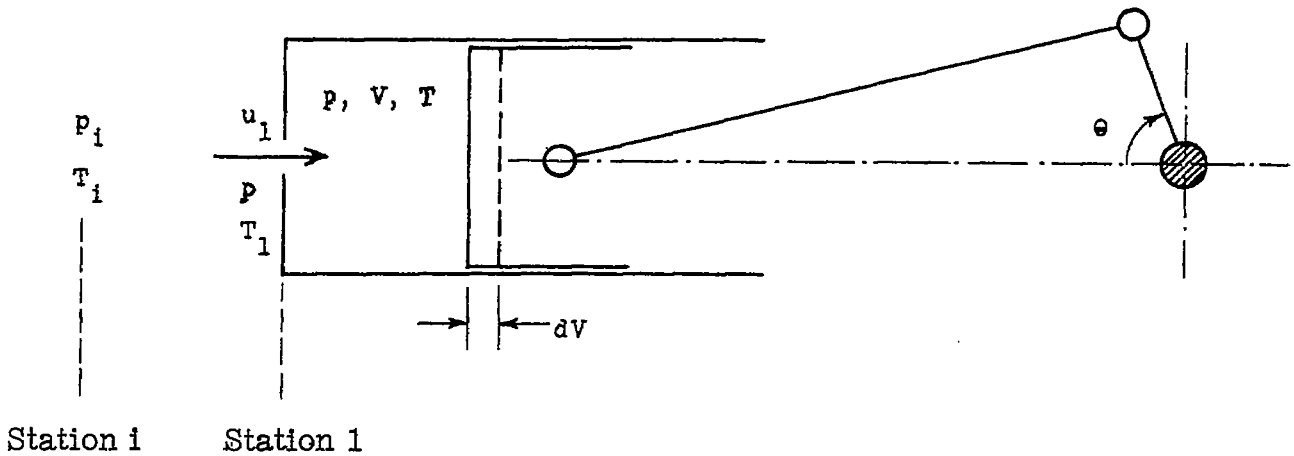

(a) Inlet process.

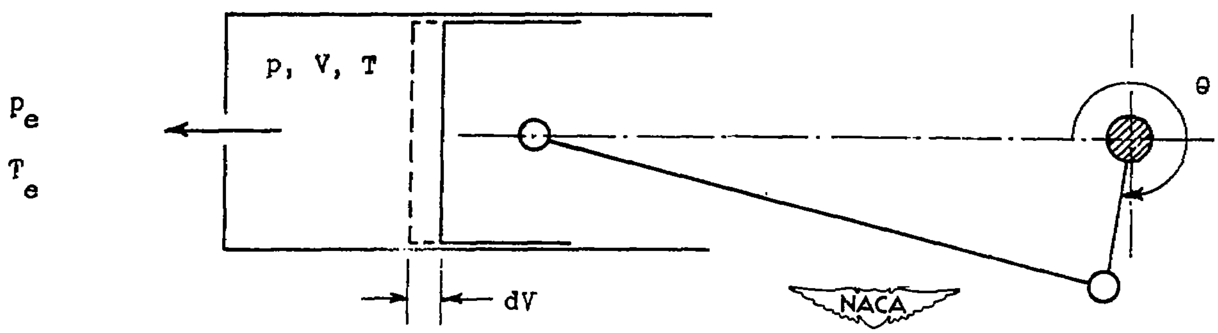

(b) Exhaust process.

Figure 1.- Diagrams of engine processes.

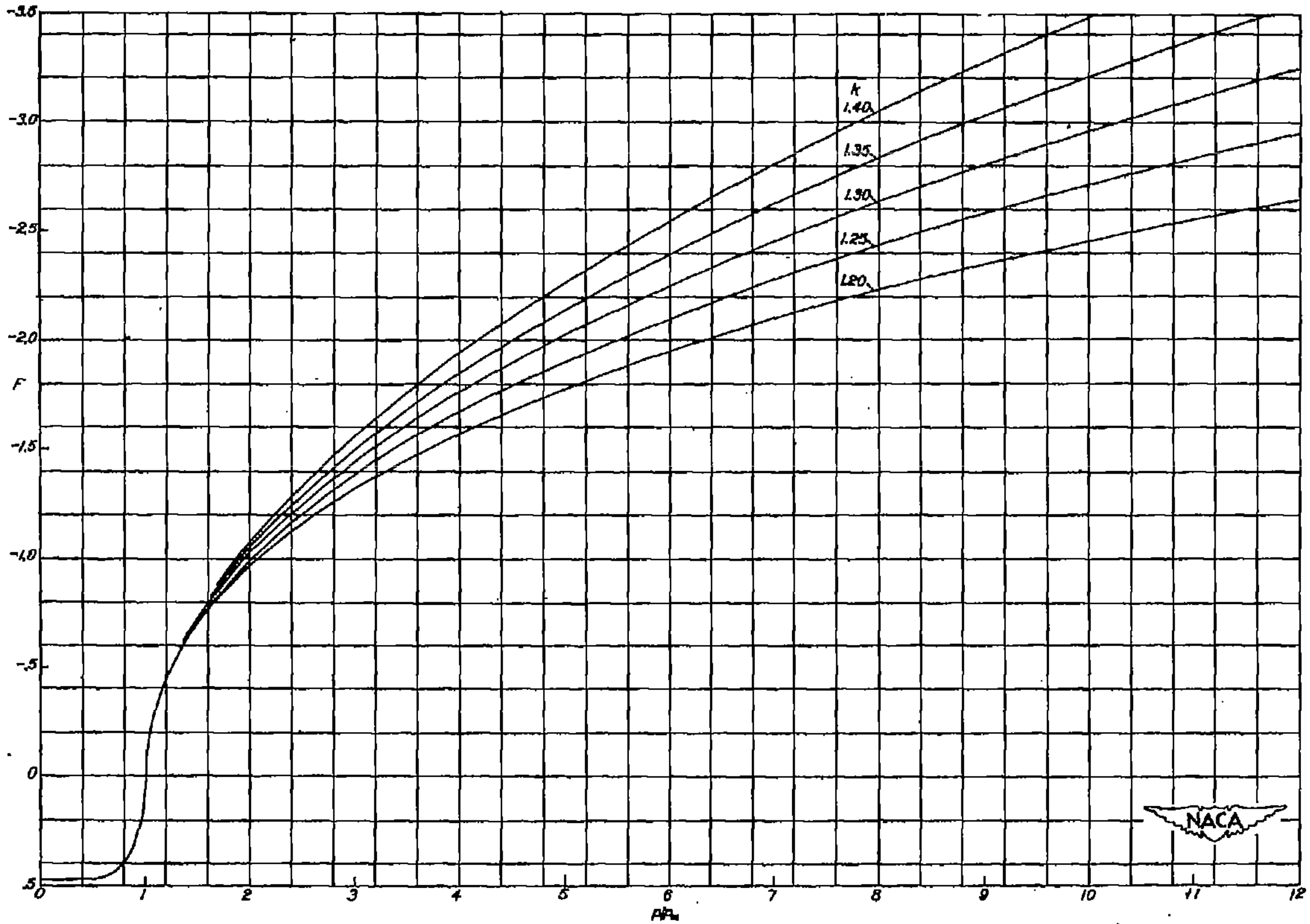

(a) Flow factor F for values of p/p_m from 0 to 12.

Figure 2.- Relation between flow factor F and ratio p/p_m.

$$F = \sqrt{\frac{k}{k-1}\left[\left(\frac{p}{p_m}\right)^{\frac{2}{k}} - \left(\frac{p}{p_m}\right)^{\frac{k+1}{k}}\right]} \text{ for } 1 > \frac{p}{p_m} > \left(\frac{p}{p_m}\right)_{cr}; \quad F = -\sqrt{\frac{k}{k-1}\left[\left(\frac{p}{p_m}\right)^{\frac{3k-3}{k}} - \left(\frac{p}{p_m}\right)^{\frac{2k-2}{k}}\right]} \text{ for } \frac{p}{p_m} > 1;$$

p, cylinder pressure; p_m, either inlet pressure p_i or exhaust pressure p_e depending on whether flow is through inlet valve or exhaust valve; k, ratio of specific heats C_p/C_v.

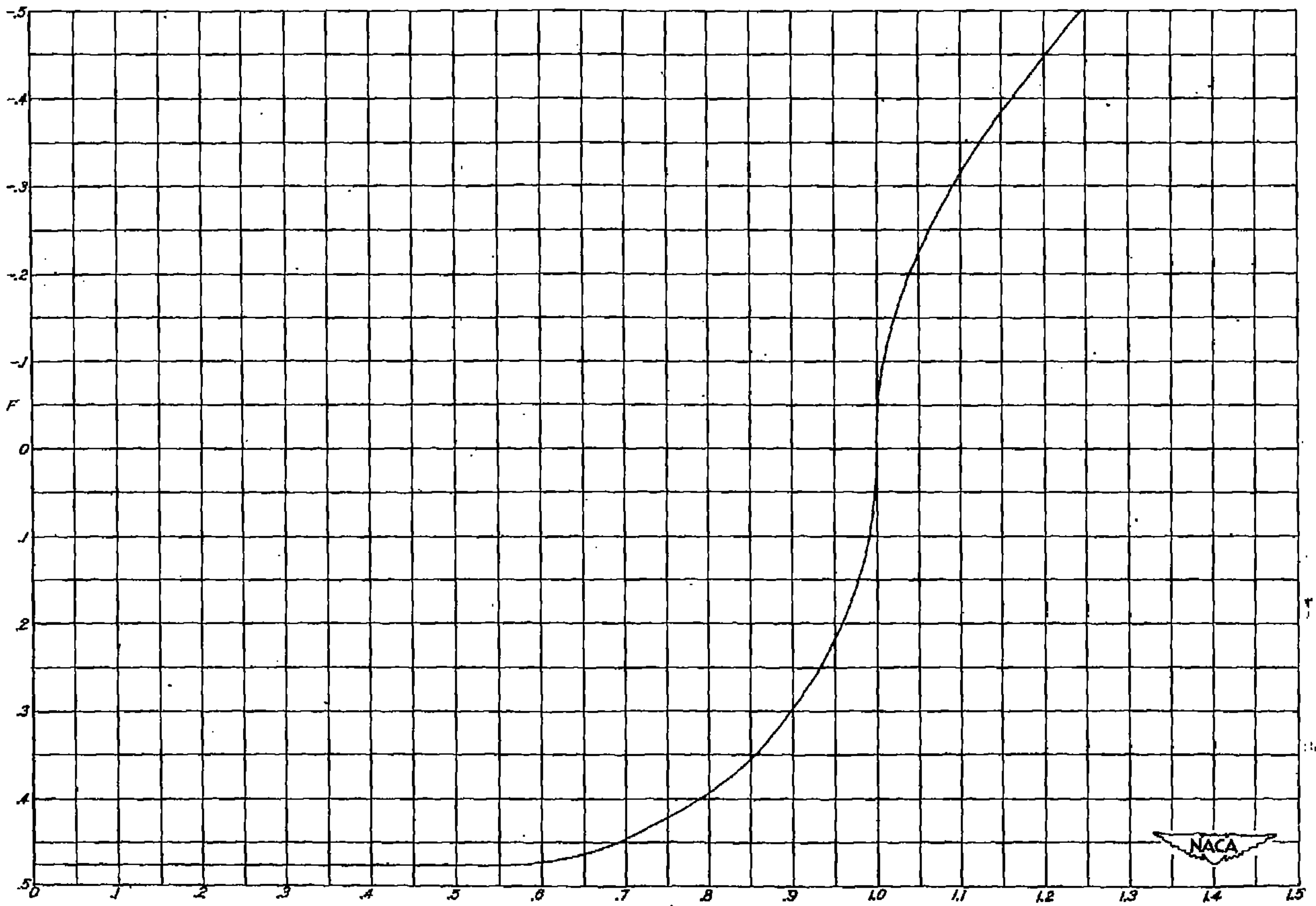

(b) Flow factor F for values of p/p_m from 0 to 1.25. (For $1.25 < k < 1.40$.)

Figure 2.- Concluded.

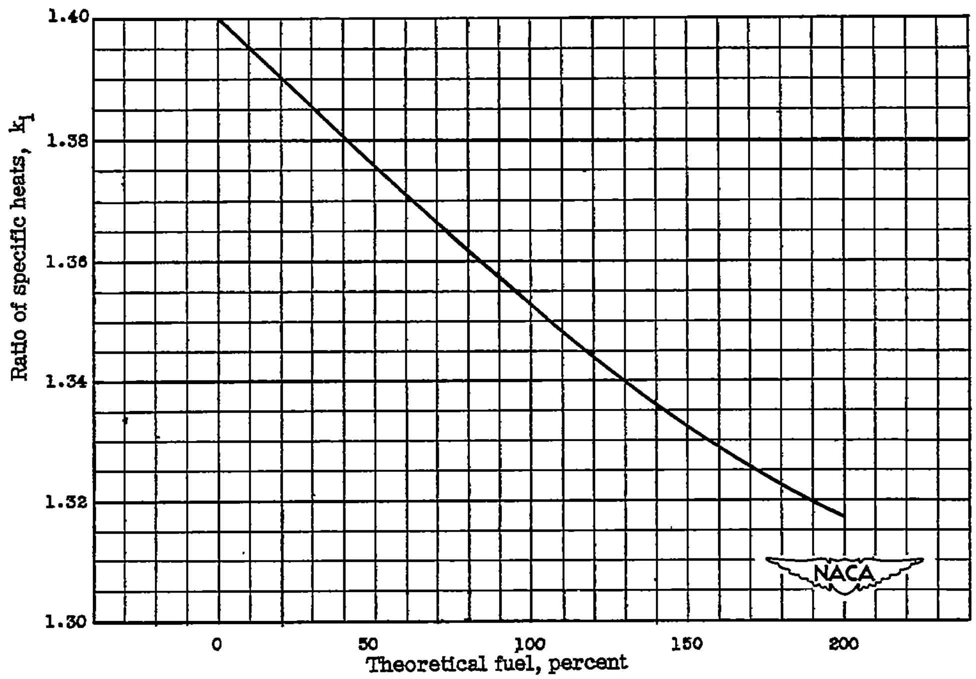

Figure 3.– Variation of ratio of specific heats with percentage of theoretical fuel. This curve is based on the following values of specific heat at constant pressure; C_p for air, 0.240 Btu per pound per $^{\circ}R$; C_p for gasoline vapor, 0.410 Btu per pound per $^{\circ}R$. The latter value is the mean C_p between 60° and 260° F.

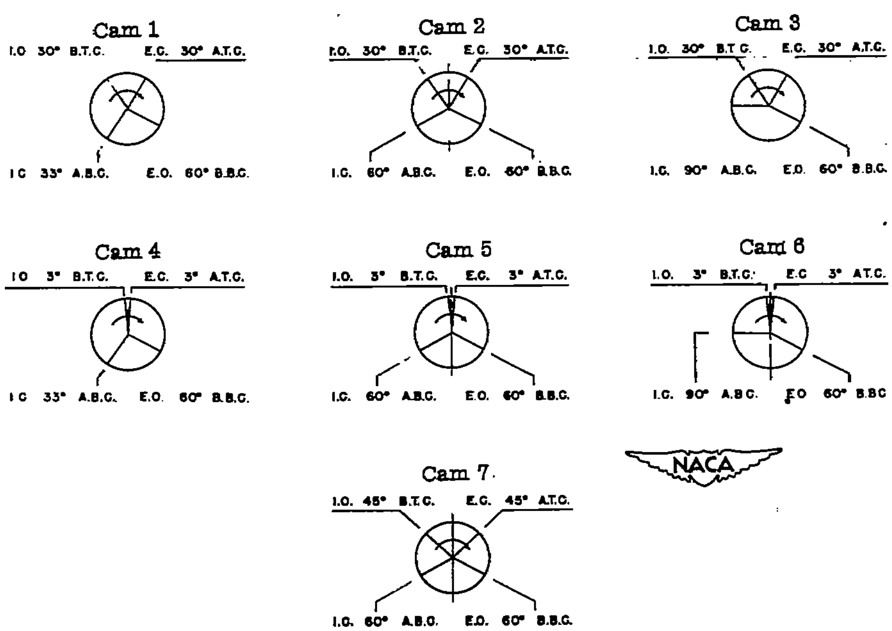

Figure 4.- Timing diagrams for cams used in CFR engine tests. I.O., inlet opens; I.C., inlet closes; E.O., exhaust opens; E.C., exhaust closes.

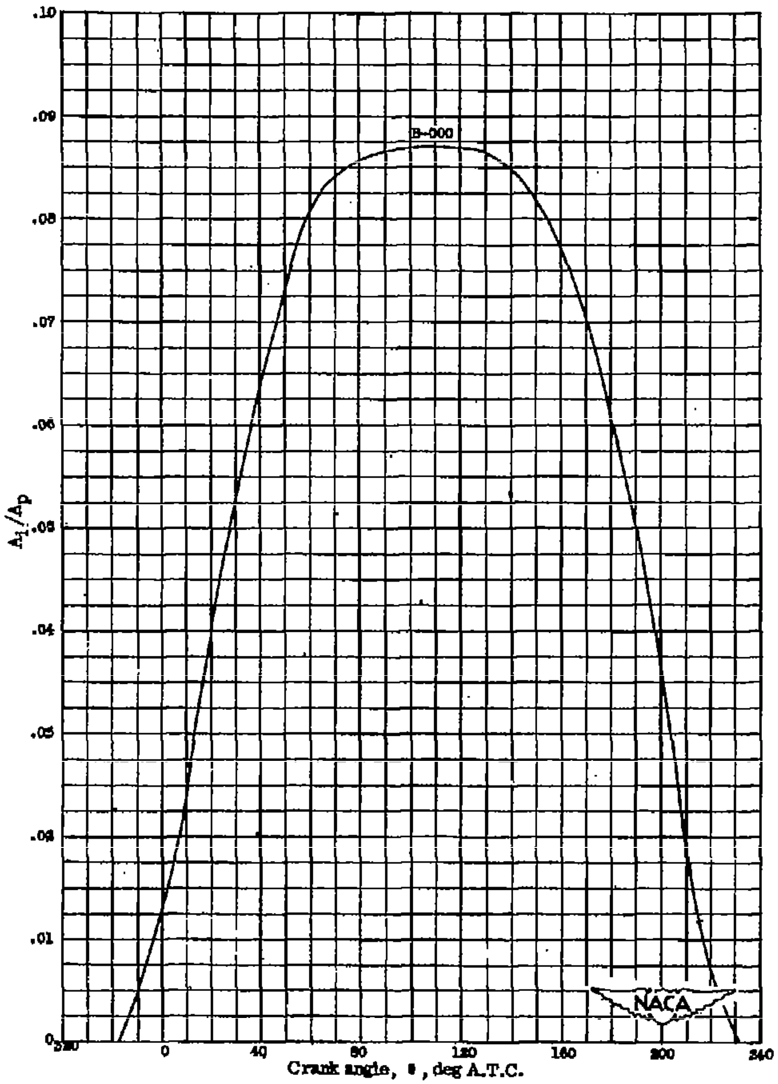

Figure 5.- Valve-opening curve of A_i/A_p against crank angle. Bore-stroke engine; inlet-valve opening duration, 250° crank angle; inlet opens, 343° A.T.C.; inlet closes, 233° A.T.C.

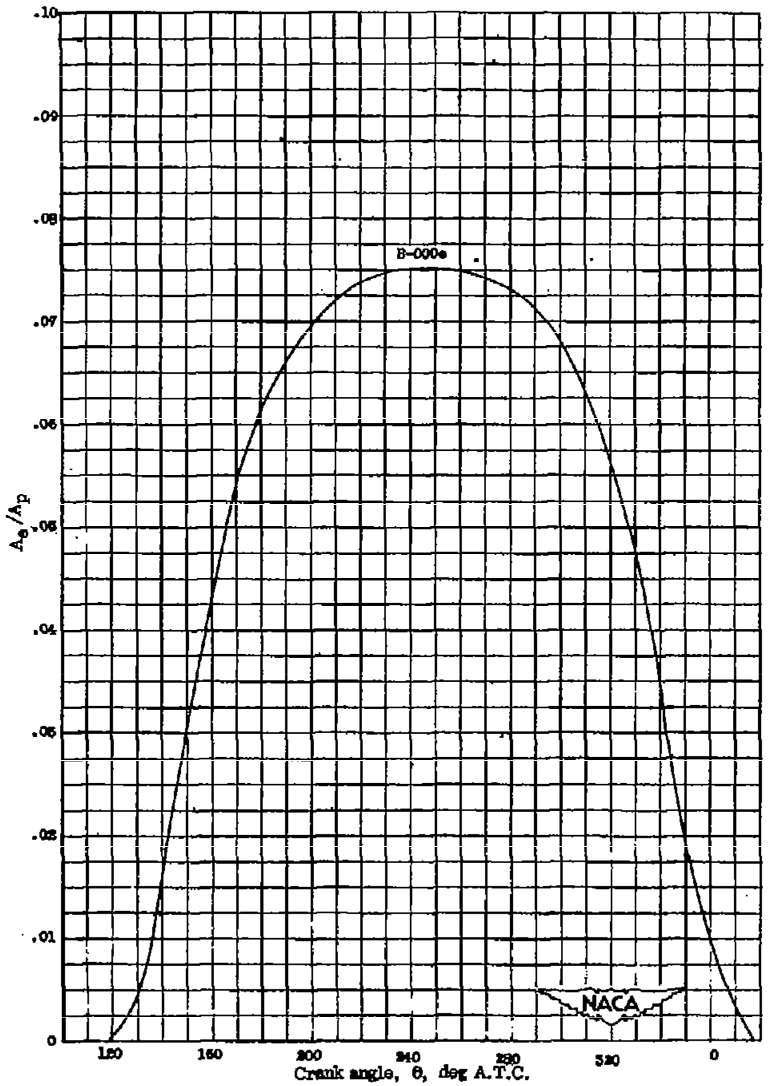

Figure 6.- Valve-opening curve of A_e/A_p against crank angle. Bore-stroke engine; exhaust-valve opening duration, 260° crank angle; exhaust opens, 119° A.T.C.; exhaust closes, 19° A.T.C.

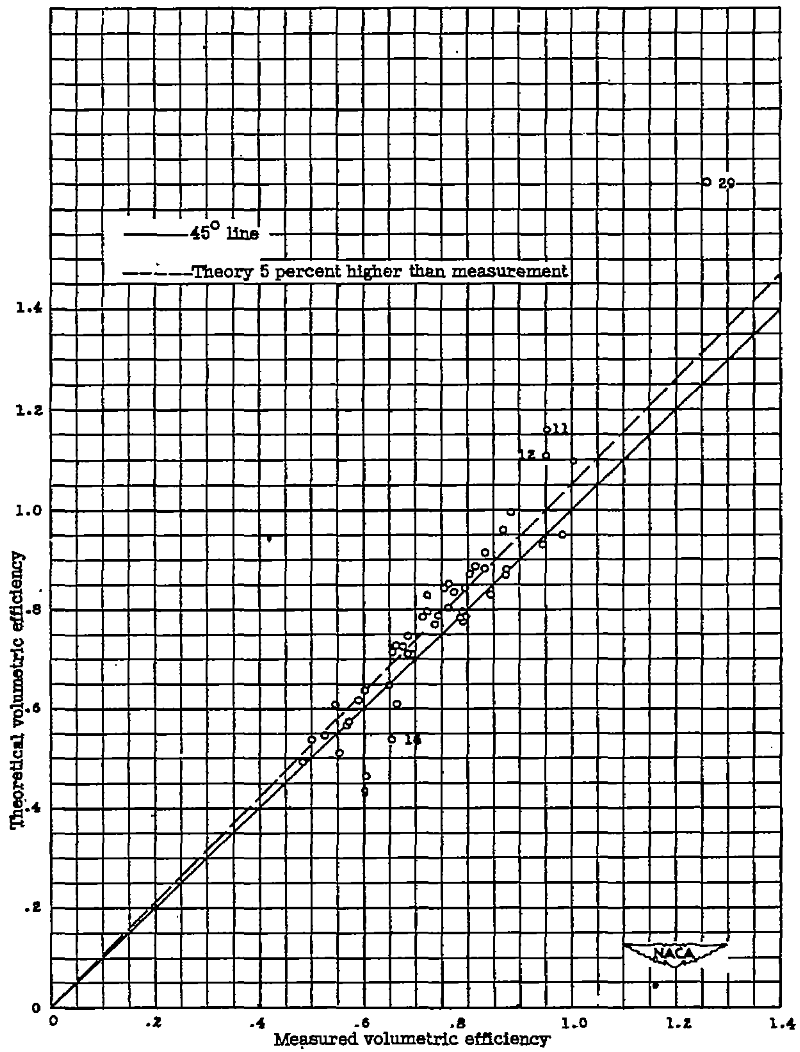

Figure 7.- Over-all comparison of calculated and measured volumetric efficiencies.
[illegible] fer to [illegible]

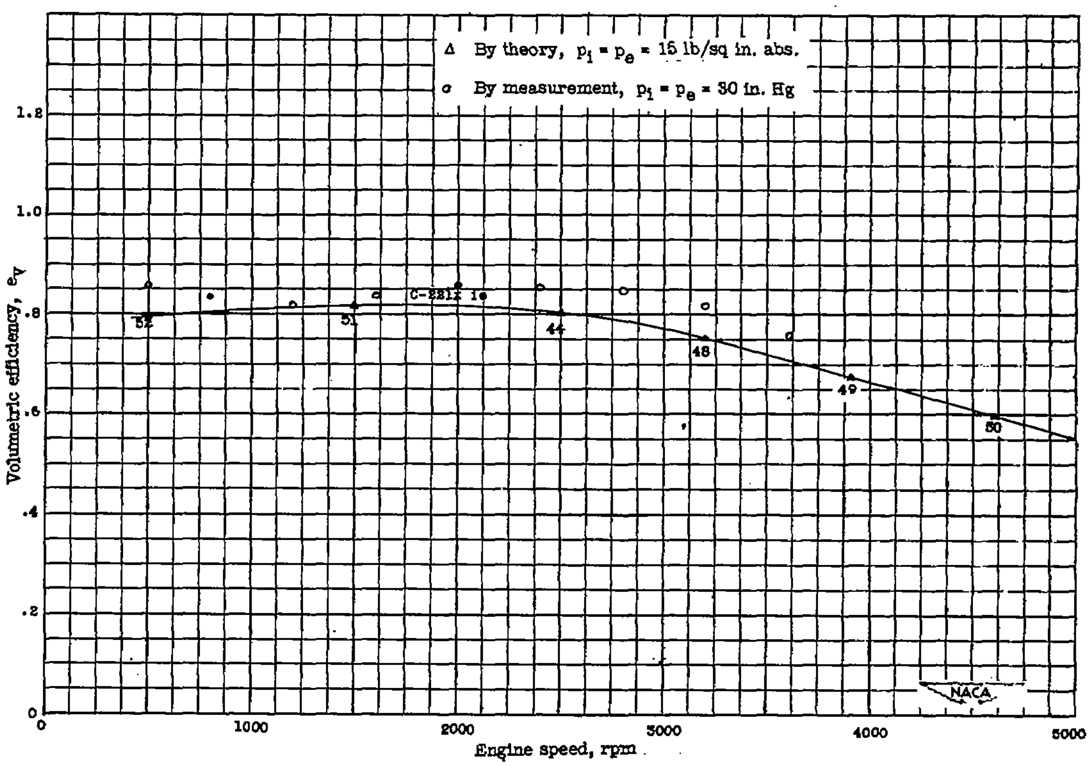

Figure 8.- Variation of volumetric efficiency with engine speed. CFR engine; cam 2: large valve, large lift. Numbers refer to solutions.

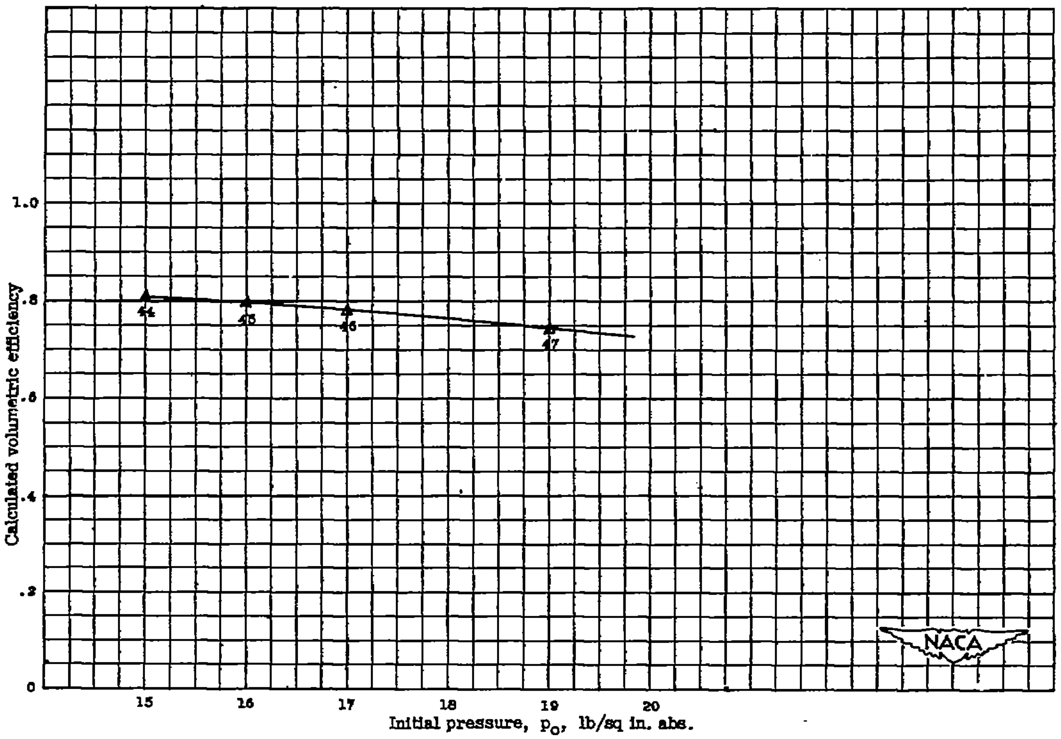

Figure 9.- Variation of calculated volumetric efficiency with initial pressure for inlet processes. $p_i = p_e = 15$ pounds per square inch absolute. Numbers refer to solutions.

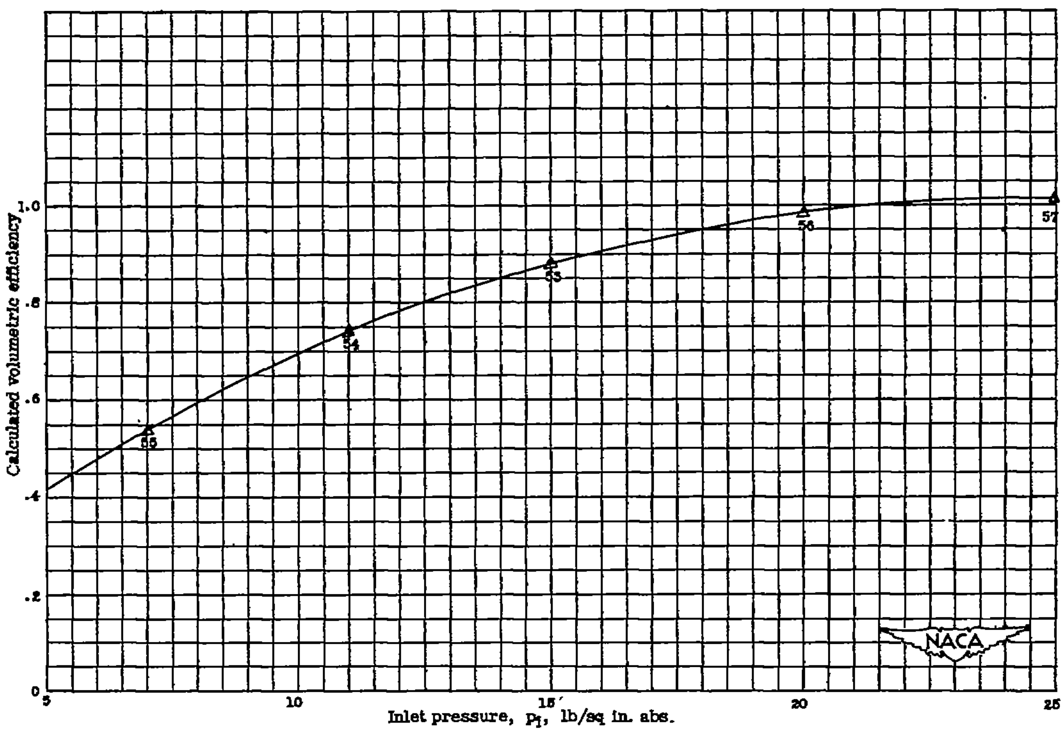

Figure 10.- Variation of calculated volumetric efficiency with inlet pressure. Exhaust pressure, 15 pounds per square inch absolute. Numbers refer to solutions.

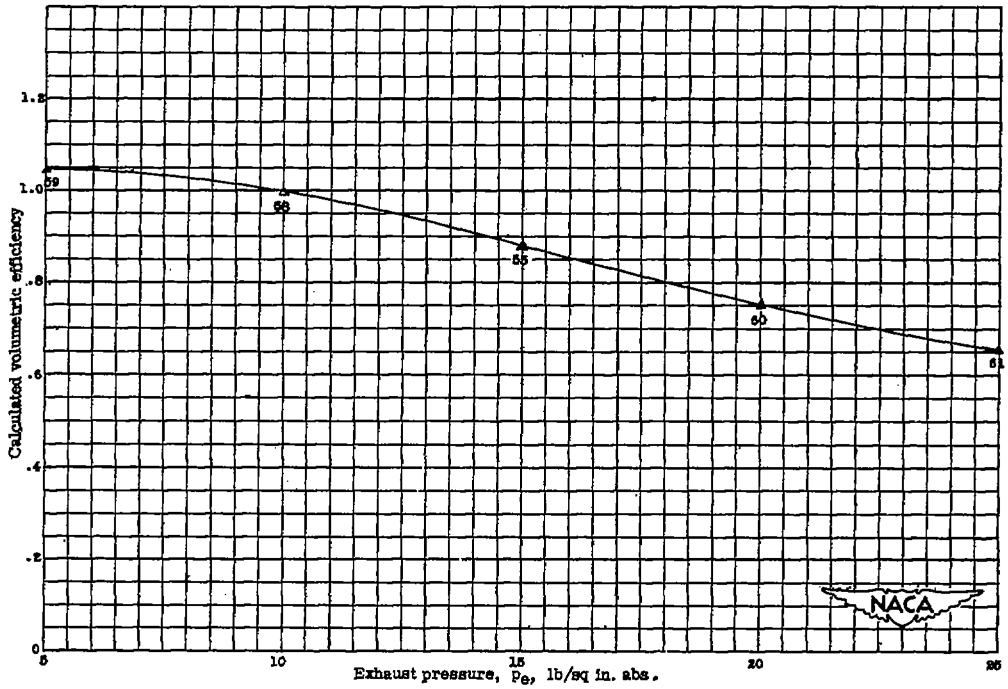

Figure 11.- Variation of calculated volumetric efficiency with exhaust pressure. Inlet pressure, 15 pounds per square inch absolute. Numbers refer to solutions.

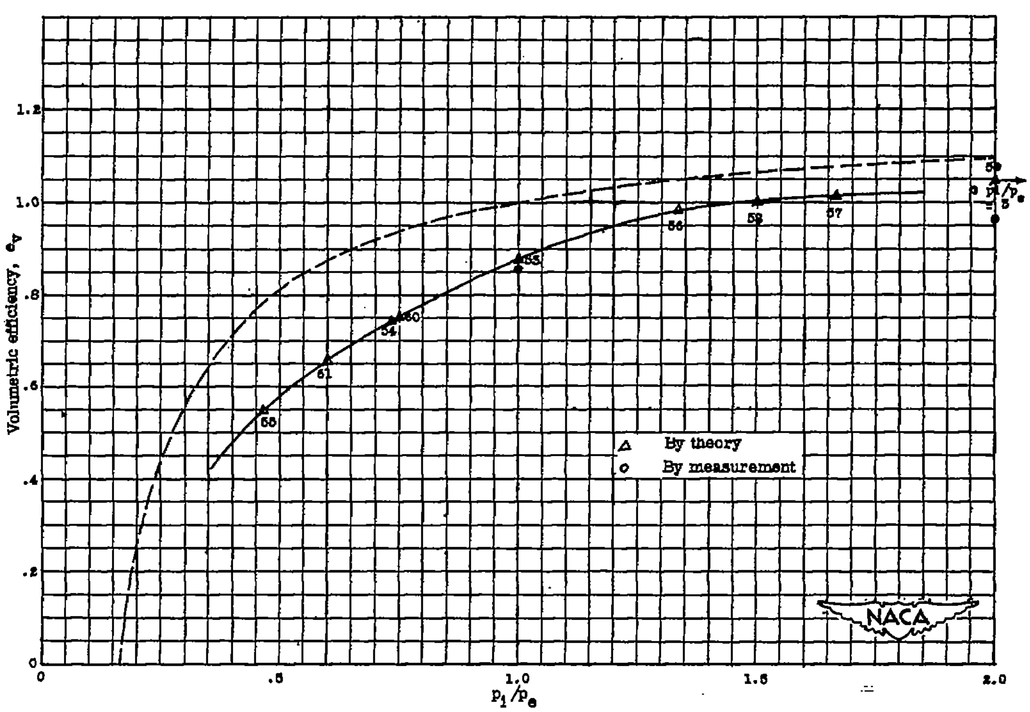

(a) Varying p_i/p_e ratio.

Figure 12.- Variation of volumetric efficiency with pressure ratio. CFR engine; large inlet valve, large lift; standard exhaust valve; engine speed, 2500 rpm; inlet opens, 30° B.T.C., inlet closes, 60° A.B.C., exhaust opens, 58° B.B.C., exhaust closes, 28° A.T.C. Dashed curve represents the equation $e_v = 1 + \dfrac{1-(p_e/p_i)}{k_i(r-1)}$ where $k_i(r-1) = 5.28$.

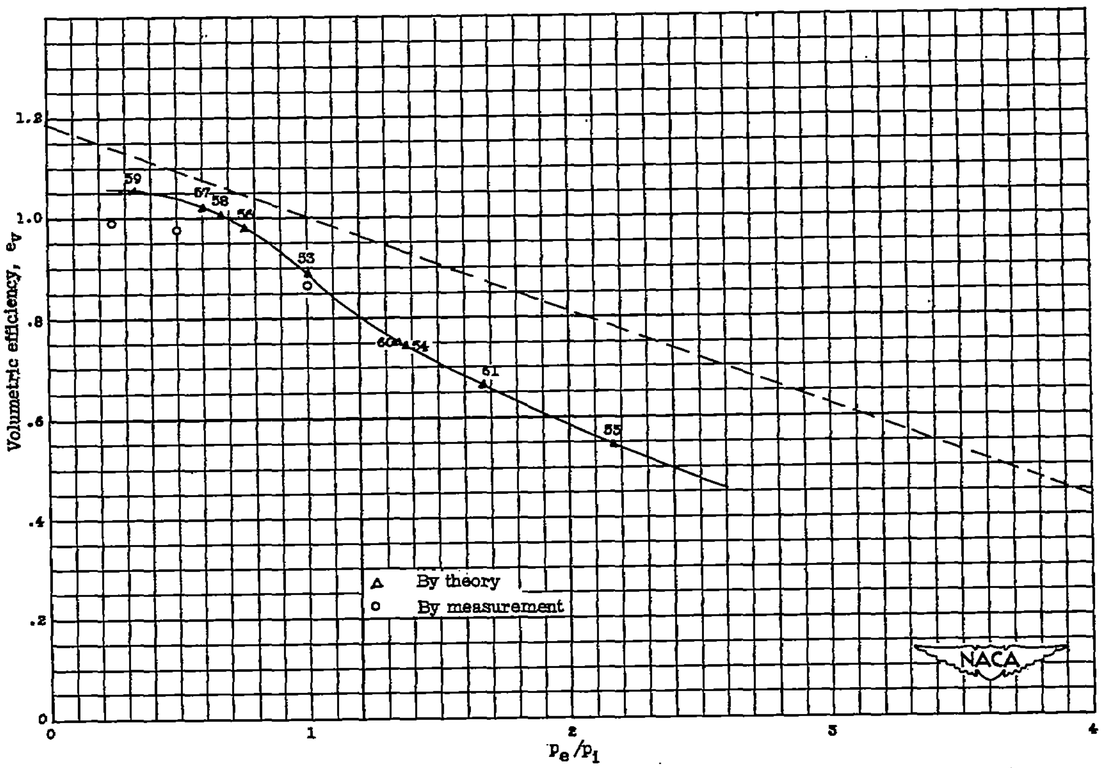

(b) Varying p_e/p_i ratio.

Figure 12.- Concluded.

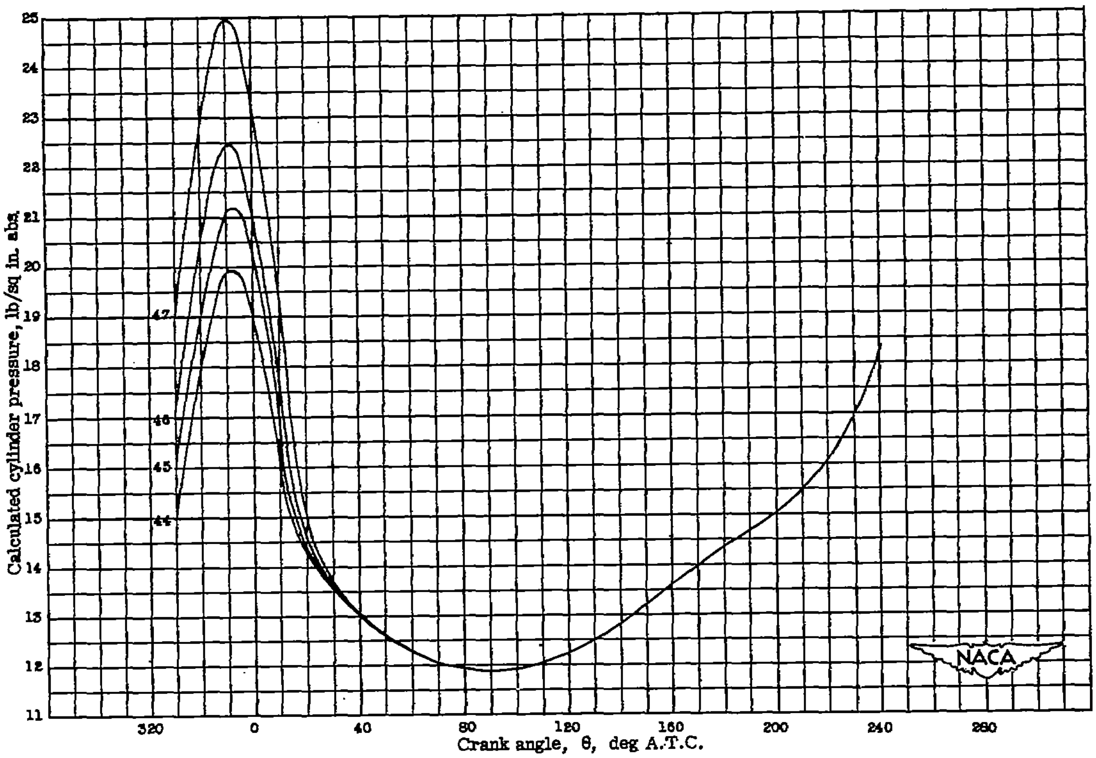

Figure 13.- Calculated indicator diagrams for inlet processes. Varying initial pressure p_o. Numbers refer to solutions.

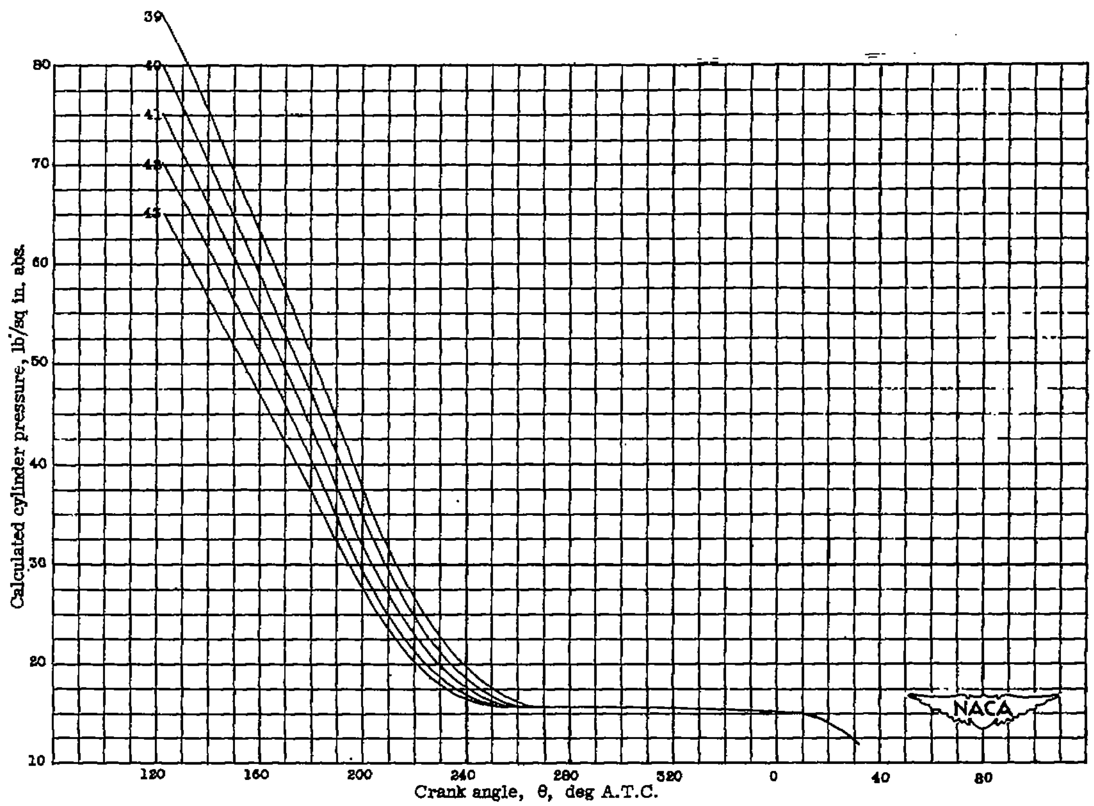

Figure 14.- Calculated indicator diagrams for exhaust processes. Varying initial pressure p_o. Numbers refer to solutions.

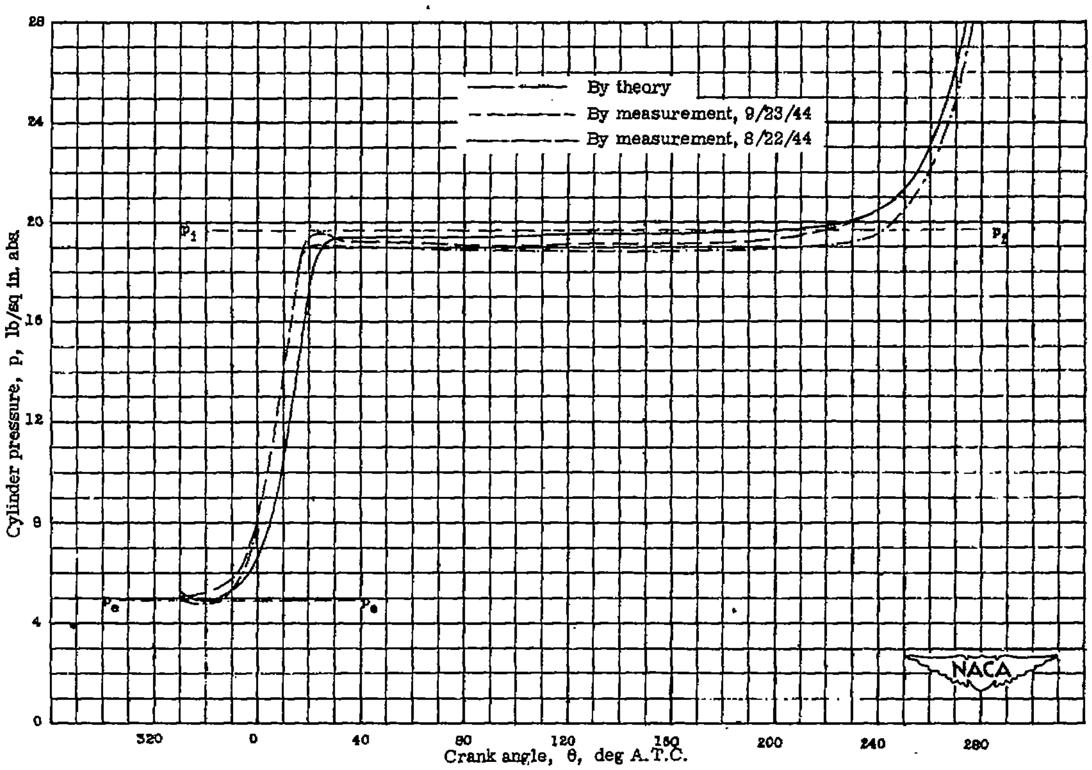

Figure 15.- Indicator diagram for solution 11. (See table II.)

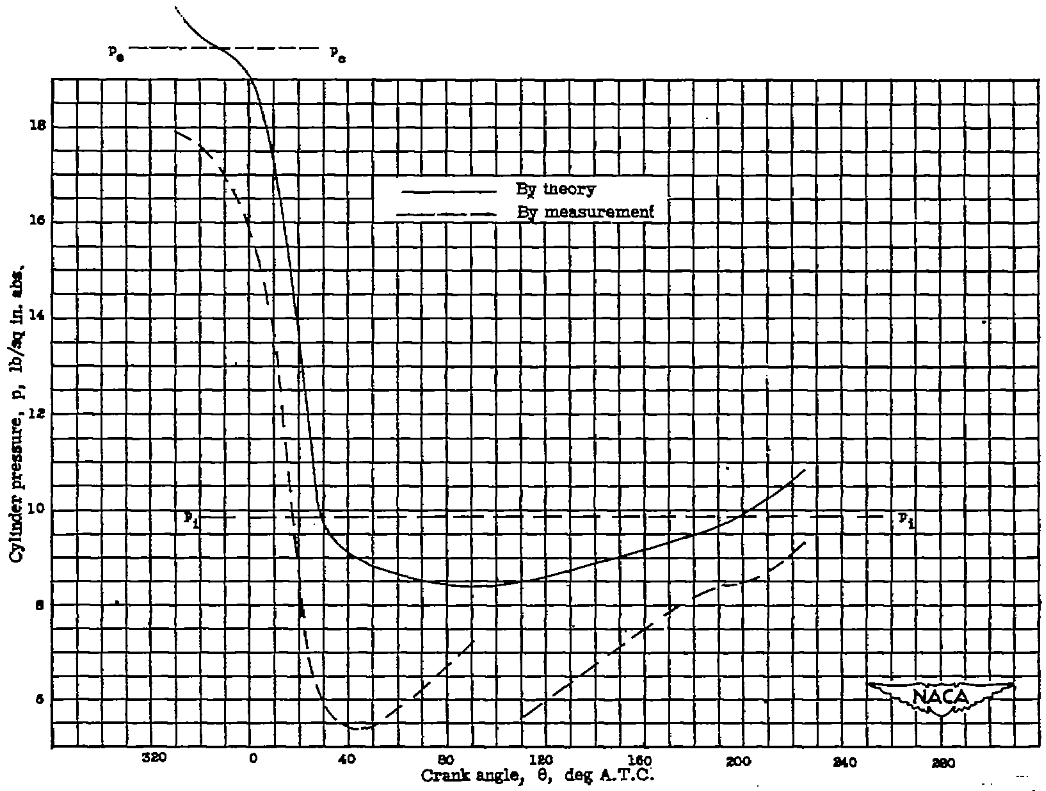

Figure 16.- Indicator diagram for solution 16. (See table II.)

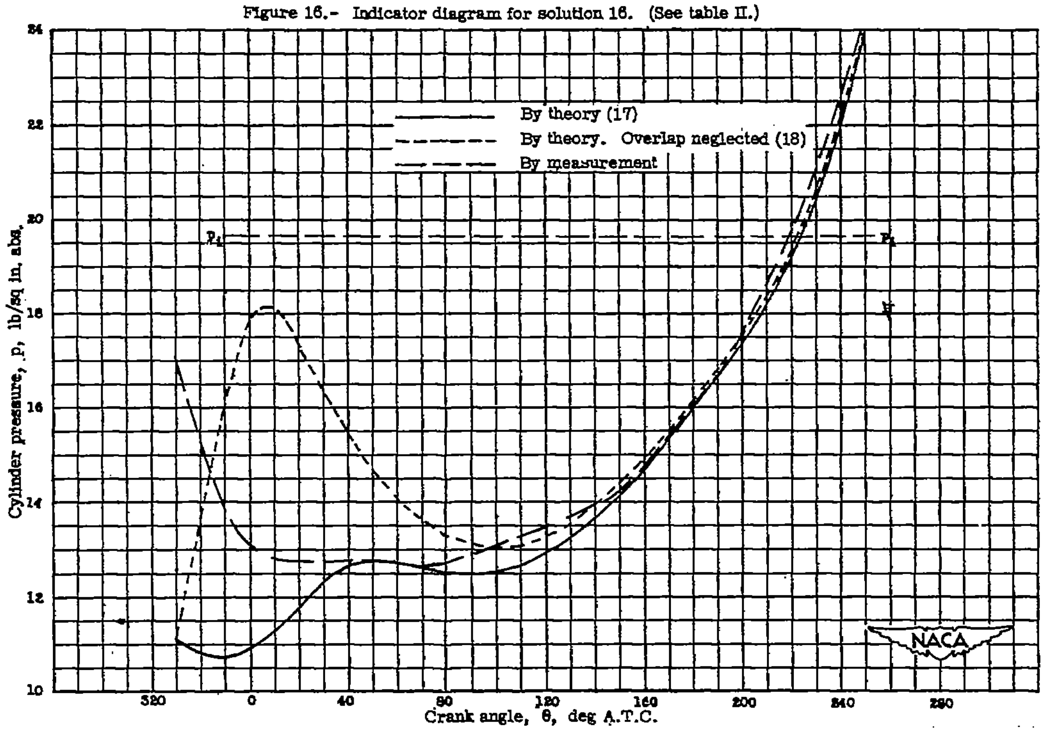

Figure 17.- Indicator diagrams for solutions 17 and 18. Exhaust pressure, 9.82 pounds per square inch absolute. (See table II.)

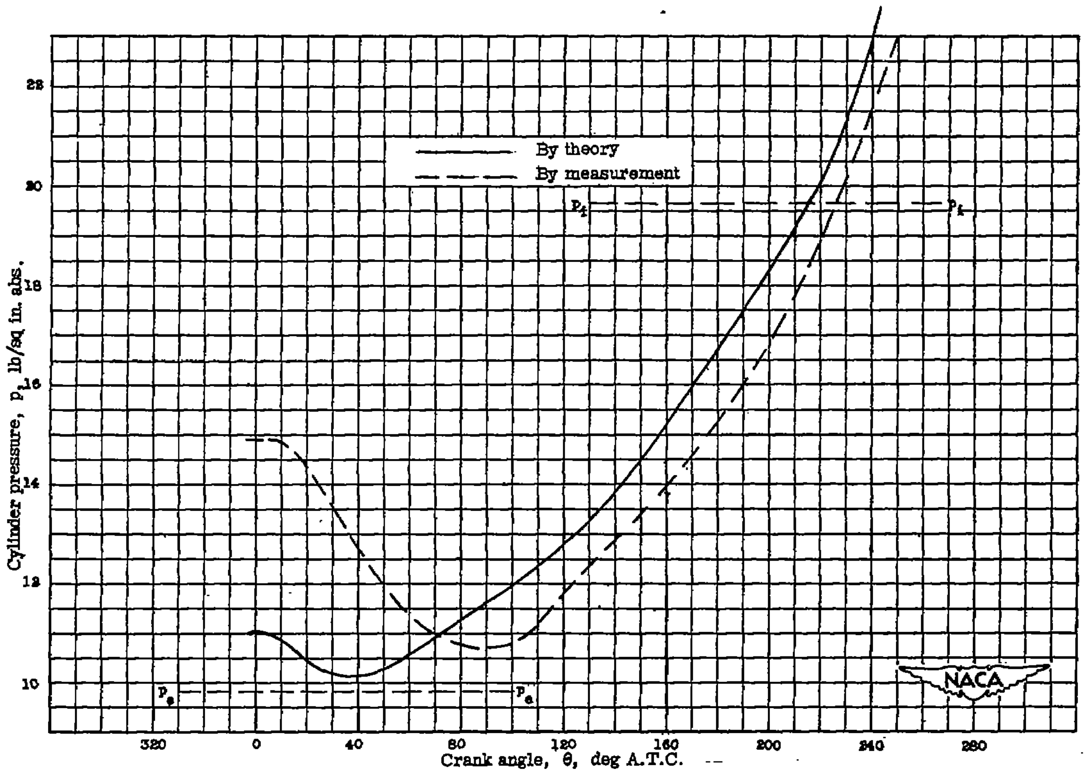

Figure 18.- Indicator diagram for solution 19.1. (See table II.)

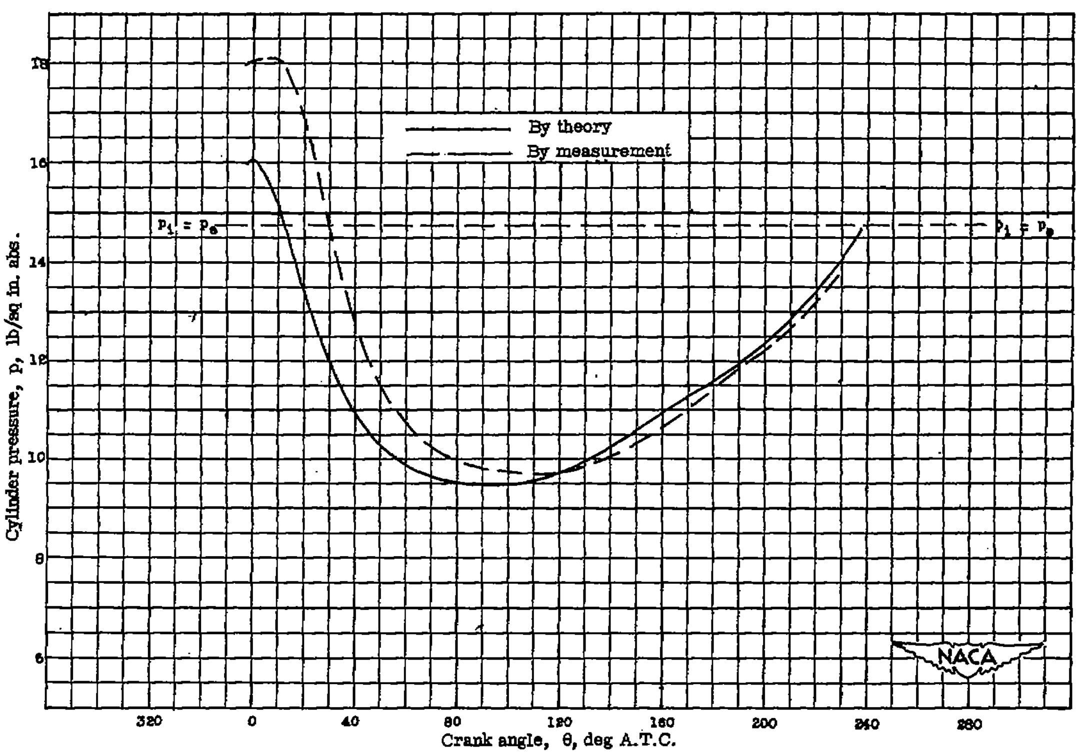

Figure 19.- Indicator diagram for solution 20. (See table II.)

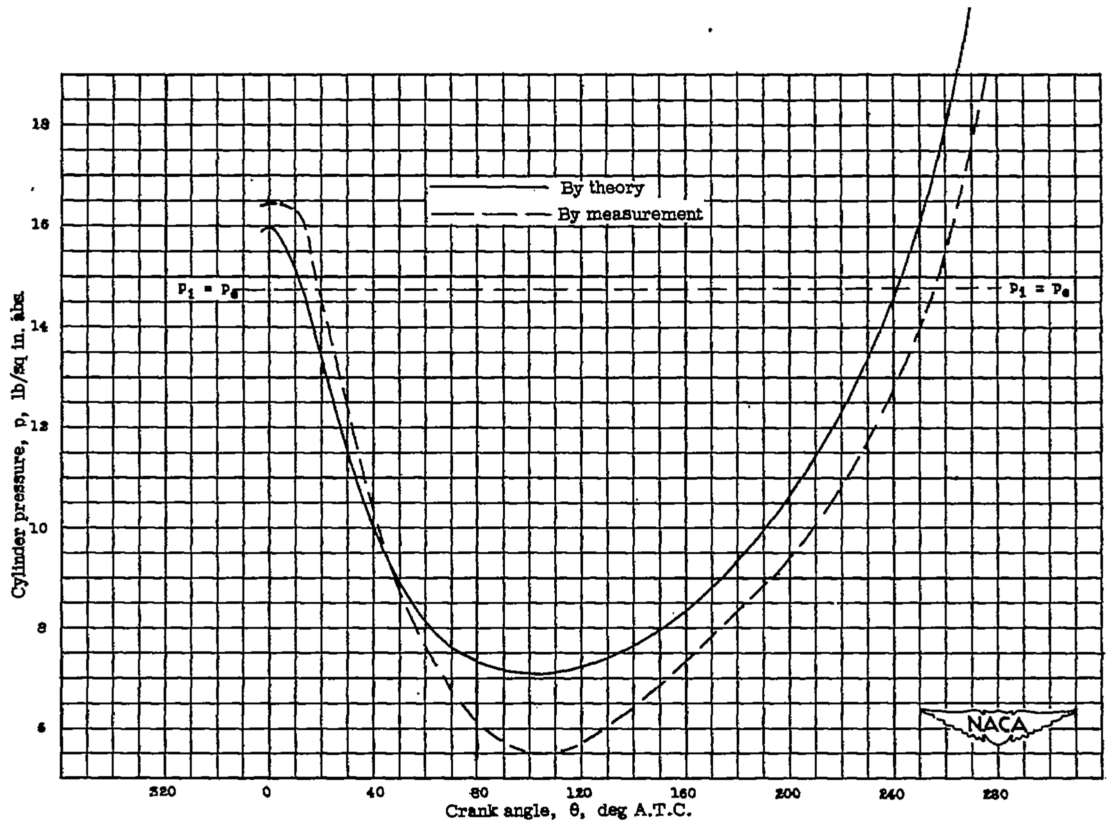

Figure 20.- Indicator diagram for solution 25.1. (See table II.)

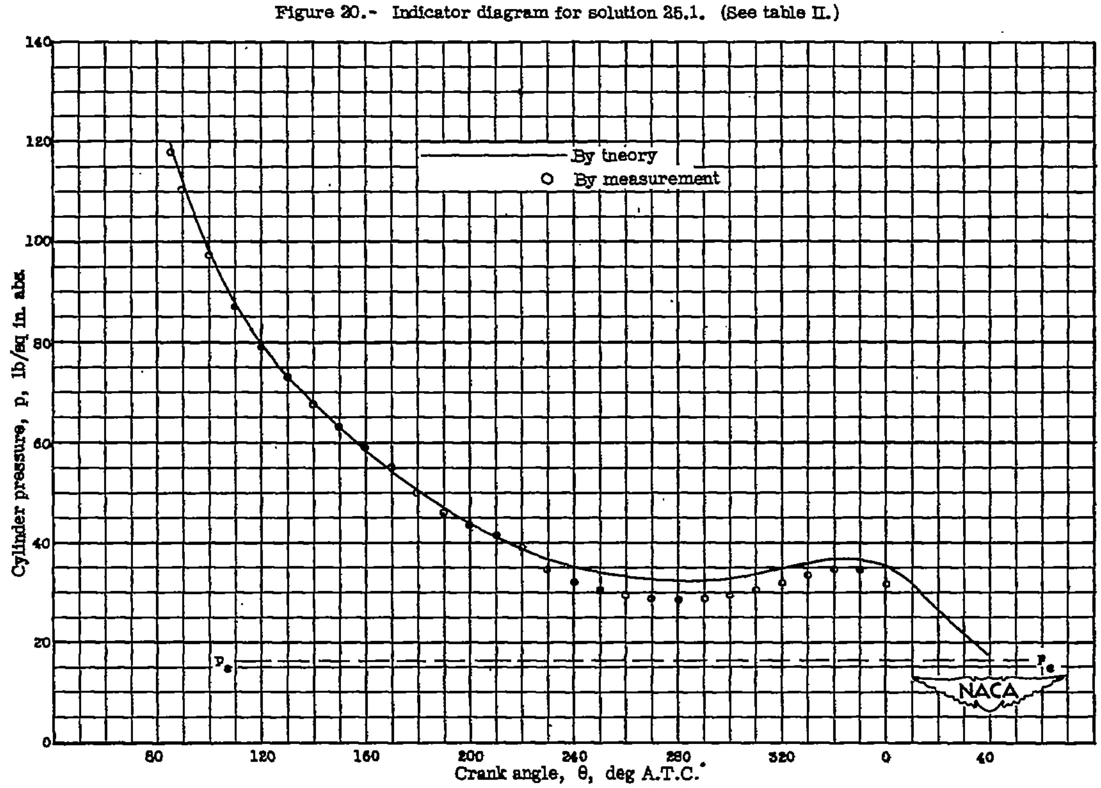

Figure 21.- Indicator diagram for solution 63. (See table II.)

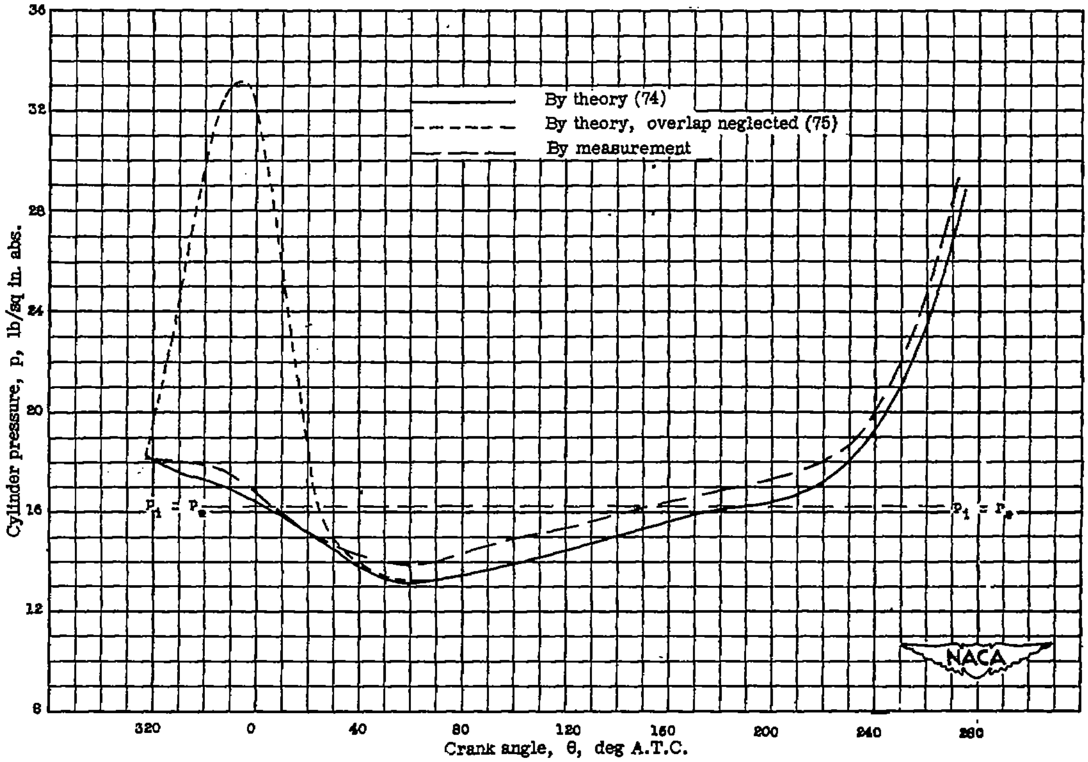

Figure 22.- Indicator diagrams for solutions 74 and 75. (See table II.)

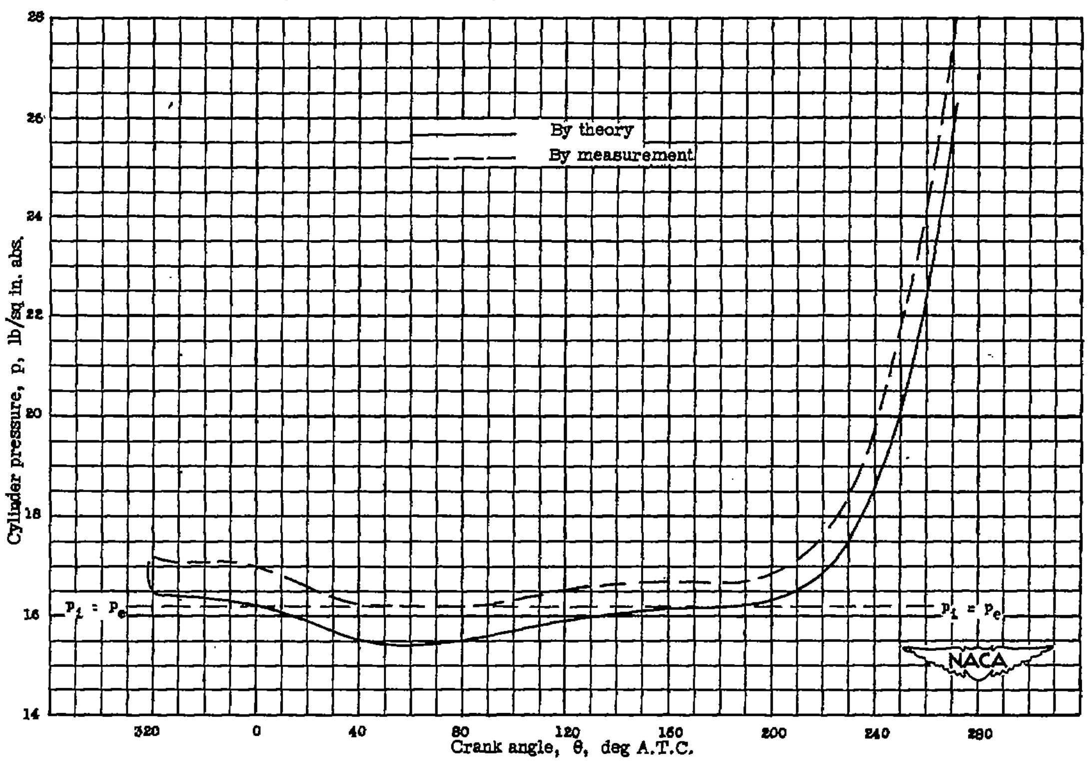

Figure 23.- Indicator diagram for solution 77. (See table II.)

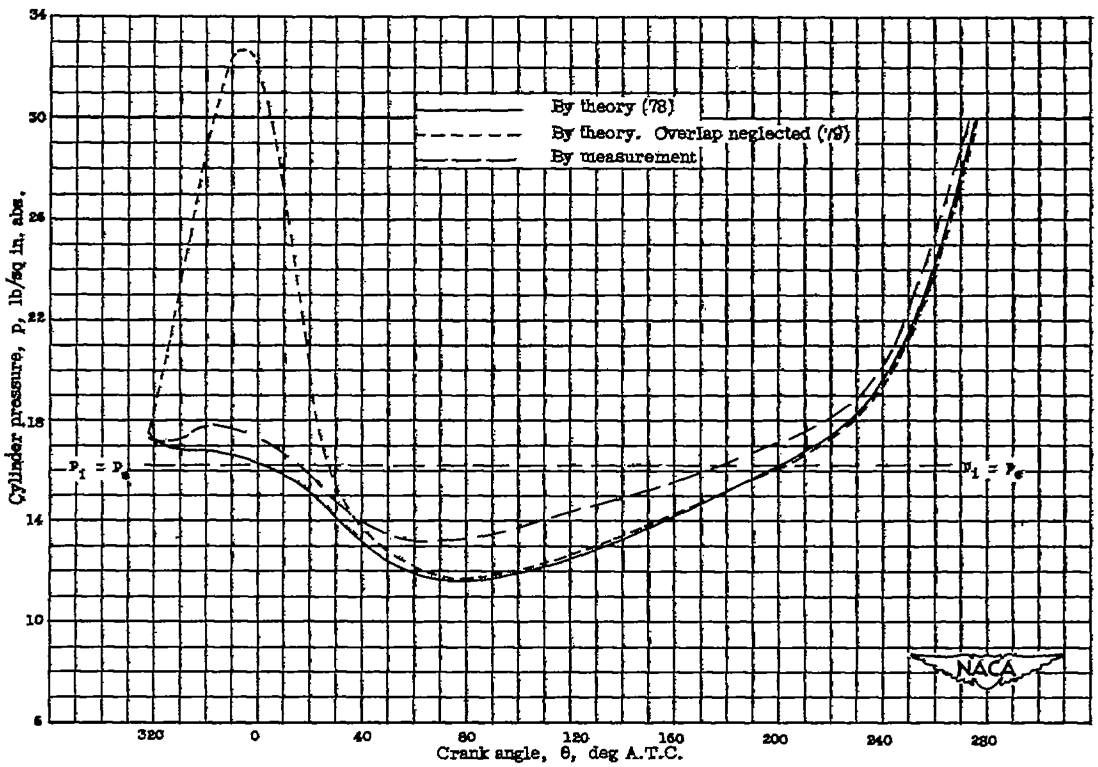

Figure 24.- Indicator diagrams for solutions 78 and 79. (See table II.)

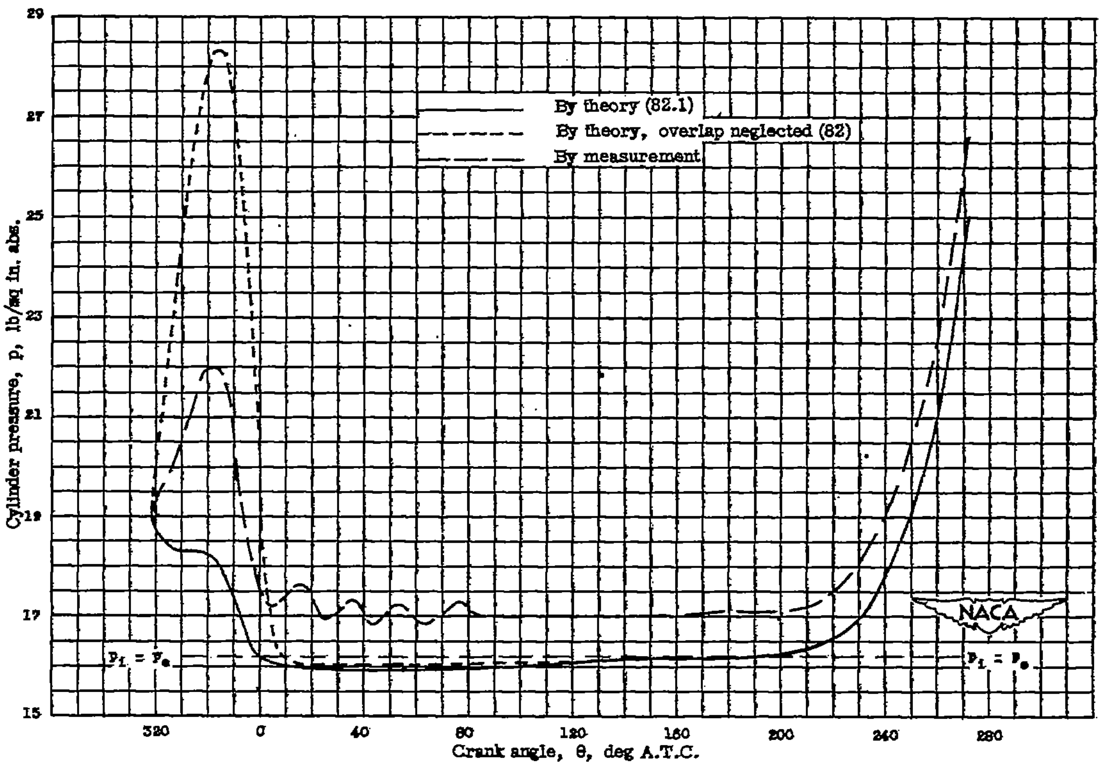

Figure 25.- Indicator diagrams for solutions 82 and 82.1. (See table II.)

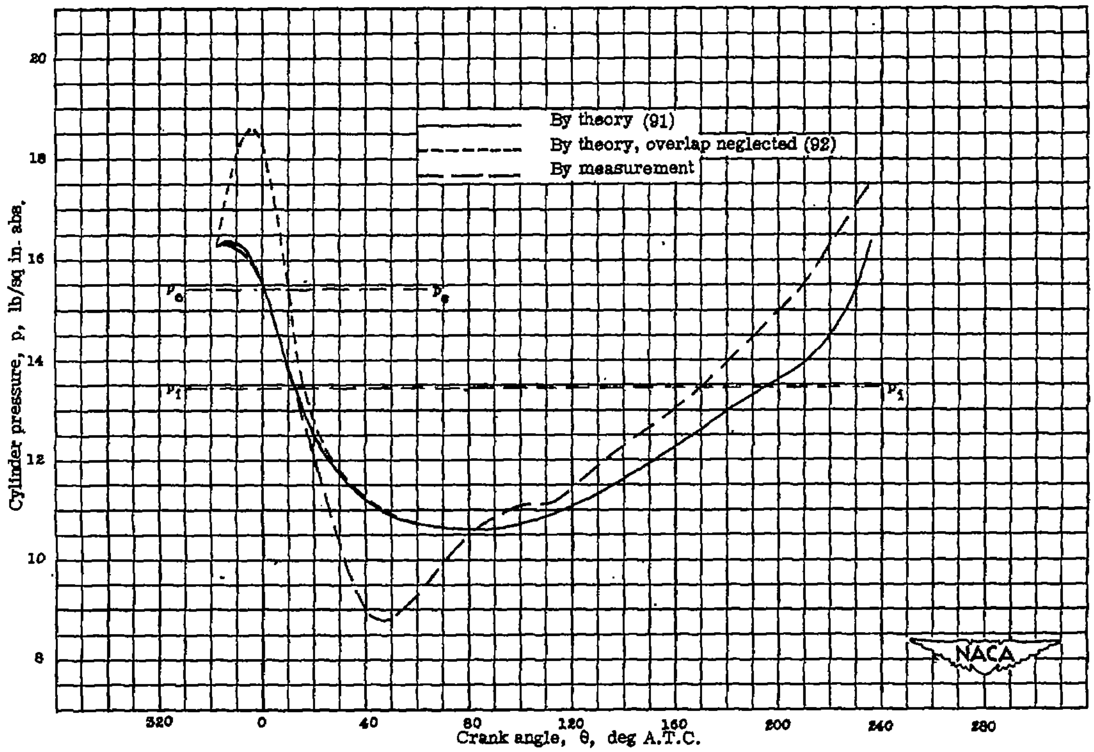

Figure 26.- Indicator diagrams for solutions 91 and 92. (See table II.)

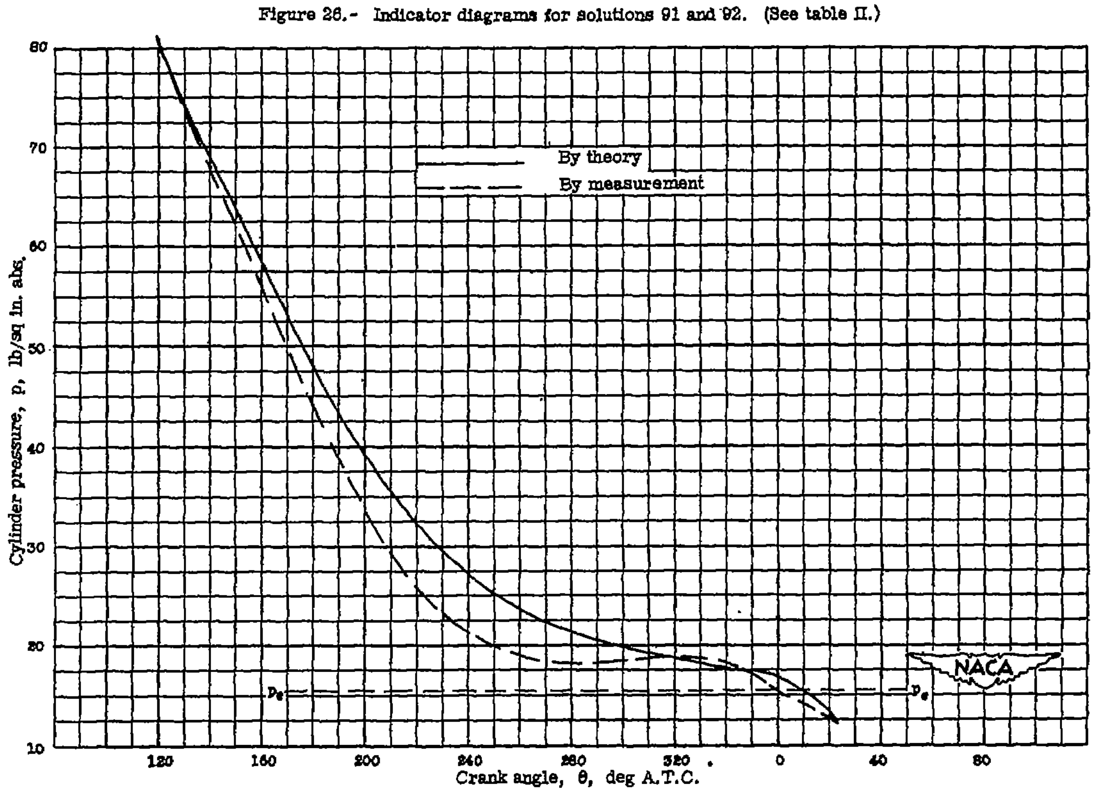

Figure 27.- Indicator diagram for solution 98. (See table II.)

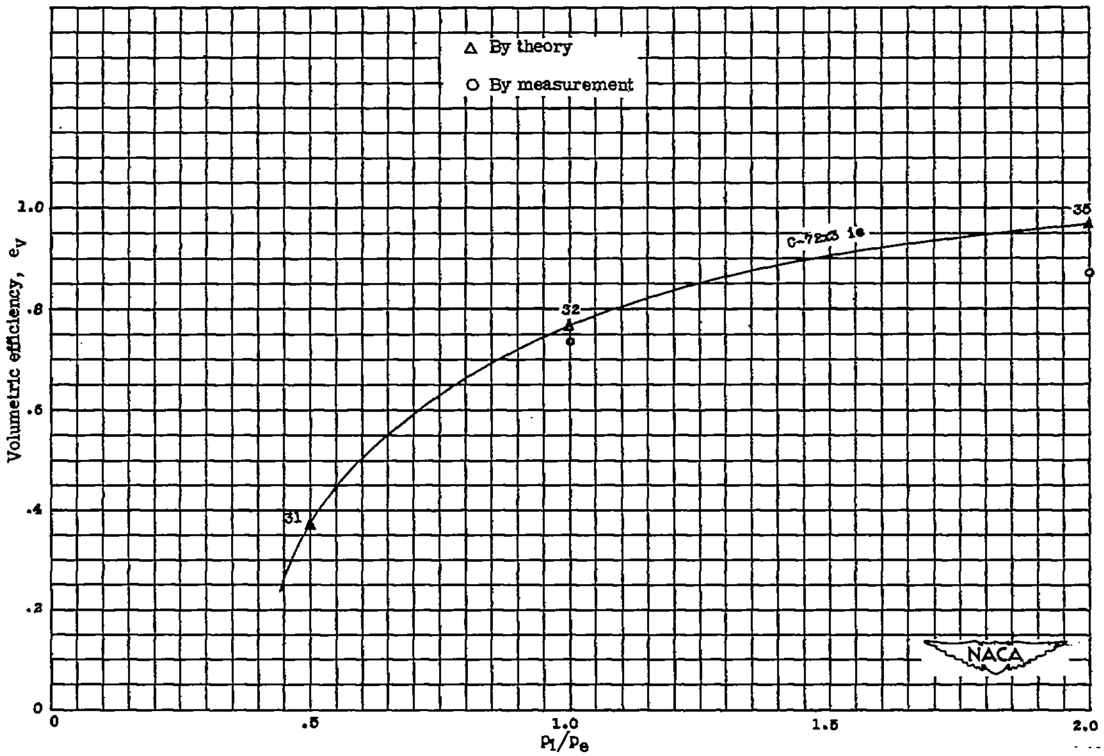

Figure 28.- Variation of volumetric efficiency with pressure ratio. Numbers refer to solutions.

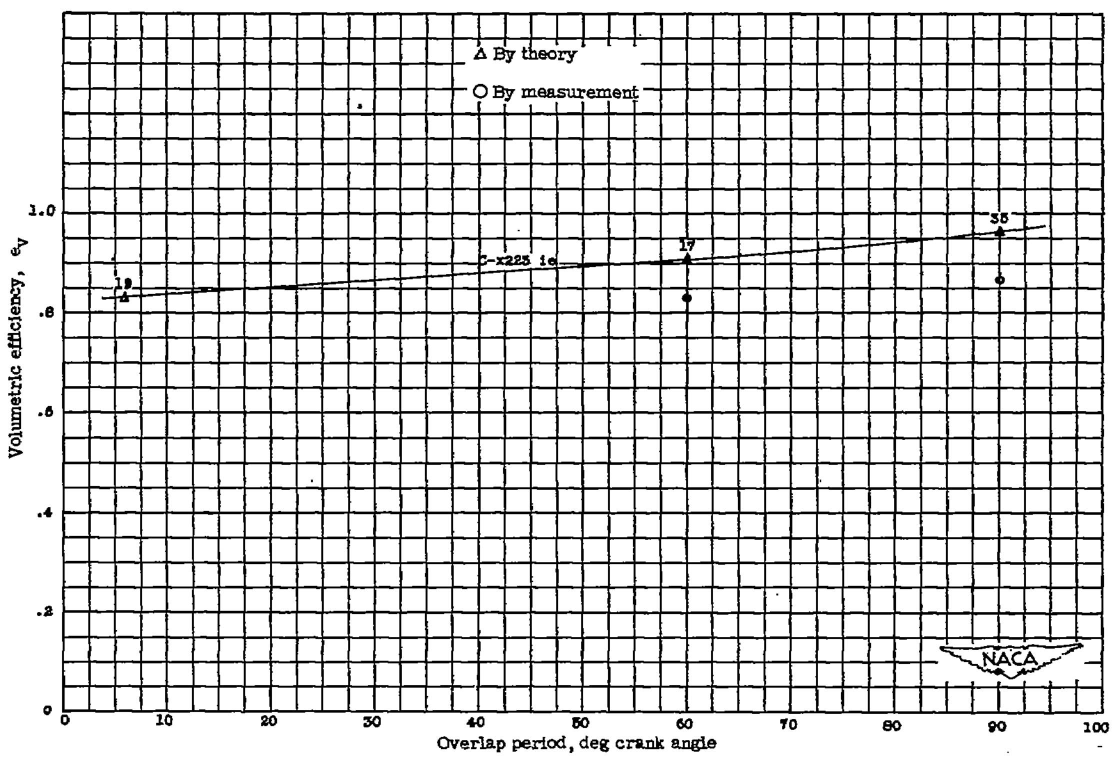

Figure 29.- Variation of volumetric efficiency with overlap period. Numbers refer to solutions.

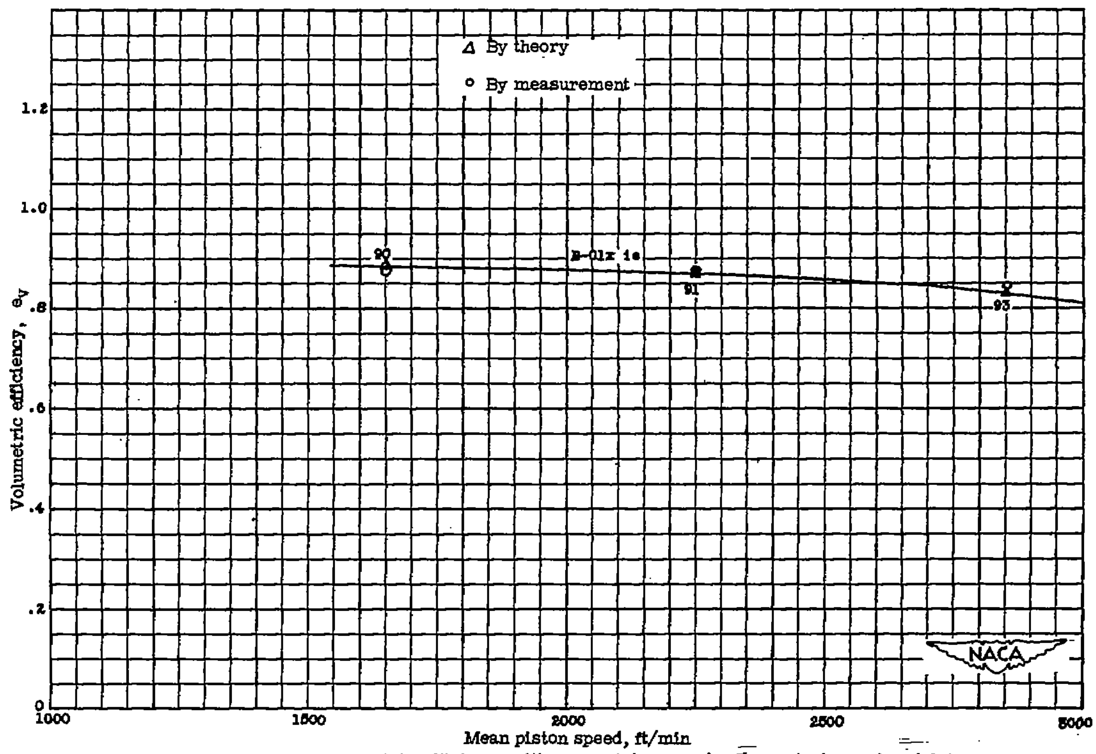

Figure 30.- Variation of volumetric efficiency with mean piston speed. Bore-stroke engine; inlet pressure, 27.4 inches of mercury; exhaust pressure, 31.4 inches of mercury. Numbers refer to solutions.

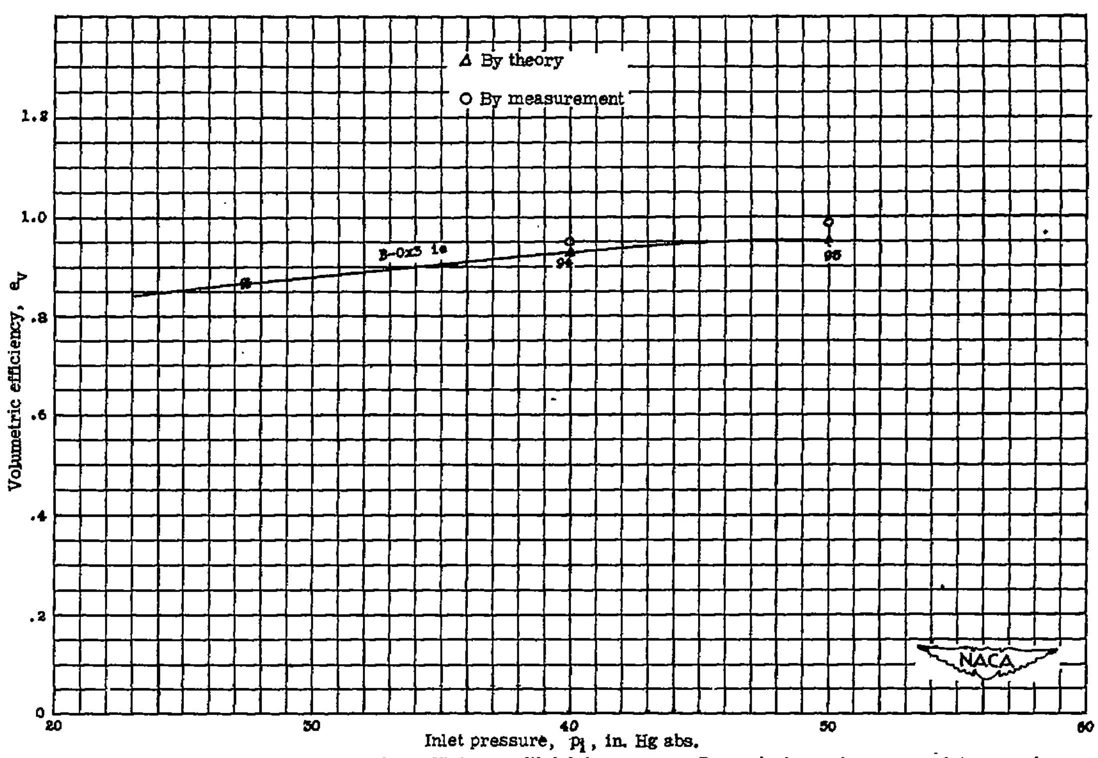

Figure 31.- Variation of volumetric efficiency with inlet pressure. Bore-stroke engine; mean piston speed, 2400 feet per minute. Numbers refer to solutions.

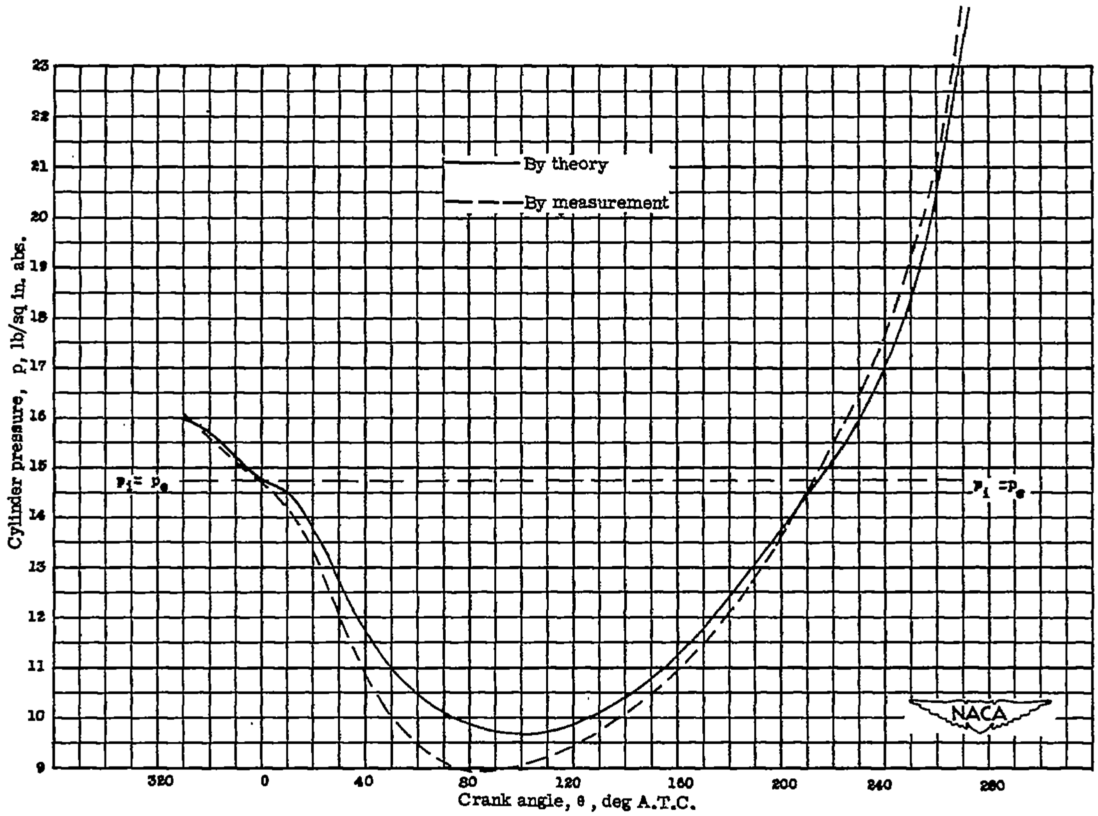

Figure 32.- Indicator diagram for solution 7. (See table II.)

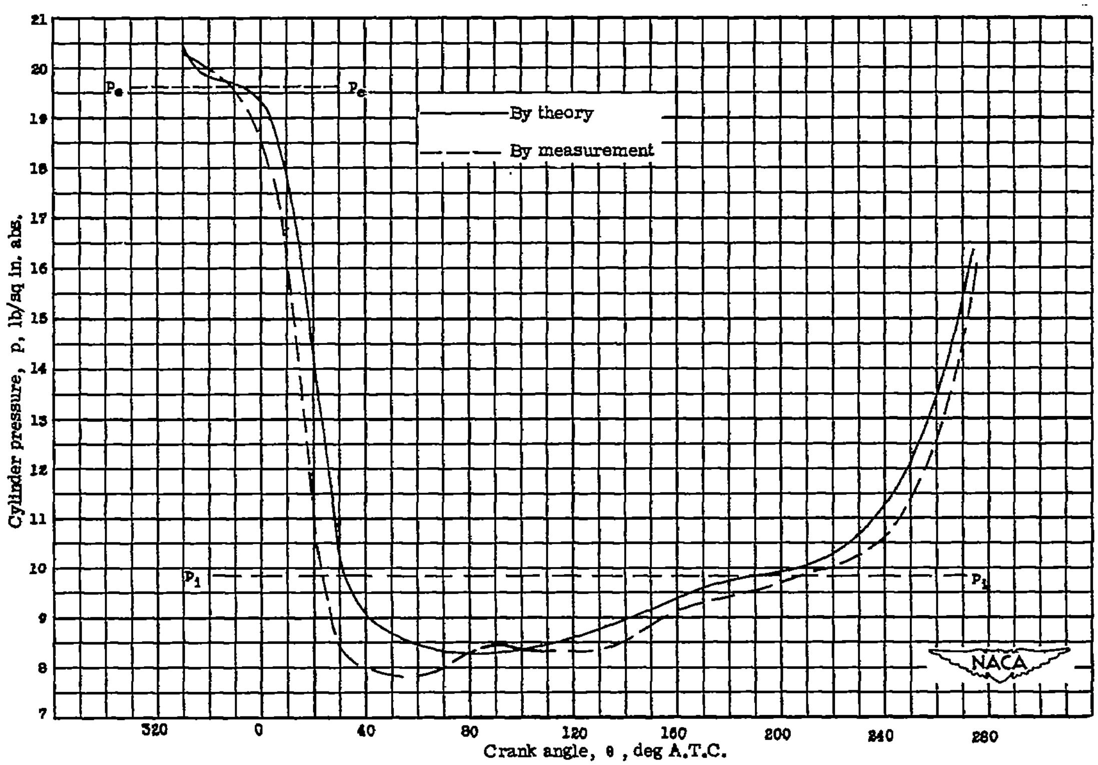

Figure 33.- Indicator diagram for solution 9. (See table II.)

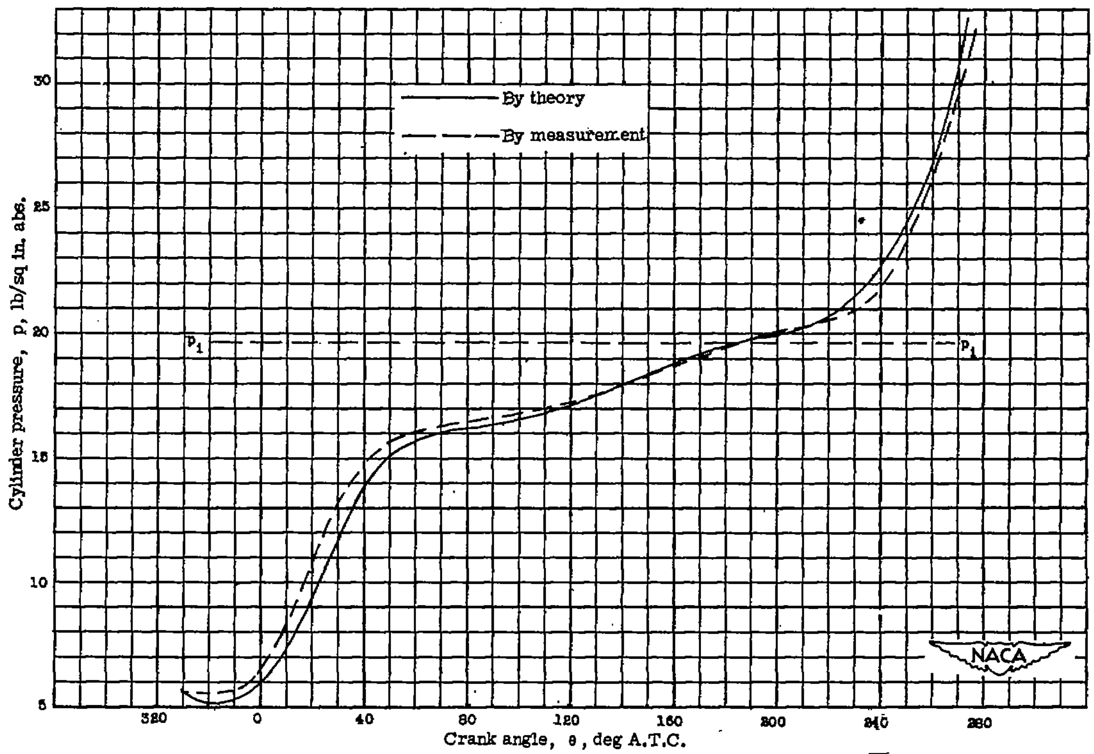

Figure 34.- Indicator diagram for solution 10. Exhaust pressure, 4.91 pounds per square inch absolute. (See table II.)

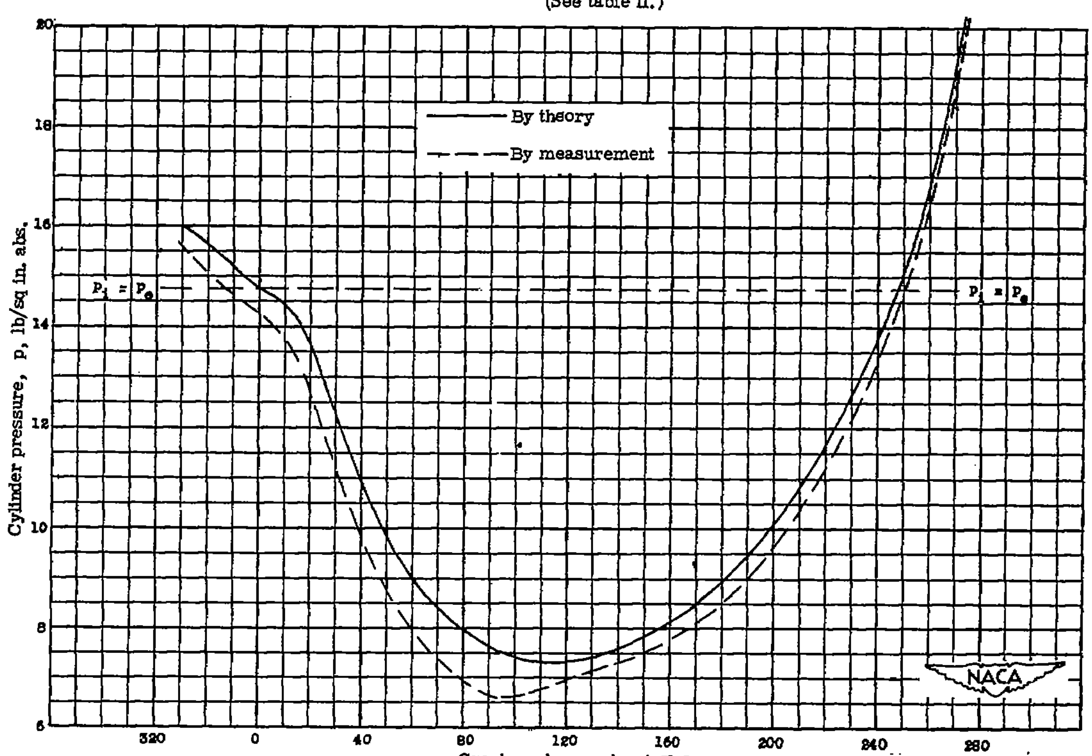

Figure 35.- Indicator diagram for solution 13. (See table II.)

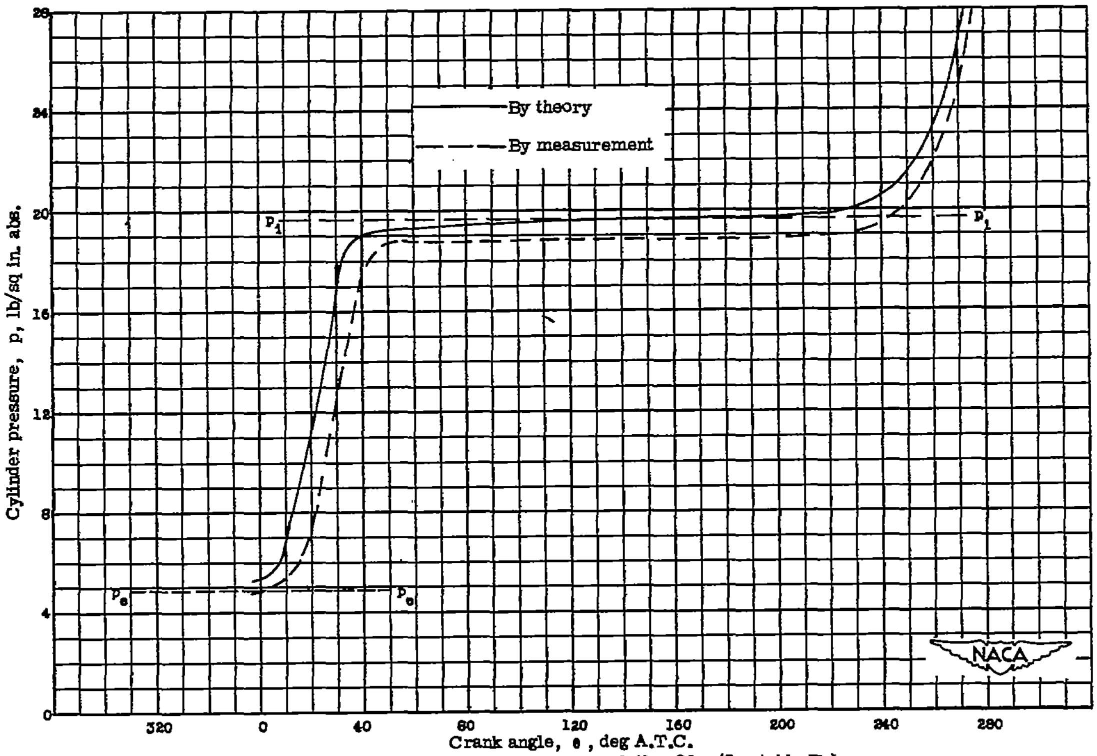

Figure 36.- Indicator diagram for solution 23. (See table II.)

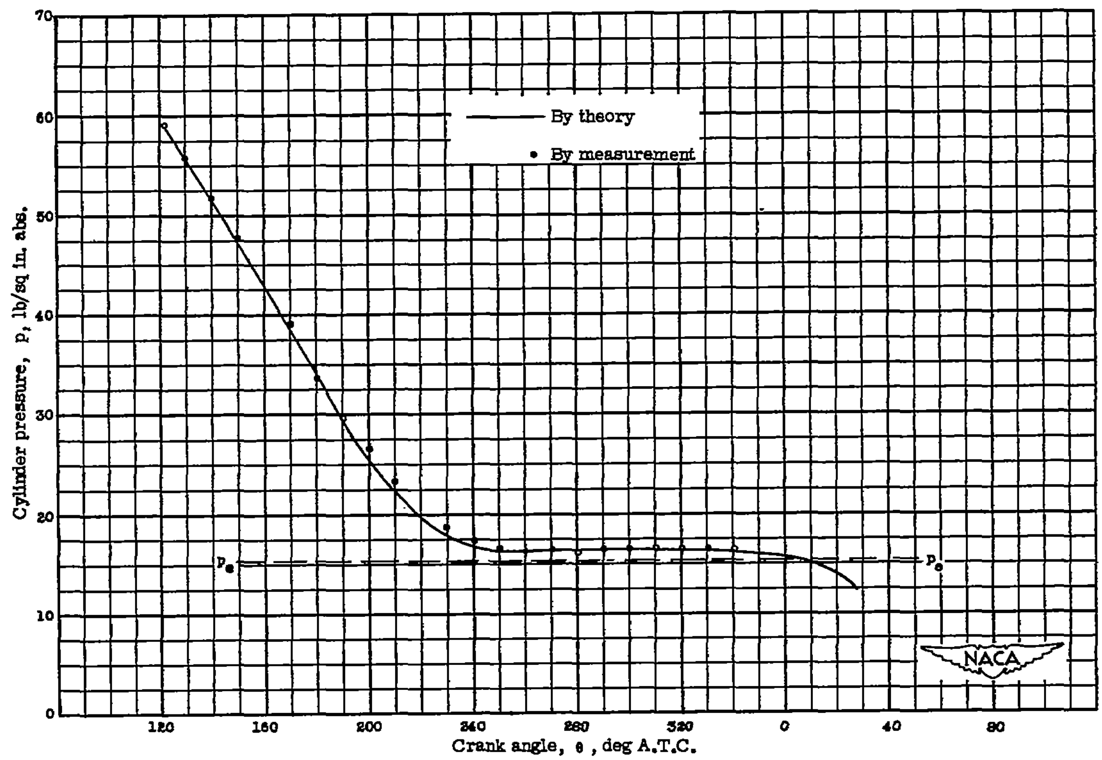

Figure 37.- Indicator diagram for solution 37. (See table II.)

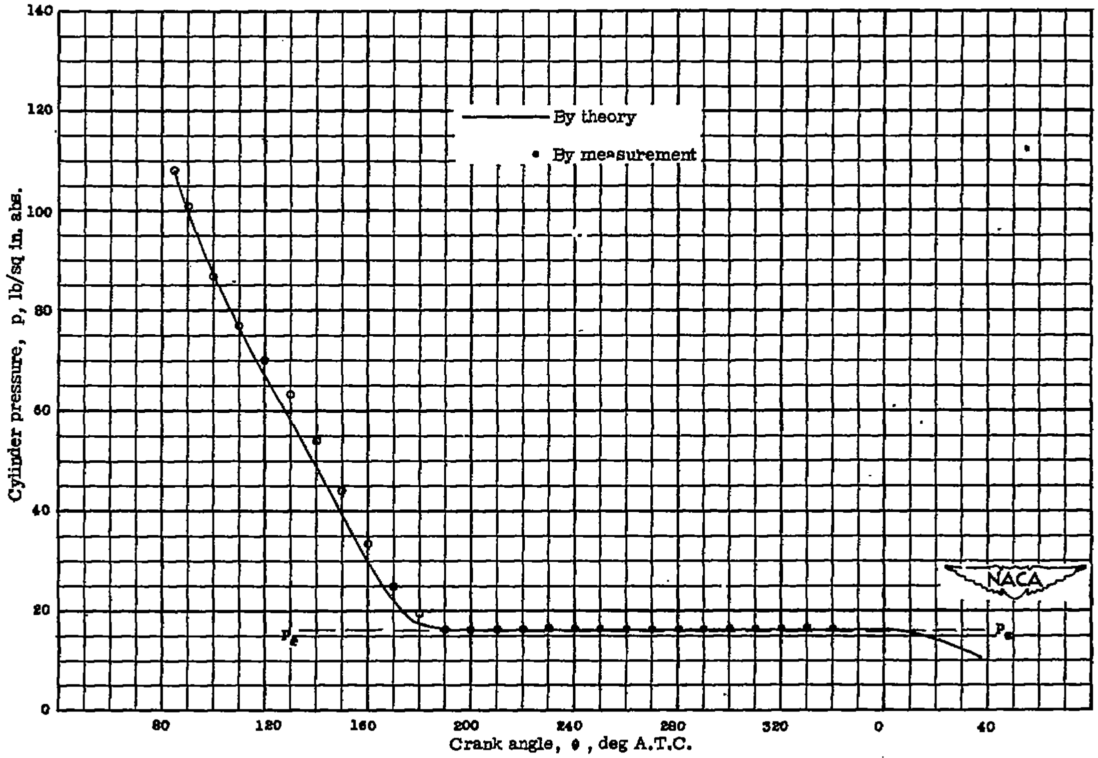

Figure 38.- Indicator diagram for solution 62. (See table II.)

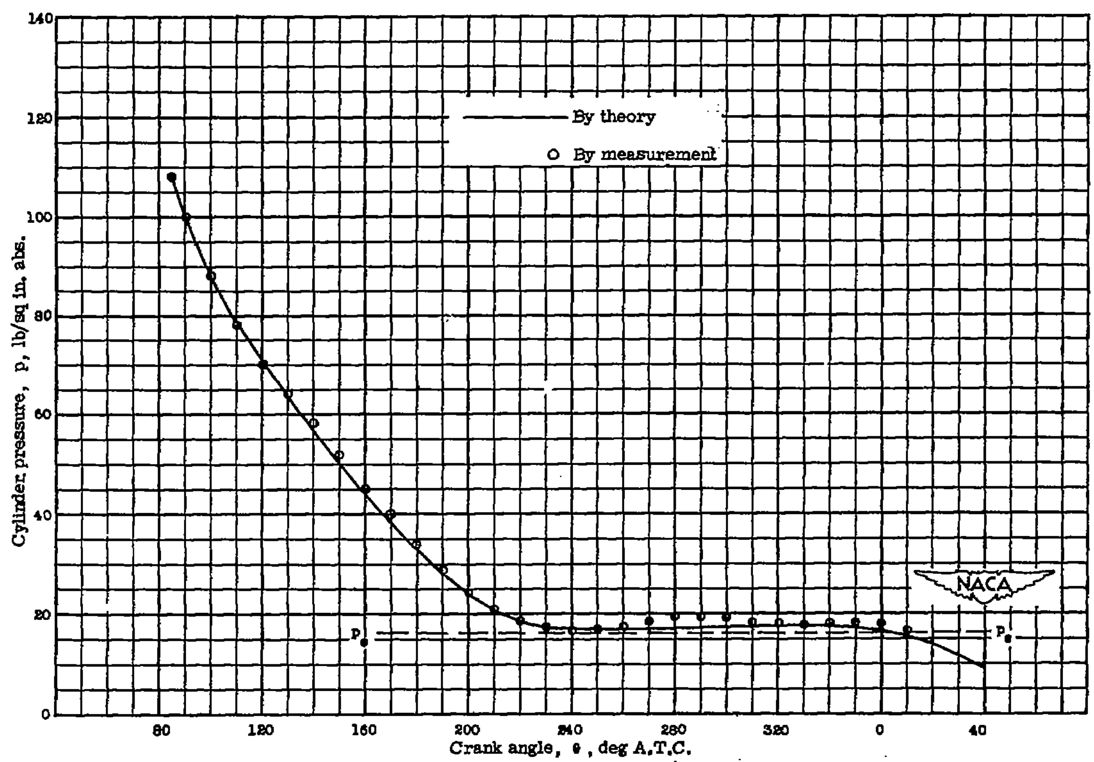

Figure 39.- Indicator diagram for solution 65. (See table II.)

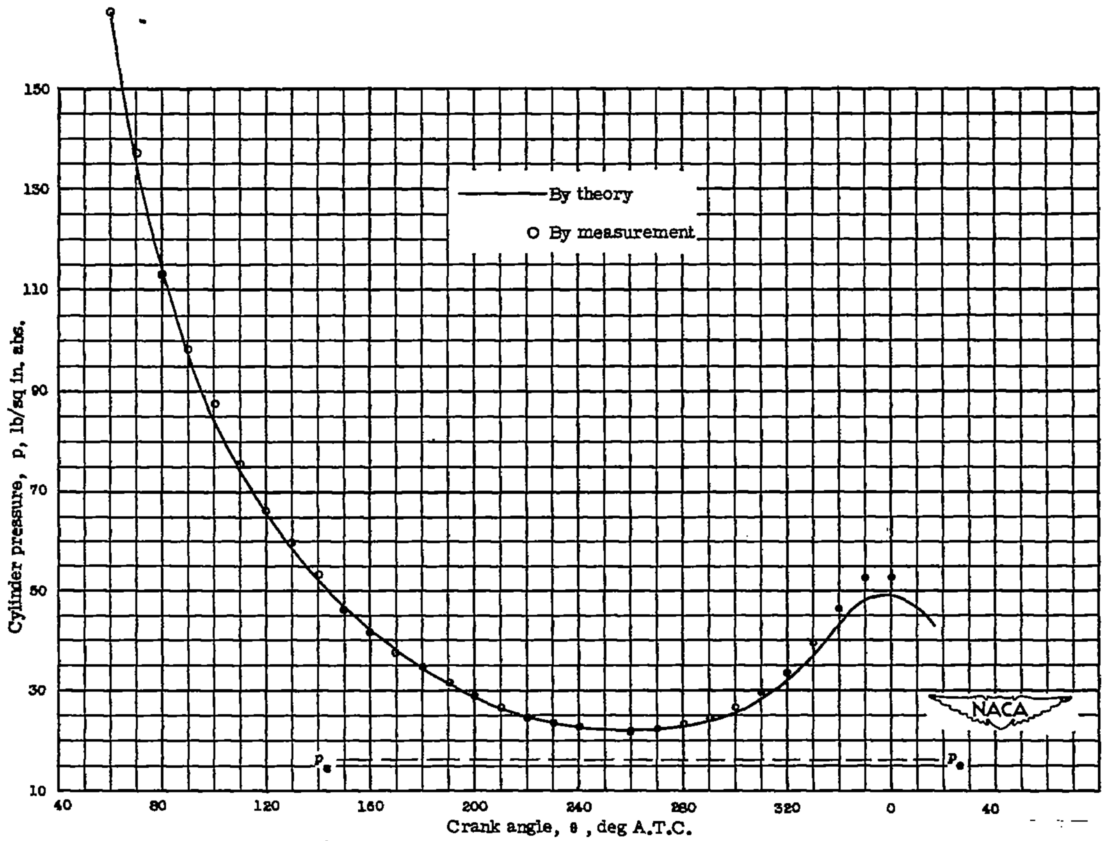

Figure 40.- Indicator diagram for solution 67. (See table II.)

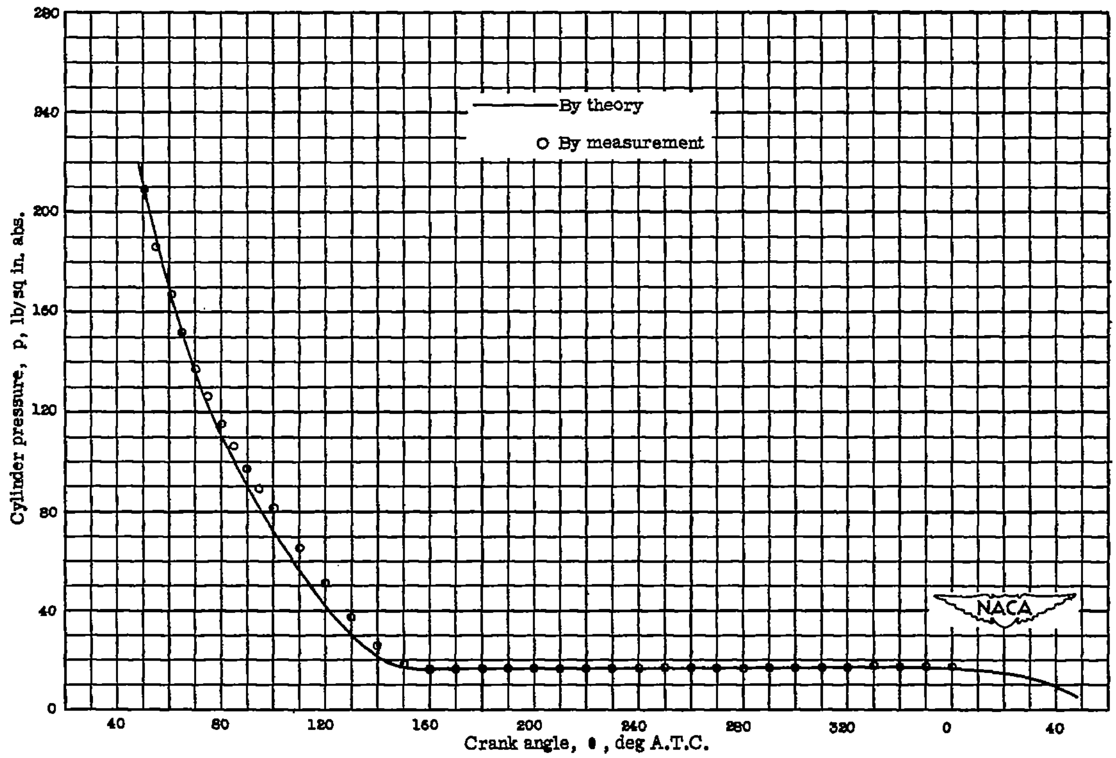

Figure 41.- Indicator diagram for solution 68. (See table II.)

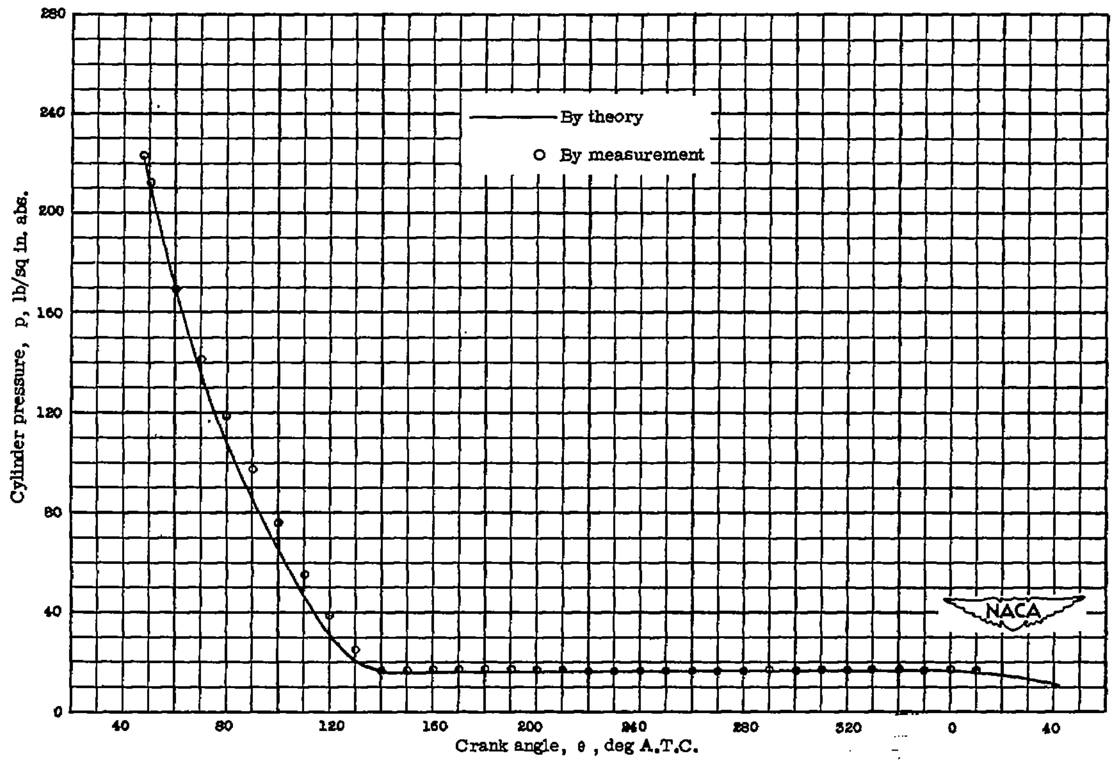

Figure 42.- Indicator diagram for solution 70. (See table II.)

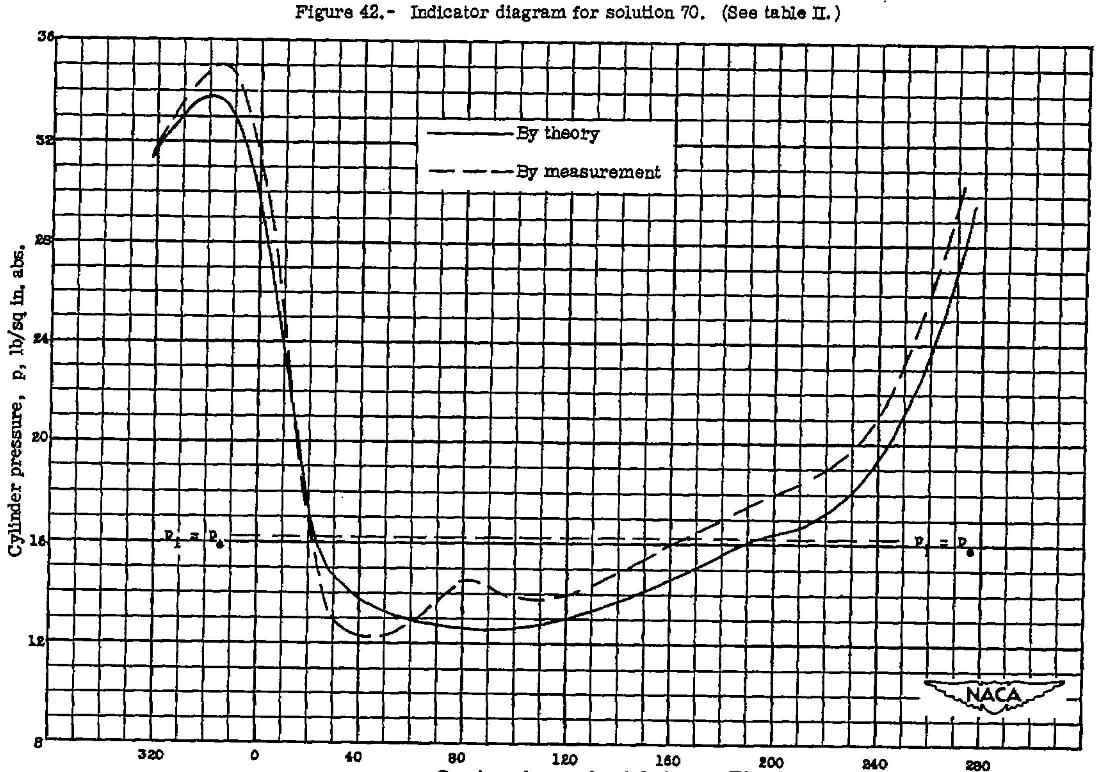

Figure 43.- Indicator diagram for solution 72. (See table II.)

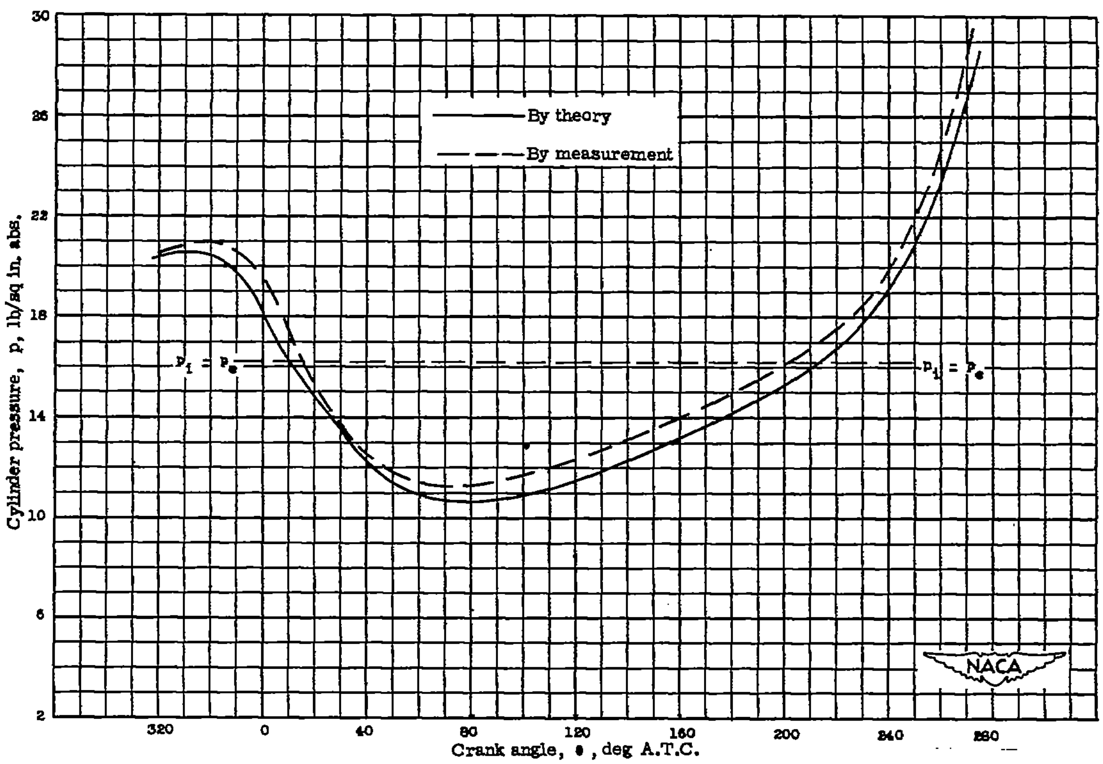

Figure 44.- Indicator diagram for solution 76. (See table II.)

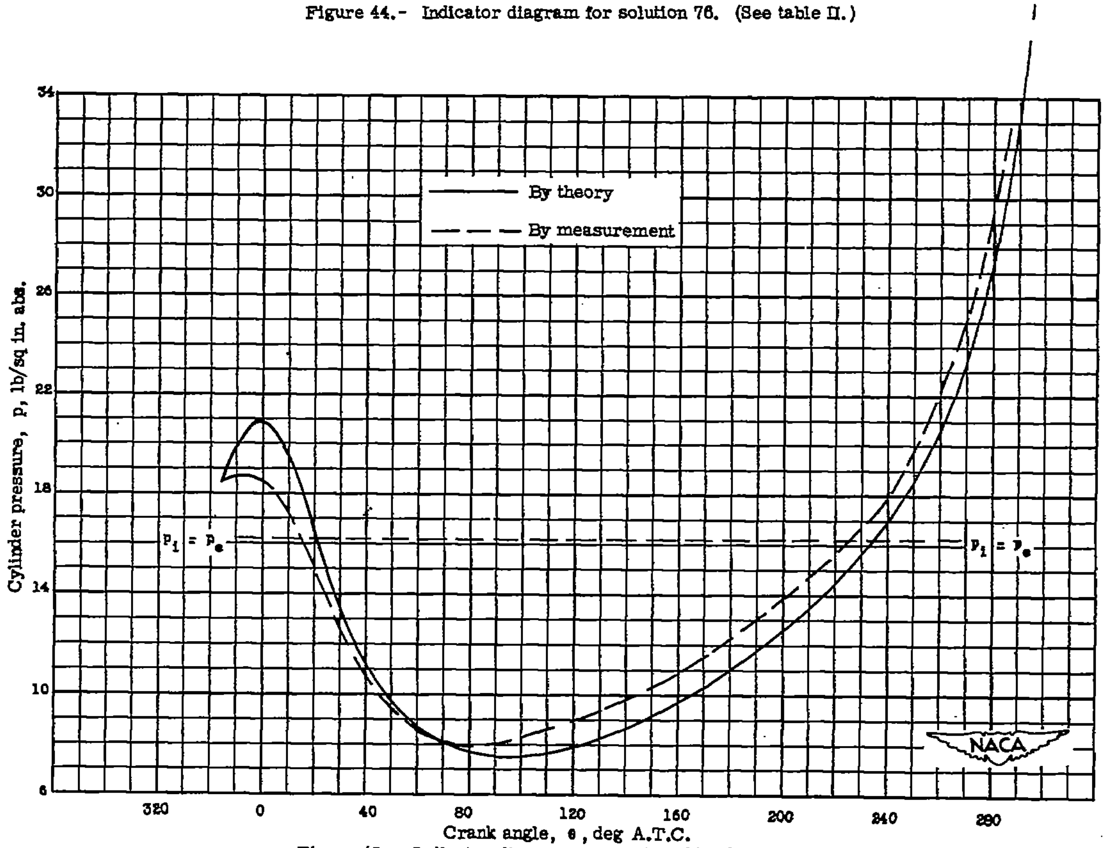

Figure 45.- Indicator diagram for solution 81. (See table II.)

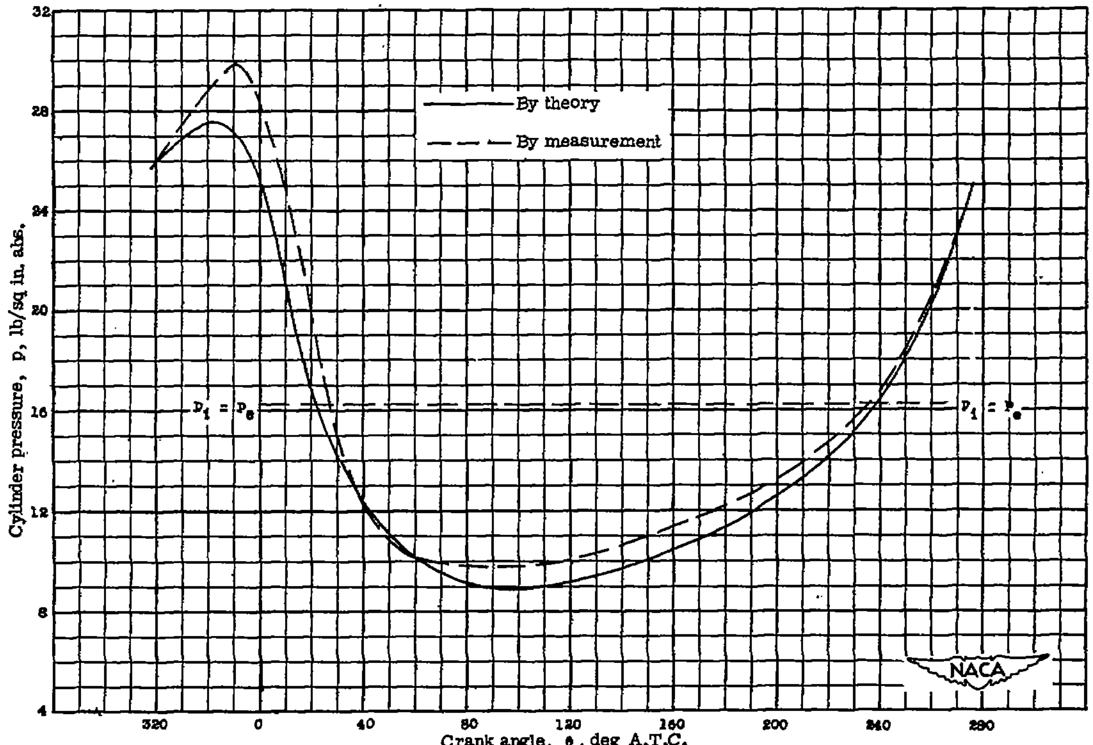

Figure 46.- Indicator diagram for solution 87. (See table II.)

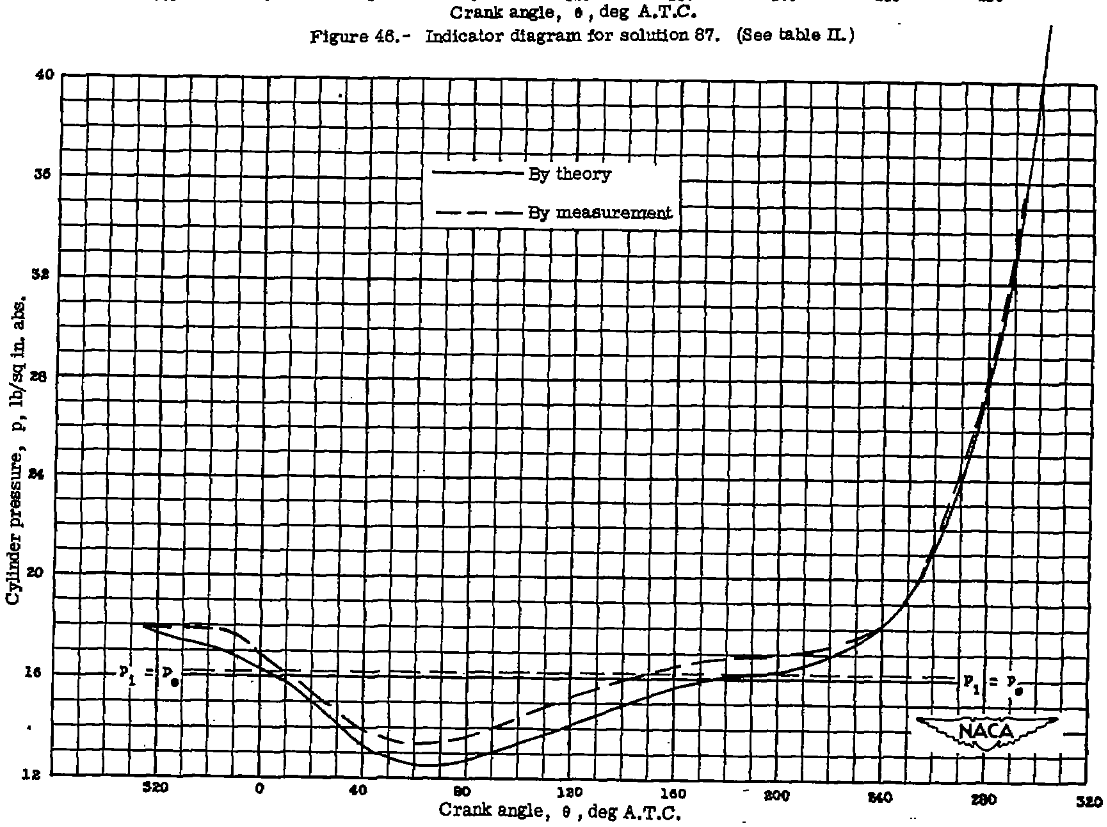

Figure 47.- Indicator diagram for solution 89. (See table II.)

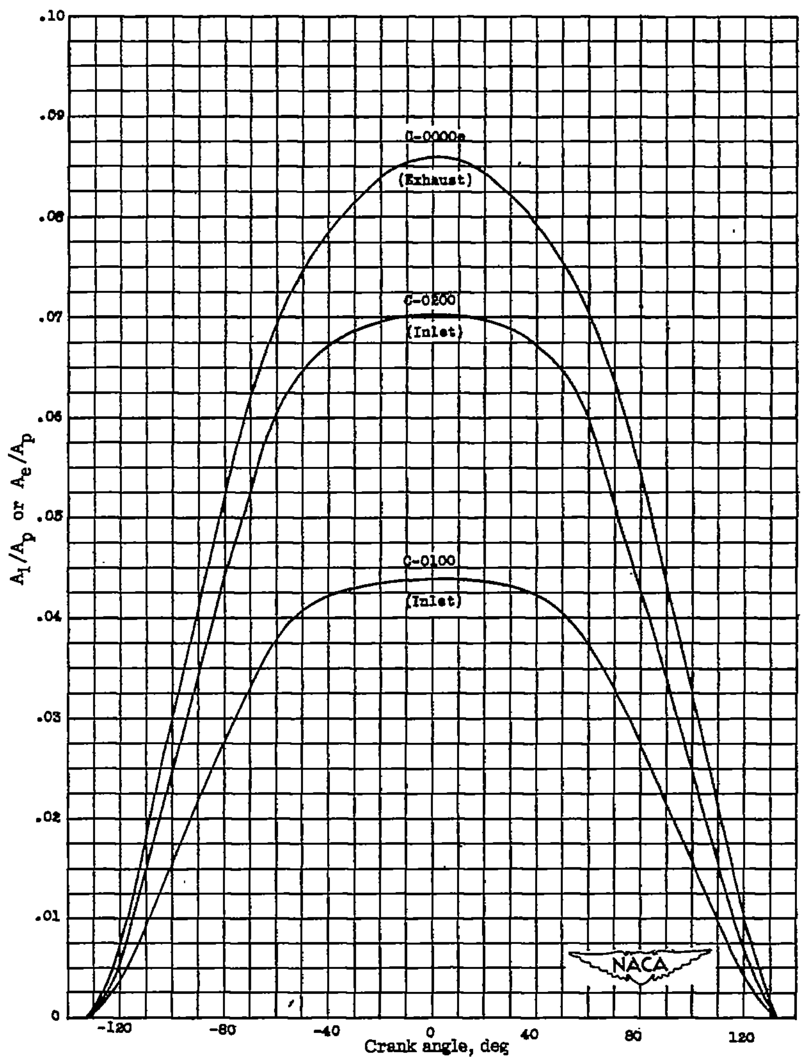

Figure 48.- Master valve-opening curves of crank angle against A_i/A_p or A_e/A_p. CFR engine. Numbers refer to curves. (See table II.) Valve opening duration, 266° crank angle.

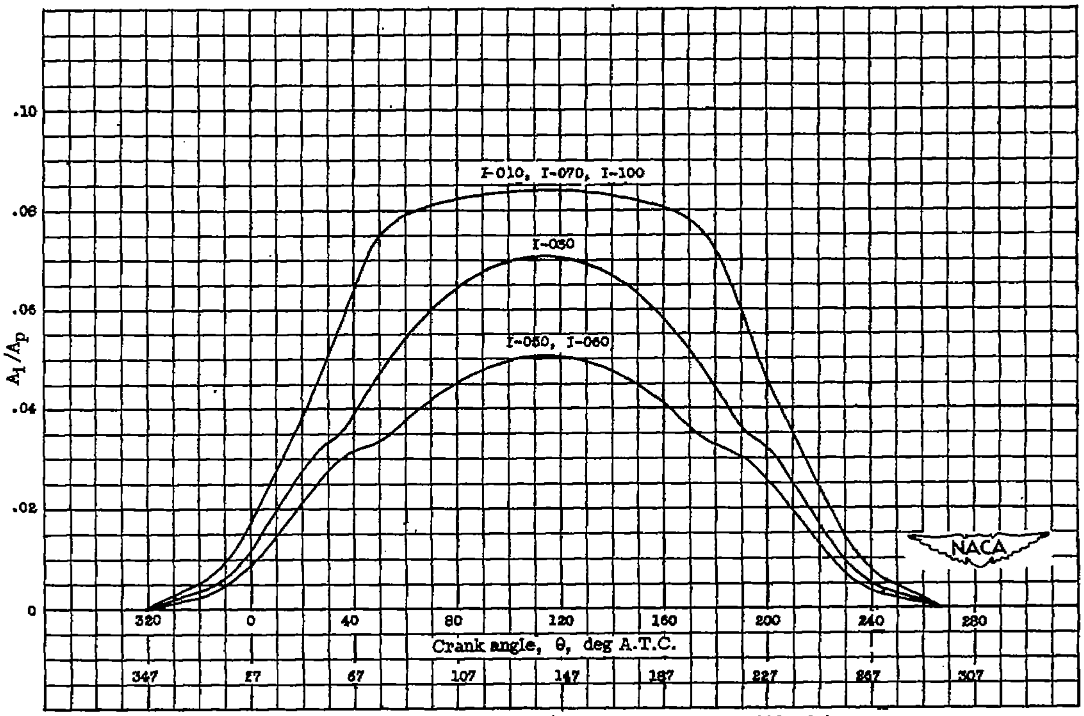

Crank angle, θ, deg A.T.C. (This scale for curve I-060 only)

Figure 49.- Valve-opening curves of crank angle against A_i/A_p. Inlet-exhaust engine; inlet-valve opening duration, 311° crank angle; inlet opens, 318° A.T.C.; inlet closes, 269° A.T.C. Numbers refer to curves. (See table II.)

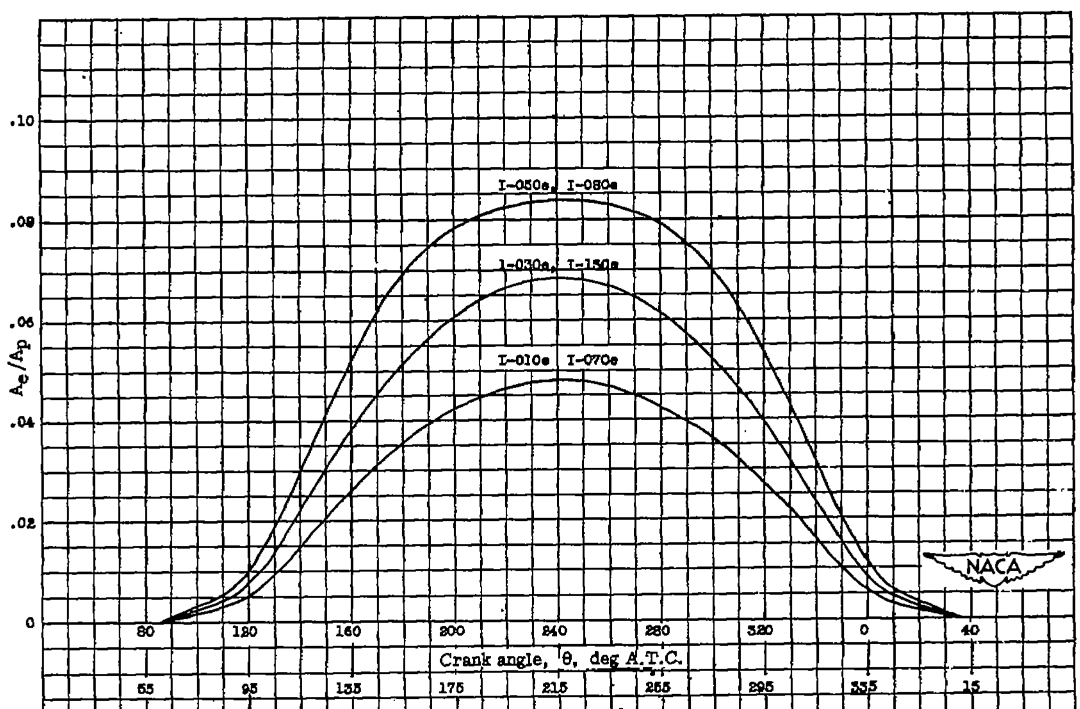

Crank angle, θ, deg A.T.C. (This scale for curve I-070e only)

Figure 50.- Valve-opening curves of crank angle against A_e/A_p. Inlet-exhaust engine; exhaust-valve opening duration, 312° crank angle; exhaust opens, 85° A.T.C.; exhaust closes, 37° A.T.C. Numbers refer to curves. (See table II.)